Normandie Université

THESE

Pour obtenir le diplôme de doctorat

Spécialité Mécanique des solides, génie mécanique, productique, transport et génie civil

Préparée au sein de l'ENSICAEN et de l'UNICAEN

Study of a unidirectional flax reinforcement for biocomposite

Présentée et soutenue par
Haomiao YANG

Thèse soutenue publiquement le 12/07/2017 devant le jury composé de		
M. Pierre OUAGNE	Professeur des Universités Ecole Nationale d'Ingénieurs de Tarbes	Rapporteur
Mme Évelyne TOUSSAINT	Professeur des Universités Université Clermont Auvergne	Rapporteur
M. Stéphane FONTAINE	Professeur des Universités Université de Bourgogne	Examinateur
M. Jun CHEN	Professeur des Universités Université de Caen Normandie	Examinateur
M. Florian GEHRING	Maitre de conférences Université de Caen Normandie	Examinateur
M. Christophe POILÂNE	Maitre de conférences HDR Université de Caen Normandie	Directeur de thèse

Thèse dirigée par Christophe POILÂNE, laboratoire CIMAP

ED PSIME

UNICAEN UNIVERSITÉ CAEN NORMANDIE

ENSICAEN ÉCOLE NATIONALE SUPÉRIEURE D'INGÉNIEURS DE CAEN & CENTRE DE RECHERCHE

ed 591

CIMAP

TABLE OF CONTENT

PRÉAMBULE/PREAMBLE

L'autorisation de rédaction d'une thèse de doctorat en langue anglaise à l'Université de Caen Normandie est conditionnée à l'incorporation au document d'une « synthèse rédigée en français, mettant en évidence les enjeux et les apports de la thèse ». Dans le présent document, cette synthèse est constituée d'un préambule, d'une introduction générale, d'une conclusion générale et d'un résumé. Les enjeux du travail demandé sont synthétisés par la feuille de route reproduite ci-dessous.

The University of Caen Normandy authorizes the PhD thesis in English with the following condition: "The manuscript should contain a synthesis to explain the challenges and the main results of the work". In this paper, the choice has been done to write preamble, general introduction, general conclusion, and abstract in both languages. Challenges of the PhD work are explained by the following proposal roadmap.

Feuille de route proposée initialement au candidat :

Roadmap as it was proposed to the PhD student:

Un « matériau composite » est le mariage d'un renfort, doté de propriétés recherchées, et d'une matrice, qui joue le rôle de liant. Partout dans le monde, les fibres végétales sont amenées à pénétrer le secteur des matériaux composites, et même à se substituer aux fibres de verre pour bien des applications. En France, la fibre de lin est le meilleur candidat pour cela. Certain secteur industriels stratégiques sont directement concernés, comme les secteurs du *Sport & loisir*, de la *Construction*, du *Nautisme*, de *l'Automobile*, de *l'Aéronautique*, et du *Transport ferroviaire*. L'incorporation de fibres végétales dans les structures à « hautes performances » n'est qu'une question de temps. Ces structures comportent essentiellement des renforts

A "composite material" is a coupling between a reinforcement from which some specific properties are interesting and a matrix which acts as a binder. All over the world, vegetable fibers are expected to more and more penetrate the composite material sector, and to replace glass fibers for numerous applications. In France, flax fiber is the best candidate. Some strategic industries are directly concerned, such as Sports & Recreation, Buildings, Boating, Automobile, Aeronautics, and Railway. Incorporating vegetable fiber in "high performance" structures is only a matter of time. High performance structures basically comprise a unidirectional reinforcement

unidirectionnels (sans torsion et sans embuvage). De nos jours, des solutions industrielles existent pour élaborer des composites renforcés par du lin unidirectionnel. Le projet décrit ici concerne l'analyse d'un nouveau type de renfort lin qui est totalement unidirectionnel. L'utilisation de ce renfort ouvre la voie à une nouvelle classe de matériau composite : les polymères renforcés par des fibres de lin unidirectionnelles (PRFL-UD).

Dans l'équipe d'Alençon du CIMAP, et ce depuis 2007, des travaux ont été conduits[45][46][47][48][49] sur du lin/époxyde haute performance dans lequel le renfort est un fil torsadés provenant de la « filature au mouillé ». L'équipe possède de ce fait une grande expérience sur ce matériau. Cependant, sa connaissance concernant le renfort totalement unidirectionnel est limitée à quelques expertises. Ce matériau est très récent en industrie ; il a fait l'objet, à ce jour, de très peu de recherches scientifiques. La principale difficulté dans l'utilisation de la fibre de lin comme renfort pour les polymères organiques est connue : « comment élaborer un matériau possédant une interface renfort/matrice performante ? ». Cette question constitue le fil rouge du présent projet de thèse.

A. Recherche bibliographique

Le travail de recherche débutera par la mise en œuvre d'une solide base bibliographique concernant les composites unidirectionnels renforcés par des fibres végétales. Cette étude

(without twisted yarn and without crimp). Industrial solutions now exist for making such unidirectional flax reinforcement. The work described below concerns the study of a new industrial flax reinforcement which is purely unidirectional. The use of such reinforcement will offer a new material for composite sector: a unidirectional flax fiber reinforced polymer (UD-FFRP).

Previous works[45][46][47][48][49] have been done in our laboratory since 2007 on high performance flax/epoxy for which the reinforcement was a twisted yarn coming from “flax wet spinning”. Therefore, we have a long experiment on this material. Nevertheless, our knowledge about purely unidirectional reinforcement of flax is actually limited. This material is very new in industry and very few research studies have been done about it.

The main difficulty in using unidirectional flax fiber as reinforcement for polymer is known: “how to make a composite with a good fiber/matrix interface?”. This question guides the proposed PhD research work.

A. Bibliographic research

In order to make a solid state of the art, the research work will begin by a bibliographic study of purely unidirectional

bibliographique sera mise à jour tout au long du travail de thèse.

B. Caractérisation du renfort

Le PRFL-UD a fait l'objet d'un brevet. Un point de départ important consiste à analyser le produit à son été initial (avant imprégnation). Les principales propriétés intéressantes sont le rapport pectines/cellulose, le degré de polymérisation, les propriétés thermiques. Il est par ailleurs essentiel de quantifier le degré de désorientation des fibres.

C. Élaboration à l'échelle mésoscopique

La matrice qui sera utilisée n'a pas fait l'objet d'un choix préalable. Elle doit cependant être adaptée à l'élaboration d'échantillon transparent à l'échelle mésoscopique. Les deux possibilités permettant d'obtenir ce type d'échantillon sont d'une part l'utilisation d'un mono-pli fibre/résine et, d'autre part, l'imprégnation d'un faisceau de fibres. L'échelle mésoscopique facilitera l'optimisation du protocole d'élaboration et formera potentiellement une base pour la caractérisation des propriétés physiques.

D. Élaboration et Optimisation à L'échelle Macroscopique

Dans le but d'expertiser les performances du PRFL-UD à l'aide des standards internationaux, et de l'optimiser à l'échelle de la structure, il convient d'élaborer des échantillons à l'échelle macroscopique. Le protocole d'élaboration n'est

reinforcements of polymer by long vegetable fibers. Nevertheless, the literature study will occur all over the PhD work.

B. Characterization of the initial product

The UD-FFRP is patented. One important subject is to characterize this reinforcement of flax at the initial state (i.e. before impregnation). The main interesting properties are the pectin/cellulose ratio, the degree of cross-linking, and the thermal properties. It is also essential to quantify the fiber disorientation.

C. Elaboration of mesoscale specimens

We have not actually decided what matrix will be used. It should be adapted to make a composite specimen which will be transparent at a mesoscopic scale. The two possibilities are one ply flax/matrix and one bundle flax/matrix. Mesoscale specimens will facilitate the optimization of composite elaboration. Then, mesoscale specimens will possibly be the base of unidirectional physical characterization.

D. Elaboration and optimization of macroscale specimens

In order firstly to test the UD-FFRP with international standards, and secondly to optimize the UD-FFRP at the scale of the structure, the elaboration of macroscale specimens is very important. The choice of

pas imposé mais les paramètres d'entrée seront rigoureusement contrôlés. Ces paramètres sont : la durée et la température de ramollissement, la température et la durée de réticulation, les proportions relatives des constituants, le type de renfort de lin, et tout autre paramètre qui entre en jeu dans l'optimisation de l'interface fibre/résine. Il sera particulièrement intéressant de fonctionnaliser le renfort par une approche scientifique. L'utilisation de la technique des plans d'expériences est nécessaire pour cette partie ; les résultats expérimentaux pertinents sont *a priori* la température de transition vitreuse et le taux de porosités.

elaboration process is not imposed but the input parameters of the process have to seriously be controlled. These parameters could be cure duration, cure temperature, softening duration, softening temperature, mix ratio, type of reinforcement of flax, and all the needed parameters to increase the fiber/matrix interface quality. It will be particularly interesting to functionalize the reinforcement with a scientific approach. The use of one or more experimental design is a necessity in this part. The cross-linking temperature and the ratio of porosity have to be quantified as output parameters.

E. Caractérisation de l'interface

Il est connu que l'efficacité de l'interface fibre/matrice gouverne les propriétés globales des composites à renfort végétal. Il est en l'occurrence très difficile d'élaborer un polymère renforcé par des fibres longues de lin exempt de porosités. Les méthodes de caractérisation *in-situ* de l'interface sont nombreuses. Les principales techniques utilisées au laboratoire jusqu'à maintenant sont la microscopie électronique à balayage (MEB) et les tests de sorption, mais d'autres possibilités existent localement comme les essais de fragmentation ou la microscopie électronique en transmission (MET). Par ailleurs, un modèle développé au laboratoire pour mieux comprendre les propriétés de sorption du lin/époxyde sera implémenté dans le cas du composite unidirectionnel.

E. Characterization of interfaces

The properties of fiber/matrix interface are a key point for global properties of UD-FFRP. For example, it is currently very difficult to make a long flax fiber reinforced polymer without porosity. Existing methods to characterize the *in-situ* interface are numerous. The main methods we are using in our team are Scanning Electron Microscopy and Sorption Tests but other possibility exists in our laboratory like Fragmentation Tests or Transmission Electron Microscopy. Furthermore, a model was developed in our laboratory in order to better understand the sorption properties of flax/epoxy. This model should be tested with the UD-FFRP.

F. Analyse des Propriétés Mécaniques

In fine, les caractéristiques les plus intéressantes pour les applications structurales sont les propriétés mécaniques. Un modèle a été développé au laboratoire pour prédire le comportement mécanique des composites lin/époxyde. Cette stratégie sera implémentée dans le cas du composite unidirectionnel. Les facteurs qui entrent en jeu dans les performances mécaniques sont la vitesse de déformation, la température d'essai et le taux d'humidité des échantillons. Le taux de désorientation des fibres sera un paramètre d'entrée privilégiée. L'analyse de la santé matière par émission acoustique sera une l'une des techniques d'analyse privilégiée.

F. Study of properties according to input parameters

Finally, the mechanical properties are the more important properties for structural applications. A model was also developed in our laboratory in order to better predict the mechanical properties of twisted flax/epoxy. This model should be tested with the UD-FFRP. The testing parameters for mechanical tests are the strain rate, the temperature and the moisture content of specimens. One of the interesting input parameters to be tested is the fiber disorientation. One of the measurement methods we use is the acoustical emission.

Apport de la thèse en terme de production/ Contribution of the thesis

C. Poilâne, F. Gehring, H. Yang and F. Richard, "About nonlinear behavior of unidirectional plant fibre composite ", in Advances in Natural Fibre Composites: Raw Materials, Processing and Analysis, Editors: Pr. R. Fangueiro and Dr. S. Rana, Springer 2017 [chapitre de livre/book chapter]

H. Yang, F. Richard, F. Gehring and C. Poilâne, "Non linear behavior of flax/epoxy unidirectional composite", International Workshop "Dynamic behaviour of green composites", ISAE-ENSMA, Poitiers (France), 27-29 September 2016 [présentationorale/oral]

F. Gehring, H. Yang, F. Richard and C. Poilâne, « Aspect inélastique du lin/époxy », JNC 20 – École des Ponts ParisTech, 28 - 30 juin 2017 [poster]

H. Yang, F. Richard, F. Gehring and C. Poilâne, "Non linear behavior of flax/epoxy unidirectional composite", 3RD Int. Conference on Natural Fibers,Braga, Portugal, 21 to 23 rd

of June 2017 [présentationorale/oral]

H. Yang, F. Gehring, and C. Poilâne, "Structural design and behavior analysis of unidirectional flax fiber composite", soumis à J. Mater. Composite [article]

INTRODUCTION

L'objectif de la thèse est de caractériser les composites à renfort lin du point de vue des propriétés mécaniques, du comportement mécanique et de la sorption. Des composites à renfort lin totalement unidirectionnels ont été élaborés suivant un protocole de presse à chaud. Deux approches mécaniques ont été explorées pour analyser les propriétés mécaniques de composites à renfort végétal.

Il est bien connu que le comportement mécanique des polymères renforcés par des fibres végétales est non linéaire – les courbes de traction comportant habituellement deux domaines distincts – et que ce comportement dépend de plusieurs conditions expérimentales (vitesse de traction, température, humidité…). Une étude expérimentale de l'influence de la vitesse de traction et de la température a mis en évidence un comportement plus général en trois domaines distincts. Le premier modèle mécanique que nous étudions suit de ce fait une approche phénoménologique visant à décrire le comportement mécanique observé via l'identification de huit paramètres matériaux. Cette approche fait l'objet du quatrième chapitre.

Le second modèle mécanique consiste à exprimer les propriétés mécaniques effectives du renfort unidirectionnel de lin à l'aide

In this PhD work, the objective is to characterize the behavior of flax fiber composite at the aspects of mechanical properties and water sorption. Purely unidirectional (UD) flax fiber composite has been designed and manufactured based on the hot platen process. Two mechanical approaches were developed to analyze the mechanical behavior of UD plant fiber composites.

As it is well known, mechanical behavior of plant fiber composite is not linear and depends on experimental condition (strain rate, temperature and humidity…): plant fiber composites normally exhibit two typical regions in the tensile test. More generally, by experimental design considering the test conditions such as strain rate and temperature effect, three regions have been identified in this work. The first studied model is a phenomenological model developed to describe the three-region tensile mechanical behavior of plant fiber composite in which more eight parameters were identified. The phenomenological model is discussed in the fourth chapter.

The second model is the development of effective mechanical properties of UD

d’une approche inverse basée sur la loi des mélanges, la prise en compte du taux de porosité, et la prise en compte de l’orientation des fibres. Pour cela j’ai introduit un paramètre d’orientation dans la loi des mélanges, la distribution statistique de l’orientation des fibres étant calculée par analyse d’image et utilisation du concept de tenseur de structure. Ce modèle de mécanique des composites est développé dans le troisième chapitre.

Les deux modèles mécaniques étudiés fournissent des prévisions pertinentes du comportement mécanique du renfort unidirectionnel lin UD et des composites associés.

Outre les résultats précédents, le comportement de sorption du composite unidirectionnel a également été analysé. Au laboratoire, de précédents résultats ont montré que dans le cas d’un polymère renforcé par du textile de lin, un modèle à deux cinétiques (Fick à deux phases ou Langmuïr) donne de meilleurs résultats que le modèle de Fick simple. Notre étude montre au contraire que la sorption du composite unidirectionnel est conforme à la théorie de Fick classique. Le résultat montre donc que la sorption d'humidité est fortement affectée par la conformation unidirectionnelle des fibres de lin et des porosités existant dans le

flax fiber reinforcement identification theory by taking orientation into account based on the rule of mixture model, and the fraction of porosity. For the latter, I introduced the orientation parameter into the rule of mixture model, statistical distribution of flax fiber orientation was obtained by using image analysis of local orientation of fiber combining structure tensor method. This composite science based model is developed in the third chapter.

Both two models provide effective forecast of the mechanical behavior of UD flax reinforcement and its composite.

Besides the previous results, sorption behavior of UD flax composite has been analyzed also. For flax textile composite in our lab, two-kinetic model (two-phase Fick’s model or Langmuïr model) has given better results than simple Fickian model. Oppositely, the sorption behavior is in line with typical Fickian model in case of unidirectional flax composite. Therefore, result shows that the moisture uptake was strongly affected by the unidirectional conformation of flax fibers and porosities existing in the composite. The sorption of UD flax composite is studied in the fifth chapter.

composite. Les propriétés de sorption sont étudiées au cinquième chapitre.

Dans le présent travail de thèse :

- J'ai étudié la littérature sur les composites unidirectionnels à fibre végétale. [Chapitre 1]
- J'ai élaboré et analysé un matériau composite à renfort unidirectionnel de lin par pressage à chaud. [Chapitre 2]
- J'ai effectué des chargements en traction (essais monotones, tractions répétées progressives, essais de fluage) du composite unidirectionnel sous différentes conditions (température entre $20°C$ et $80°C$, vitesse de traction entre $10^{-3}s^{-1}$ et $10^{-8}s^{-1}$). Un modèle viscoélastoplastique à huit paramètres, développé précédemment dans notre équipe, a été testé avec le composite unidirectionnel. Nous montrons qu'une rigidification apparente cyclique en traction n'est pas possible à identifier avec le modèle viscoélastoplastique précédent. Nous proposons comme hypothèse que l'ajout de paramètres de durcissement au précédent modèle est une solution pertinente pour améliorer la simulation. [Chapitre 4]
- J'ai mesuré les orientations locales du renfort. Nous avons ajouté un nouveau paramètre (orientation) dans la loi des mélanges permettant d'analyser

Generally, in this PhD work:

- I studied the literature on unidirectional plan fiber composite. [Chapter 1]
- I designed, manufactured and analyzed one purely unidirectional flax fiber composite based on the hot platen. [Chapter 2]
- I have done tests under tensile loading (repetitive progressive load, creep tests, and monotonic tensile tests) of UD composite at varies conditions (temperature from $20°C$ to $80°C$, and strain rate from $10^{-3}s^{-1}$ to $10^{-8}s^{-1}$). Eight parameters viscoelastoplastic model previously developed in the team has been tested with the UD composite. I showed an apparent cyclic strengthening in tensile which is not possible to simulate with the previous viscoelastoplastic model. We propose a strong assumption that the addition of strengthening parameters to the initial model offers a good solution to improve simulation. [Chapter 4]
- I measured the local orientations of reinforcement. I introduced new parameter (orientation) into rule of mixture model for UD reinforcement effective mechanical properties analysis. UD flax fiber shows high mechanical properties (Young's

l'efficacité du renfort dans le composite lin unidirectionnel. La fibre de lin UD présente des propriétés mécaniques élevées (supérieures à $80\,GPa$) à température ambiante ($20°\,C$) et vitesse de traction standard ($10^{-4}s^{-1}$). [Chapitre 3]

- J'ai mis en œuvre des essais de sorption en immersion du composite unidirectionnel. Ce composite montre une capacité de prise d'eau rapide et élevée (environ 22% d'eau en masse à saturation), le mécanisme de diffusion est conforme à une loi de Fick. [Chapitre 5]

modulus higher than $80\,GPa$) in room temperature ($20°C$) and standard strain rate conditions ($10^{-4}s^{-1}$). [Chapter 3]

- I designed and performed sorption experiment for UD composite. This composite has a high moisture uptake (about 22% by mass percentage). Diffusion mechanism is finally conform to Fickian model. [Chapter 5]

Chapter 1 STATE OF THE ART

1.1 Characteristic of plant fiber composite

Plant Fiber Composites (PFC) – also known as Plant Fiber Reinforced Polymer (PFRC) – are low environmental impact and low cost and renewable source fiber with lightweight reinforced polymers compared to artificial fiber reinforced polymers. One of their potentials is to replace artificial fiber composites such as glass fiber composites at lower cost with improved sustainability[1]. The use of plant fiber reinforced polymers is main in the aspects of construction and infrastructure (such as beams, roof panels and bridges), sports and leisure (for boat hulls, canoes, bicycle frames and tennis rackets), furniture and consumer goods (such as packaging, cases, urns, chairs, tables, helmets and ironing boards) etc.[2]. Although plant fiber reinforced polymers exhibit good prospects, the artificial fibers, specifically E-glass, dominate today fiber reinforced polymer (FRP) market[3]. In many of plant fiber composite applications, they are being employed primarily as little or no structural role but environmentally friendly materials because of reinforcement characteristics summarized below that will transfer into the final product performance. Plant fiber advantages and disadvantages are shown in Table 1.1.

Table 1.1 Main advantages and disadvantages of plant fibers[4]

Advantages	Disadvantages
Low cost	High moisture absorption
Renewable resource	Poor dimensional stability (swelling)
Low density	Poor microbial resistance
High specific property	Low thermal resistance
High Young's modulus	Discontinuous fiber
Good tensile strength	Anisotropic fiber properties
Nonabrasive to tooling and molds	Low transverse strength
No skin irritations	Low compressive strength
Low energy consumption	Local and seasonal quality variations
CO_2 neutral	Demand and supply cycles
No residues when cremated	
Biodegredable (±)	

1.2 Characteristic of plant fiber as a reinforcement

Plant fibers primarily consist of: cellulose, hemicelluloses, lignin, and pectin for some of them. The individual percentage of these components varies with the different types of fibers. Generally, higher performance is achieved with varieties having higher cellulose content and with cellulose microfibrils (see Fig. 1.1) aligned more in the fiber direction, which tends to occur in bast fibers (e.g. flax, hemp, kenaf, jute and ramie) that have higher structural requirements in providing support for the stalk of the plant[5]. Numerous studies on the characterization of plant fibers were conducted. Table 1.2 gives properties of plant fibers compared with those of the main types of artificial fibers.

Table 1.2 Mechanical properties of plant fibers as compared to conventional fibers[5][6][7][8]

Fiber	Density $(g\ cm^{-3})$	Length (mm)	Elongation (%)	Tensile strength (MPa)	Young's modulus (GPa)
Cotton	$1.5-1.6$	$10-60$	$7-8$	$287-597$	$5.5-12.6$
Jute	1.3	$1.5-120$	$1.5-1.8$	$393-773$	$10-55$
Flax	1.5	$5-900$	$2.7-3.2$	$345-1830$	$27.6-80$
Hemp	1.5	$5-55$	1.6	$550-1110$	$58-70$
Ramie	1.5	$900-1200$	$3.6-3.8$	$400-938$	$61.4-128$
Sisal	1.5	900	$2-2.5$	$511-635$	$9.4-28$
Alfa	1.4	350	$1.5-2.4$	$188-308$	$18-28$
Coir	$1.25-1.5$	$20-150$	$17-47$	$105-175$	$4-6$
Bamboo	0.9	–	$1.4-1.73$	$341-503$	$19.7-35.9$
Wood	1.3	$38-152$	6.9	$50-315$	$2.3-5$
E-glass	2.5	continuous	2.5	$2000-3500$	70
S-glass	2.5	continuous	2.8	4570	86
Aramid	1.4	continuous	$3.3-3.7$	$3000-3150$	$63-67$
Carbon	1.4	continuous	$1.4-1.8$	4000	$230-240$

The density of the plant fibers is much smaller than that of glass fibers. This is a major asset for the use of them as reinforcement combining the ecological protection advantages. The Young's modulus of plant fiber such as flax is comparable to that of glass fiber if one is interest in the best results regarding the ecological cycle and carbon emission. However, in terms of failure stress, the artificial fibers are well above the plant fibers. Furthermore such

comparison from bibliographic results could be not meticulous, because for most of articles the authors do not make any difference between elementary fiber and bundle of fibers (see next section). For example, it is the case for flax fiber in Table 1.2, for which the length varies from 5 mm (elementary fiber) to 900 mm (bundle of fibers)!

1.3 Flax fiber as reinforcement

1.3.1 Structure and composition

Flax fibers which originate from renewable resources are a possible alternative to artificial fibers. They have many advantages such as low density, high specific stiffness, recyclability and especially have a CO_2 neutral life cycle fitting well into ecological environment in contrast to the artificial fibers (glass, carbon, etc.), and these constitute the major incentives for their use in composites. The flax fiber has a complicate structure consisting of cellulose, hemicellulose, pectin, lignin, water soluble and others[7]. Fig. 1.1 presents the general structure of a flax fiber. The flax fibers which are grouped in bundle forms exist in the phloem parenchyma between the wood part and the bark of the stem of the plant (Fig. 1.1(a) & Fig. 1.1(b)). The fiber bundles are composed of several tens of elementary fibers. Flax fiber is a hollow fiber where the chemical components (cellulose, hemicellulose, lignin and pectin) are organized into cell walls in a multilayer structure. Each fiber has a complex, layered structure consisting of a primary cell wall (PCW), a secondary cell wall (SCW) and a lumen (L) (Fig. 1.1(c) & Fig. 1.1(d)). The primary wall which is the first layer contains randomly oriented microfibrils in a matrix consisted mainly by pectin and deposited during cell growth encircling a secondary wall. The secondary wall representing 80% of the fiber section is made up of three layers: S1 ($0.5-2$ µm), S2 ($5-10$ µm) and S3 ($0.5-1$ µm). S1 is the external layer, S2 is the thick middle layer determining the mechanical properties of the fiber, and S3 is the thin internal layer that surrounds the fiber lumen. A lumen which is somehow porosity in the center of the fiber can be as small as 1.5% of the cross section. S1 and S3 are arranged in parallel layers in different orientations. In addition, the cellulose microfibrils are highly oriented in the S2 layer with a low angle (microfibril angle between 8° and 11°) relative to the axis of the fiber Fig. 1.1(d)). The elementary fibrous cells with lengths mainly between 2 and 5 cm, and average diameters mainly between 10 and 30 µm are glued together by means of the middle lamella interphase which mainly consisting of pectin and hemicellulose, that is a mixture of different lower molecular weight branched

polysaccharides. The various layers can be differentiated according to their chemical composition, thickness and organization in microfibril structure, but each layer consists of cellulose microfibrils in a matrix of hemicellulose, pectin and optionally lignin. This confers tensile strength in cell walls, where cellulose microfibrils are meshed into a polysaccharide matrix[9][9][11][7][12].

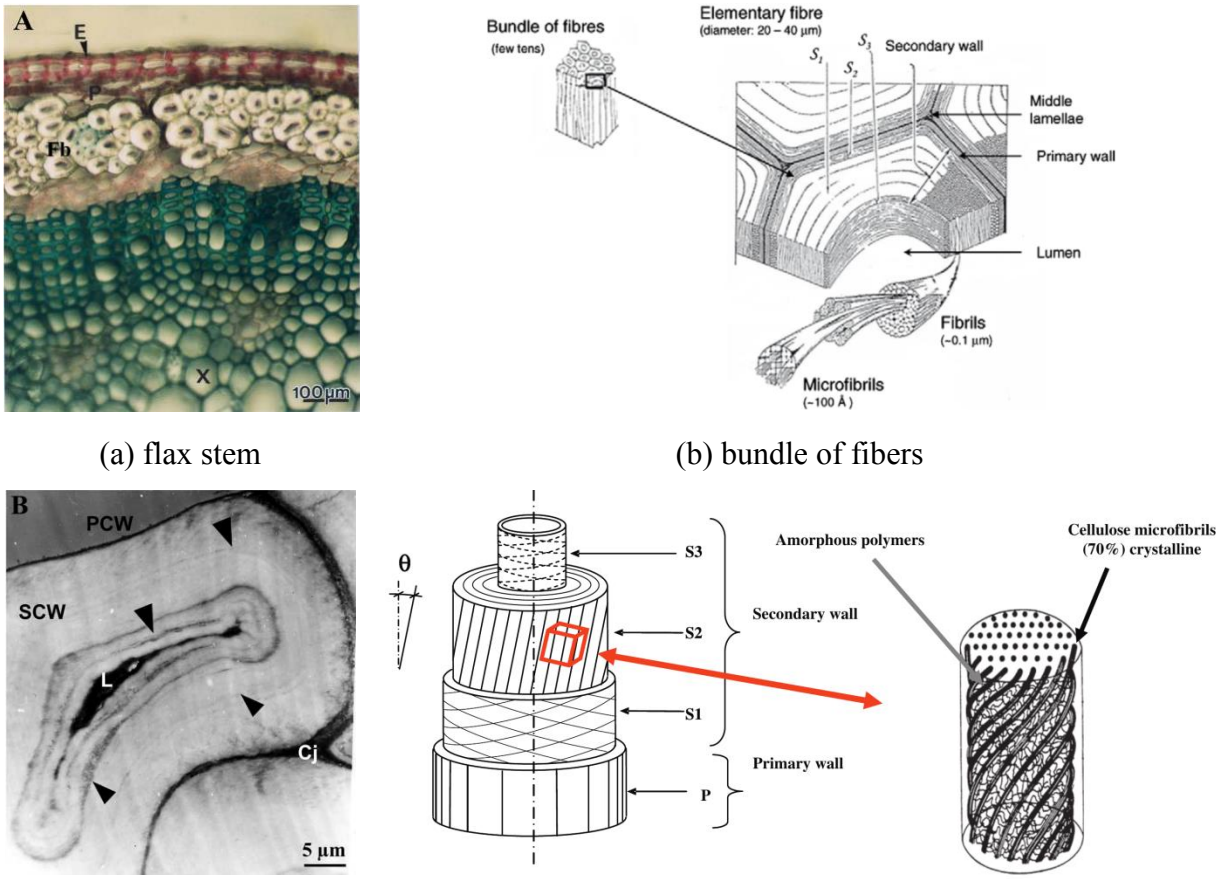

(a) flax stem (b) bundle of fibers

(c) elementary fiber (d) elementary fiber (S1–S3 reversed)

Fig. 1.1 Structure of a flax fiber from the stem to the microfibrils[11][9]

Flax fibers are mainly made up of cellulose “fibers”, consisting of helically wound cellulose microfibrils bound together by an amorphous matrix. Plant fibers, in particular flax fibers, comprise four main components: cellulose, hemicellulose, lignin, and pectin, but also waxes and water. Main component proportions are summarized and determined in several studies as in Table 1.3.

A large variation of the values has been found in the literature. That is mainly because a set of parameters such as the variety, quality of the soil, the climatic conditions, the quality of the retting process, the degree of maturity or measurement conditions.

Table 1.3 Chemical composition of flax fiber (mass fraction)

Cellulose	Hemi-cellulose	Pectin	Lignin	Wax	Water soluble	Water	References
65.2 – 72.2	10.1 – 17.1	2.8 – 5.6	2.3 – 7.7	2.2 – 3.0	–	–	[13]
61.5 – 86.5	–	2.4 – 3.8	2.1 – 2.6	–	–	–	[14]
77	8.7	–	2.8	–	–	4.5	[15]
71	19.6	2.3	2.2	1.7	–	10	[16]
60 – 80	10 – 15	–	0.4 – 4	–	–	–	[17]
65	16	3.0	2.5	1.5	4	8	[18]
64.1	16.7	1.8	2.0	1.5	3.9	10	[7]
62 – 72	18.6 – 20.6	2.3	2 – 5	1.5 – 1.7		8 – 12	[19]

a. Cellulose

Cellulose consists of crystalline and amorphous regions and is an organic compound with the formula $(C_6H_{10}O_5)_n$, a polysaccharide consisting of a linear chain of several hundred to many thousands of $\beta(1 \rightarrow 4)$ linked D-glucose units (Fig. 1.2). In the cellulose chain, the glucose units are in 6-membered rings, called pyranoses[20]. The multiple hydroxyl groups on the glucose from one chain form hydrogen bonds with oxygen atoms on the same or on a neighbor chain, holding the chains firmly together side-by-side and forming microfibrils with high tensile strength. Meanwhile, a large numbers of hydroxyl groups could leads to a strong hydrophilic property of cellulose.

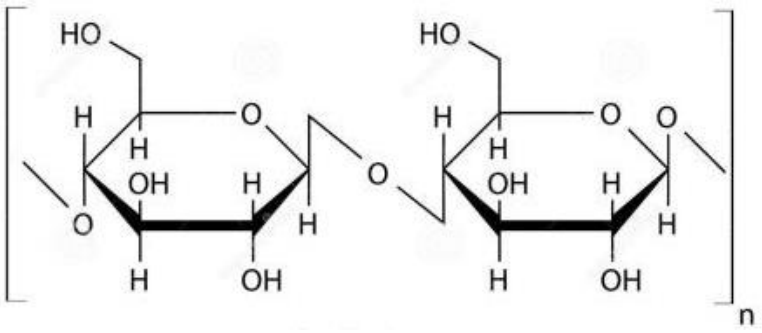

Fig. 1.2 Cellulose molecular structure

b. Hemicellulose

Hemicelluloses are wall polysaccharides, and branched whereas cellulose is unbranched. In contrast to cellulose, hemicellulose is derived from several sugars in addition to glucose, especially xylose but also including mannose, galactose, rhamnose, and arabinose[21]. These are amorphous polysaccharides with a lower molecular weight than that of cellulose, which explains their low chemical resistance. Hemicellulose which can be extracted with alkaline treatment consists of shorter chains, between 500 and 3000 sugar units as opposed to $7000-15000$ glucose molecules per polymer seen in cellulose[22]. The main role of hemicelluloses is to tether cellulose microfibrils, thereby strengthening the cell wall. Hemicelluloses are very hydrophilic, they are primarily responsible for the water absorption in plant fibers. They also have links with lignin and constitute the interphase between cellulose microfibrils and pectin cements[23].

c. Pectin

Pectin consists of a complex set of polysaccharides such as galacturonic acid and neutral sugars of various compositions (rhamnose, galactosexylose and arabinose) with galacturonic acid residues constituting up to 70% of its overall structure. It consists of four pectin domains: homogalacturonan (HGA), rham-nogalacturonan I (RGI), rhamnogalacturonan II (RGII) and xylogalacturonan (XGA)[24]. Pectins are contained in the primary cell wall of the plant fiber and particularly abundant in the non-woody parts, and ensure the cohesion of the cellulose or other non-cellulosic polysaccharides, similar to tethered liquids. A direct relation can be observed between the humidity and the hemicellulose/pectin percentages. There is a linear increase of the moisture index with the hemicellulose/pectin percentage in natural plant fibers[25].

d. Lignin

Lignin is a three-dimensional complex molecule composed of phenyl groups. Lignins are particularly important in the formation of cell walls, especially in wood and bark, because they lend rigidity and do not rot easily. Chemically, lignins are cross-linked phenol polymers[26]. Lignin is after cellulose the second most abundant natural polymer on the earth[27], however it is present in small quantities in flax fiber (Table 1.3). Microfibrils are cross-linked together by hemicellulose homopolymers. Lignins assist and strengthen the attachment of hemicelluloses to microfibrils. The non-polysaccharide components of

plant cell walls are highly hydrophilic and thus permeable to water, whereas lignin is the more hydrophobic.

e. Waxes

By the way, waxes are a diverse class of organic compounds that are hydrophobic with a low melting point above about $40°C$. Plants secrete waxes into and on the surface of their cuticles as a way to control evaporation, wettability and hydration. No significant effect of wax on the mechanical properties of the flax fiber composite was found.

1.3.2 Physical properties

a. Density and defect

The values of the mass density of a flax fiber reported in the literature are widely scattered, ranging from 1380 to 1550 $kg\ m^{-3}$ [28][29][7][5][30]. This difference may be explained in part by the growth conditions of the plants, the position of the fiber in the rod and of the species in question, and secondly, by the measurement method. Particularly, taking in account the volume of the lumen on one hand and the humidity inside fiber on the other hand has an important effect on the measured density. One retains the value $1540\ kg\ m^{-3}$ for fiber percentage computation of FFRP[31][47]. Elementary flax fibers contain cell-wall defects known as various organizational forms called dislocations, kink bands, nodes, or slip planes, etc.[32]. Defective secondary walls also exist in the growth of plant cell wall[33][34]. Ultrastructural studies reveal a common set of cell wall defects in dividing embryonic and root cells. These defects are linked to a specific reduction in cellulose coupled with ectopic callose and lignin deposits and by which cell-wall gaps are resulted in. The most obvious defect observed was the appearance of incomplete cell walls[34]. The rupture properties of the flax fiber are affected by the defects of those weakest links of a chain (kink bands zone) causing initiate failure under load[32]. A non-homogeneous distribution of defects exist in the fibers may be one reason for the large variations in mechanical properties of the flax fibers. Many defects are also induced through the standard mechanical preparation of the flax – typically scutching, hackling, spinning and weaving (see Fig. 1.6) – in addition to the discontinuity and possible misalignment of the fibers. These defects lead to weakening of the fibers and result in a decrease of composite mechanical properties[35].

b. Thermal stability

The thermal degradation of cellulose-based fibers is greatly influenced by their structure and chemical composition. Thermal stability seems to be one drawback limiting the application of flax fiber. Several-condition thermogravimetric analysis carried on between room temperature and $800°C$ with $10°C\ min^{-1}$ [36] is shown in Fig. 1.3 where the mass of the fibers remain stable until $160°C$ and weight loss of the previous portion (below $100°C$) is mainly due to evaporation of water. After that the fibers gradually begin to decompose. Derivative thermogravimetry displayed in blue dotted curve shows that the maximum weight loss rate is around $334°C$. Flaxtape™ which is comprised of unidirectional flax fibers is found to be more thermally stable in argon than air. It should be the same with other flax product because oxidation reaction takes place at around 440°C in the air atmospheres. The first decomposition of the fiber components are the wax (above $120°C$) and pectin (above $180°C$) then cellulose and hemicelluloses[37] followed by the lignin[38].

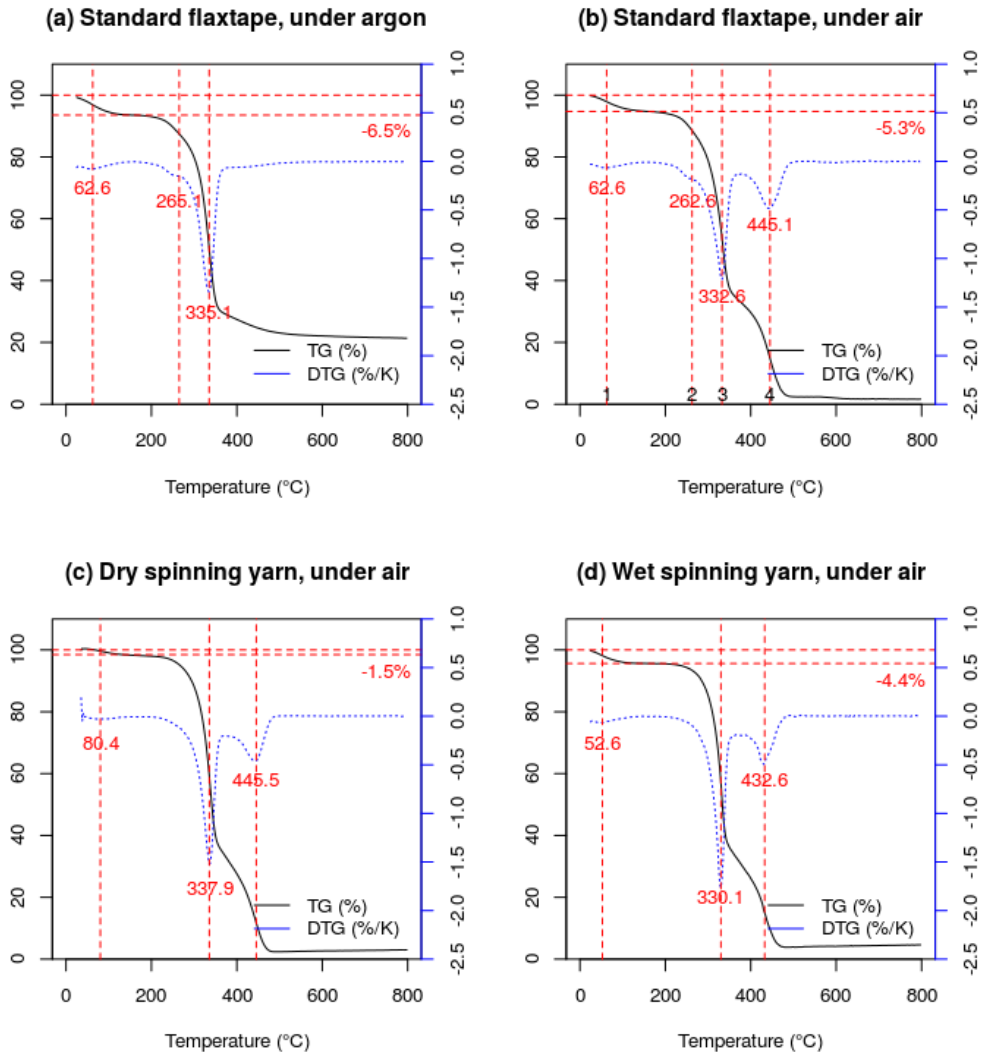

Fig. 1.3 Thermogravimetric analysis of flax fiber[36]

According to the literature, the first loss of mass at around $60°C$ on Fig. 1.3 is due to the release of water, the third loss of mass at around $334°C$ is due to cellulosic substance degradation, and the fourth loss of mass at around $440°C$ is due to oxidation of some woody matter (lignin). The second loss of mass at around $264°C$ is mainly due to pectin degradation[39]. This loss of mass is usually not noticed[37] but particularly visible with Flaxtape™ (Fig. 1.3(a) & Fig. 1.3(b)). That is due to the use of pectin as a binding agent in case of Flaxtape™, these pectins being mainly eliminated in case of traditional textile processes (Fig. 1.3(c) & Fig. 1.3(d)). Beyond this simple analysis, it is well known that when cellulose-based materials are heated in the range of $100°C$ to $250°C$, some of the changes in physical properties of the fibers can be explained in terms of alteration in either physical or chemical structure such as depolymerization, hydrolysis, oxidation, dehydration, decarboxylation and recrystallization.

The thermal stability is a key factor for the flax fiber used as reinforcement during composite production and temperature has a greater effect on the resistance mechanical properties. Normally, for exposure temperatures up to $170°C$, both the recrystallization and the differences in thermal expansion coefficient seem not to be significant enough to have a remarkable influence on the tenacity of untreated flax fibers[40]. Van de Velde et al.[37] reported that after exposure to $120°C$ up to two hours, no significant decrease of the tensile strength is observed in hackled long flax. However, after two hours exposure to $180°C$, stress retentions of 64 to 68% and retained strains of 44 to 60% are observed, respectively. Strain properties are more influenced than stress properties.

c. Tensile mechanical properties

Tensile mechanical properties of flax fibers are a basic performance considering that as reinforcement in the composite. The tensile deformation is influenced by various factors such as external conditions of strain rate, humidity, temperature etc. and internal conditions of fiber variety such as chemical composition (e.g. cellulose rate) and the structure (e.g., size of the lumen, microfibril angle), fiber diameter, fiber length considering the defect, etc. Generally, the mechanical properties (Young's modulus and failure stress and strain) of flax fibers exhibit significant dispersions. In addition, the extraction process of the fibers operations can be varied resulting in a variation in mechanical properties. Charlet et al.[41] performed a tensile test with displacement rate of $1\ mm\ min^{-1}$ and gauge length $10\ mm$ in room condition. Results show a mean strength $1200\ MPa$ and Young's modulus $56\ GPa$, respectively. The

stress-strain curve of a tensile test of a flax fiber is shown as in Fig. 1.4 with three regions considering: first linear region (strain from 0% to 0.3%); second non-linear region (0.3– 1.5%) and the final linear region (1.5% to rupture). Bos et al.[12] evaluated the hand decorticated elementary fiber can give a strength as high as 1800 MPa at a clamping length 3 mm and strain rate 0.005 s^{-1}. The clamping length has an influence on the tensile mechanical properties, especially when it is small.

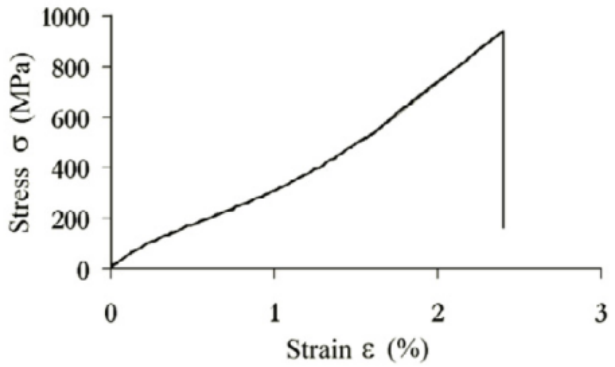

Fig. 1.4 Stress-strain curve of an elementary flax fiber[41]

Pillin et al.[42] investigated different flax fiber varieties from the same cultivation environment. The test parameters are the same such as gauge length and speed as Charlet et al.[41]. The ultimate stress of different kinds of flax fibers varies from 733 to 1111 MPa and for modulus, it is from 45.6 to 71.7 GPa using the second region to calculate. Both Pillin et al. and Charlet et al. show a typical stress-strain curve with linear and nonlinear regions in small deformation (0– 0.3 & 0.5%) or higher deformation about the flax fibers (actually, they hold different views on the linear region), see Fig. 1.4 and Fig. 1.5. The nonlinear tensile mechanical behavior could be explained by the structure parameters described in Section 1.3.1. A widely accepted view is due to the deformation of each cell wall caused by the reorganization and alignment of the cellulose microfibrils along the tensile axis direction of the flax fiber. Worth to point out, there is a decrease tendency of mechanical properties (tensile rigidity and strength) of flax fiber accompanied by an increase in fiber diameter. One reason could be the size change of lumen, another reason could due that defective secondary walls do not have as many defects as when it is fine.

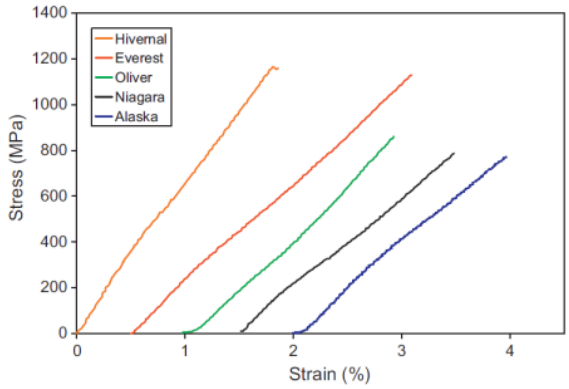

Fig. 1.5 Tensile stress-strain curves of different varieties of flax fiber[42]

1.3.3 Manufacture processes of flax

Plant fibers can be categorized according to the region of the plant they are extracted from, which are leaf fibers, seed fibers, stem fibers, and other fibers (including grasses, reeds, roots, and wood fibers, etc.). Flax fiber comes from the stem of the plant undergoing further processing to make reinforcement. This means retting, scutching, hacking, folding, etc. determined by the final reinforcement product we want to get. Fig. 1.6 gives a schematic overview of the processing of flax fibers. In the normal way, flax fiber bundles have been obtained by a retting process firstly, which consists in the biological action of bacteria in an aqueous medium where some waxes and pectins are removed[43].

Then the mechanical processes are implemented including scutching and hackling, etc. Scutching is the process consisting of extracting fiber bundles contained in the stems. Hacking process makes phloem fiber bundles into the technical fibers which contain several dozens of elementary flax fibers in an increasing fine status. Folding/drawing of the flax reinforcement allows coalescing fibers into greater length so as to obtain ribbons or tapes with several meters long. At the same time, the variability of reinforcement decreases and the flax color homogenizes itself. In the spinning process by flax spinning mills, the ribbons undergo successive torsions and stretches by which the flax ribbons are transformed and the desired yarn titration or woven reinforcement can be obtained[44]. Experienced more or less process steps, flax fiber reinforcements with different forms (mat, sew, UD) can be acquired (Fig. 1.6).

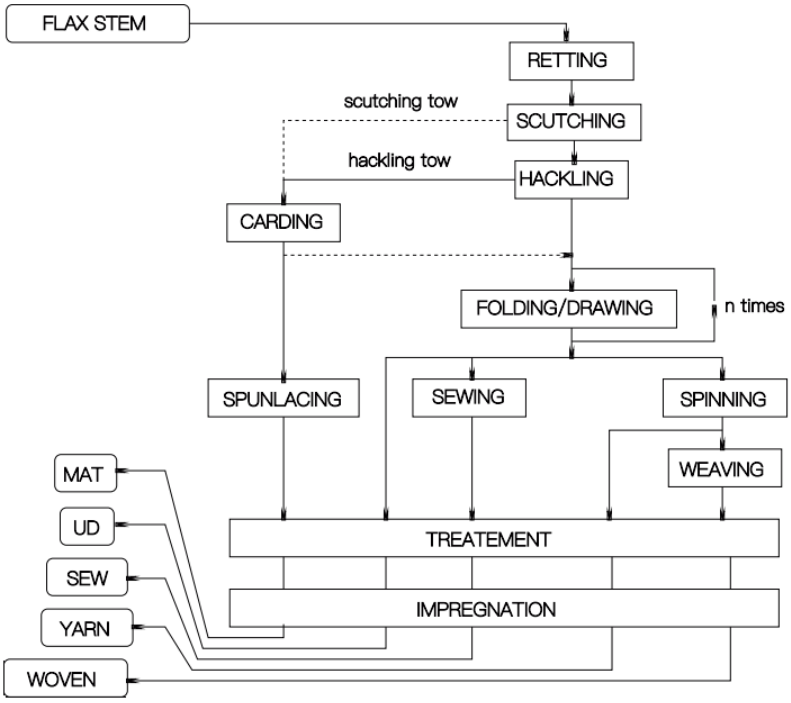

Fig. 1.6 Production processes of technical flax fibers as reinforcement

1.4 Mechanical properties of flax fiber composites

Resins used for composite matrices are cataloged into thermoplastic and thermosetting polymer. Commonly used matrices of thermosetting polymers for flax fiber studying as the reinforcement are epoxy[45][46][47][48][49], unsaturated polyester (UP)[50], phenol formaldehyde (PF)[51] polyurethane (PU)[52], bio-based thermoset soybean oil[53] and furan[54] etc. Thermoplastics are those of polyamide (PA)[55], polypropylene (PP)[56], poly lactic acid (PLA)[57][58], polystyrene (PS)[59], aliphatic polyester[60] and polyvinyl chloride & polyethylene[61] etc. Although a wide variety of polymers are used to manufacture composite as basic matrices, the influence of the polymer type apparently is of secondary importance at the finally mechanical properties. However the polymer type plays a more important role in the forming process and non-mechanical properties of products such as chemical degradation. Mechanical behavior of flax fiber composites are determined by many factors that are not only matrix system but also reinforcement form (such as mat, unidirectional, sew, yarn and woven, etc.); methods and materials used in the forming process (e.g. hot platen method, resin transfer molding, vacuum infusion method, etc.); previous flax surface treatments (silane treatment, esterification, acetylation, anhydride treatment, mercerization/alkali treatment, etc.). It means that mechanical performances cannot be directly compared, mainly because

processes result in variation of component form and fraction in the final products. Tensile mechanical properties of flax fiber composite are summarized in Table 1.4. Note that compared to ultimate stress of flax fiber composite, calculation of Young's modulus has more variations and non-repeatability due to the chosen regions for measurement in tensile curve. In the cited studies, porosity effects are not considered always, however, it is an important factor affecting on the mechanical properties of composite and inevitably exists in flax fiber reinforced polymer.

Table 1.4 Tensile mechanical properties of flax fiber composite

Flax	Resin	Fiber fraction (%)	Porosity fraction (%)	Forming process	Tensile strength (MPa)	Tensile stiffness (GPa)	Ref.
Arctic flax	Epoxy	47 (vol.)	-	RTM	279	39	[62]
Woven fabric	Epoxy	55 (vol.)	-	Vacuum bagging tech.	120	9.2	[63]
Woven UD yarn (warp knit)	UP	31 (vol.)	-	RTM	143	14	[64]
Natural cellulose of flax	Biodegradable polyester	25 (vol.)	-	Compression molding	$19.4-25.5$	$4.3-16.2$	[65]
Unidirectional fiber (UD)	PU	32 (vol.)	16.3	Vacuum assisted resin transfer molding	≈ 230	≈ 12.5	[66]
Retted (roving)	PLA	30/40 (wt.)	-	Compression molding	$44-53$	$7.3-8.3$	[67]
Retted (roving)	PP	30/40 (wt.)	-	Compression molding	29	$5-7.6$	[67]
Interwoven fabric	PP	40 (vol.)	-	Hot pressing	71.2	5.8	[68]
Woven fabric	Bio-based thermoset soybean oil	60 (wt.)	-	Hot press molding	$137-146$	$14-18$	[69]
Extremely short fiber	PE	30 (wt.)	-	extrusion molding	≈ 17	–	[70]

1.5 Unidirectional plant fiber composite

Flax fiber as described in Section 1.3.3 or plant fiber has varies kinds of forms as reinforcement for the utilization in the composite products. Amongst them, purely unidirectional fiber gain many attentions by some research teams. Bourmaud et al.[71][72] studied influence of processing temperature on mechanical performance of unidirectional flax fiber/polyamide 11 composites. They discern two regions, the mean values of flax fiber stiffness show results $E_1 = 39.0 \pm 13.3\, GPa$ in region one and $E_2 = 35.8 \pm 12.8\, GPa$ in region two, respectively, and regardless of the used matrix unidirectional composites exhibit a good correlation between the fiber volume fraction and their Young's modulus or tensile strength. By analysis of evolution of rheological properties, they found a drop of viscosity of

flax/PA11 mainly attributed to morphological changes of the fibers. Pucci et al.[73] investigated purely quasi unidirectional flax reinforcements after a thermal treatment at $220°C$ for $2h$ and without treatment. They found that treated flax fibers show a better dimensional stability and less hydrophilic/sensitive to liquid sorption, in addition the composite reinforced by treated purely flax fibers has a lower porosity content through the same liquid composite molding (LCM) process. By inducing laccase catalyzed cross-linking of feruloylated polysaccharides and/or by generating covalent bonds during lignin polymerization, Liu et al.[74] investigated mechanical properties of purely unidirectional hemp fiber reinforced composites and found a stiffness increase from $33.8\ GPa$ (without treatment) to $42.5\ GPa$ (with treatment). Mahjoub et al.[75] investigated the tensile properties of continuous unidirectional kenaf fiber reinforced epoxy polymer composites, which showed a tensile mechanical properties of strength and modulus of $731.6\ MPa$ and $40\ GPa$, respectively, with a maximum elongation 1.8%. Liu et al.[76] investigate the epoxy composites reinforced with unidirectional abaca fiber or bamboo fiber fabricated by using RTM. They found the transverse thermal conductivity of composites with plant fiber show a great dependence on the lumen structure but a little on crystal structure and chemical compounds. Ntenga et al.[77] studied elastic properties of purely unidirectional sisal fiber by making sisal epoxy composite with the vacuum infusion method and given out sisal fiber elastic constants of modulus. An obvious decrease of modulus with an increase in the loading angle was observed about unidirectional sisal fiber composite, where modulus is from $6.92\ GPa$ to $3.56\ GPa$ versus loading direction $0\ deg$ to $30\ deg$, respectively. Brahim et al.[78] found average Young's modulus and ultimate stress of $21.5\ GPa$ and $247\ MPa$, respectively, with an ultimate strain 1.96%, by analyzing purely unidirectional alfa unsaturated polyester composite fabricated by wet layup method.

1.6 Conclusion

In this chapter, characteristics of plant fiber composite – in particular flax fiber and their composites – were reviewed. Plant fiber has a lot of advantages considering the utilization in composites, e.g. they have relatively high specific ultimate stress and specific stiffness and come from renewable resource, and they are environmental protection compared with the artificial fibers such as carbon and glass fiber in the same application area. However plant fibers also have some disadvantages such as sensitivity to moisture. Flax fiber whose ultimate

stress of element fiber could be more than $1000\ MPa$ as a member of plant fiber family shows superiorly stronger mechanical properties than others, even better than magnesium alloy or aluminum alloy, and could be compared to conventional fiber in parts of specific tensile ultimate stress and specific Young's modulus and has been used in many aspects of consumer products with a prospective field of view. Flax fiber as reinforcement composes many resin systems. In this work, unidirectional flax fiber (Flaxtape^{TM}) will be used to make biocomposite with epoxy. Unidirectional flax fiber composite – which performs better tensile properties in the loading direction along fiber orientation than textile flax fiber composite – has been deeply studied in this work, mainly on the behavior of mechanical properties and sorption.

Chapter 2 MATERIALS AND METHODS

2.1 Material

2.1.1 Matrix

Epoxy resins belong to the class of thermosetting. The resin used in this study is a standard Huntsman industrial resin for laminating system with low viscosity and high flexibility. This warm-curing epoxy system is based on Araldite LY1564SP associated with a polyamine accelerator Hardener XB3486/XB3487. The reactivity may be easily adjusted to demands through the combination with one of both hardeners. The “long” pot life of XB3486/XB3487 facilitates the production of very large industrial parts. The optimal mix ratio recommended by the manufacturer is 100 parts by weight of Araldite LY1564SP and 34 parts by weight of accelerator hardener XB3486 or XB3487. In our unidirectional flax fiber reinforcement, we selected the Araldite LY1564SP and XB3486 forming system because of the longer gel time for matrix infiltrating fibers than the other system.

2.1.2 Reinforcement

The flax fiber reinforcement is originated from plant of flax stem, after harvesting, the fibers are treated according to the usual steps: retting, scutching, hackling and combing folding/drawing (see Fig. 1.6, Chapter 1). After all these usual steps (from retting to folding/drawing) flax ribbon is obtained. We can obtain flax fibers for unidirectional reinforcement. Indeed, with *n* times folding/drawing process (Fig. 2.1), the flax fibers are then subjected to a refining which involves stretching the technical fibers to form ribbons like in Fig. 2.3(a).

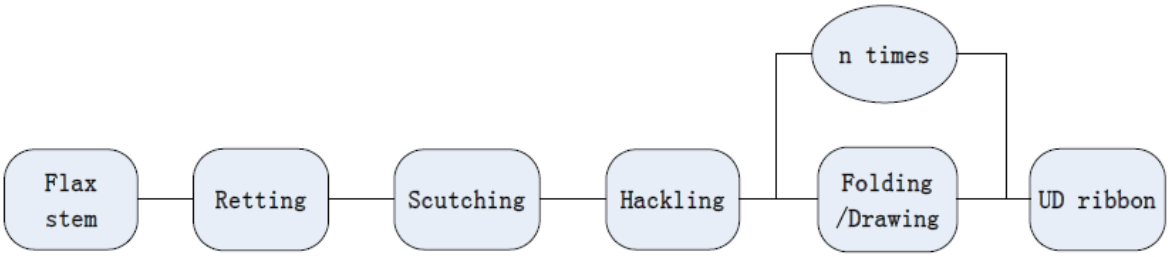

Fig. 2.1 Manufacturing process of unidirectional flax ribbon

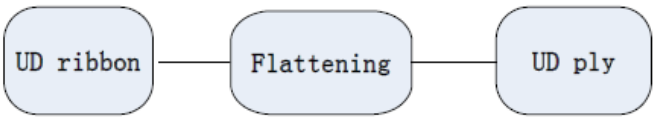

Fig. 2.2 Manufacturing process of unidirectional flax ply

After this stage, the product is ready for spinning for flax yarn reinforcement (Fig. 1.6, Chapter 1). The flax ribbons is usually processed in spinning stage in three types which are wet spinning, semi-wet spinning or dry spinning. However, the products of unidirectional flax plies are manufactured by one more step just after folding/drawing: a widing/flattening process (Fig. 2.2). In that step, several strands are connected in parallel, with the help of pulverized water, in order to make the natural pectins softer and to use them as glue between fibers. The output of this step is a purely unidirectional ply of flax, the Flaxtape™ (Fig. 2.3(b)). We consider this product of unidirectional flax fibers as non-pretreated reinforcement which not undergoes any particular flax selection by the manufacturer. The reinforcement used in this work weighs $70\ g\ m^{-2}$, $110\ g\ m^{-2}$ or $200\ g\ m^{-2}$ (values from manufacturer).

(a) Ribbon of flax (courtesy from Lineo) (b) Ply of unidirectional flax

Fig. 2.3 Unidirectional flax fiber reinforcement

Actually, the properties of plant fibers are affected by many factors such as variety, climate, harvest, maturity, retting degree, decortication, mechanical disintegration, fiber modification, textile and technical processes[79]. However, if the flax stems were obtained from a same source, as the technical flax fibers were obtained from the same manufacturer, it may be assumed that the fibers were grown under “similar environmental conditions”. In this way, growth environmental effect may be thought to be reduced, meanwhile with same technical processes.

2.1.3 Composite

Usually, number of the plies is selected according to the desired architecture. Ten plies at 0 deg are used to manufacture composite laminates required in that study. The process of the development of the composite plates is carried out by liquid composite mold with a hand layup method using contact forming consisting of a male mold and a female mold (also named hot platen press method) according to the detailed stages as follow (see also Fig. 2.4):

1. Cleaning and waxing the mold three times, ten minutes interval for each waxing.
2. Cutting selected plies with the same orientation and optimizing the size.
3. Preparing matrix according the required partition for composites, and leave them in the air with a short time for bubbles disappearing.
4. Putting adjusted metal block in the mold sideway which allows us to guide the upper and lower molds in the correct position and prevent resin leakage at these two sides.
5. Stacking the plies in the mold meanwhile utilizing prepared matrix by a brush which can make the matrix penetrates the reinforcement everywhere from the upper left to the bottom right to fabricate the composite ply by ply.
6. Placing and tightening the mold by preset method (preload by screws or metal) and preset pressure, and then leaving it at ambient temperature to promote the liquid matrix dispersion for two hours.
7. Curing in enclosure equipped with a thermostat in a certain temperature at atmospheric pressure for a certain period recommended by the manufacturer to allow the crosslinking of the resin.
8. Cooling to surroundings means that releasing the composite plate from the mold when the temperature returns to room temperature.
9. Polishing the edges of plate each time after releasing composite from the mold with abrasive paper 200#.

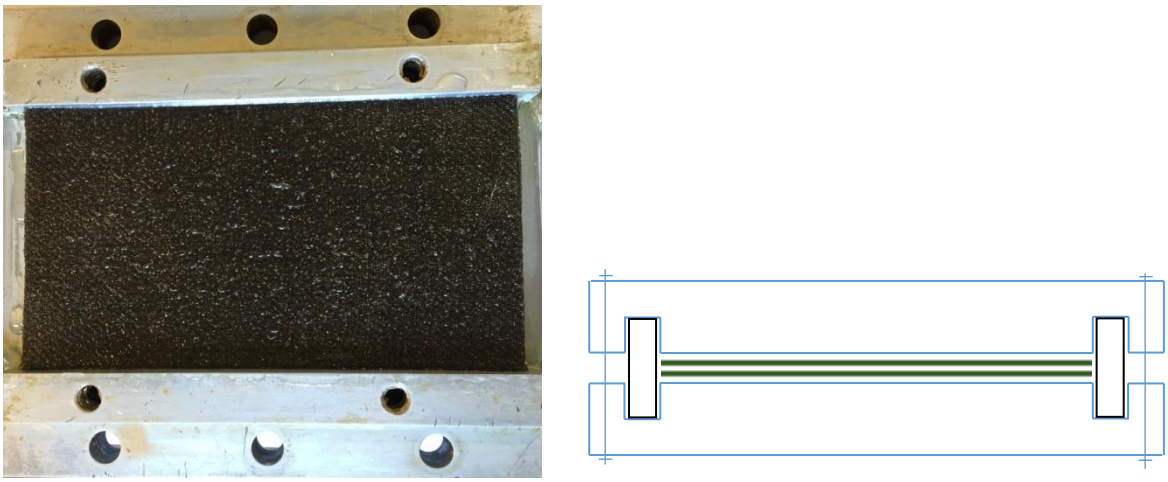

(a) Curing mold with (step 5) (b) Schematic diagram of stacking (step 7)

Fig. 2.4 Curing mold used in flax fiber composite

The curing process is in conformity with one of the manufacturer's instructions (8 hours at $80°C$). We chose $80°C$ as curing temperature to reduce both the thermal impact on fiber mechanical properties[80] and the effect of expansion coefficient of aluminum mold on surface conditions of composite. With the specific process development above, flax composite laminates with a length and width size of $200\ mm \times 110\ mm$ or $330\ mm \times 250\ mm$ have been manufactured (about ten laminates for each mold for the present work). Our UD flax composite has been manufactured with an excellent surface condition. An evaluation of the dimensional stability is summarized in Fig. 2.5 for six small laminates of textile composite (that I made for a study which is not presented in this document). Note that the size fluctuation is very low.

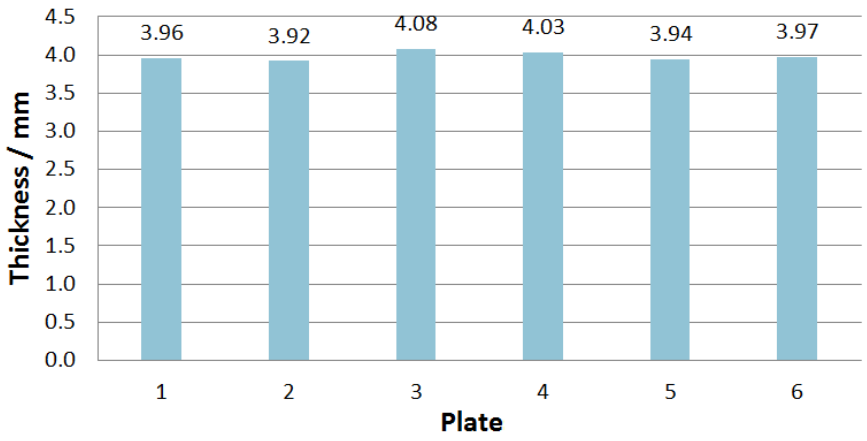

Fig. 2.5 Repeatability of laminates thickness with hot platen process (S300)

2.2 Specimen preparation and experiments

2.2.1 Samples for microstructure observation

Table 2.1 Polish process parameters for microscope samples

Polish parameter					Fine grinding
Abrasive paper	#220	#1200	#2400	#4000	MD-Nap (velvet)
Force (kN)	20	20	15	15	18
Speed (rev min^{-1})	200	200	200	200	200
Time (min)	0.8	1	2	2	5
Lubricant	DP-Blue	DP-Blue	DP-Blue	DP-Blue	DP-Brown

Observations of specimen microstructure carry on specimens cut in the initial blank plates. They are made for optical microscopy (OM) or scanning electron microscopy (SEM). To do this, samples are optionally polished for OM and polished and coated with a thin layer of gold when used in the SEM observation. The sample making process for optical microscopy is that after fine cutting, the samples are cut into small piece of $20\ mm$ in length with their thickness and then embedded in the resin, consisting of acrylic shaped in a cylindrical mold (sample holder). Once the resin are cured in the sample holder, the whole can be promoted into the next stage which is polished on grinding sheets (Struers MD-System) for decreasing particle size and gaining good surface status.

The apparatus used in this operation is a polishing machine Struers (Fig. 2.6(a)). Several steps are carried out on the initial sample with a special lubricant developed by the same company. Finishing is carried out with a sheet coated with a disk paste up to soft velvet and lubricated with alcohol. Detailed polish guidance exploited is given in Table 2.1.

(a) Polishing machine

(b) Coating machine

Fig. 2.6 Systems used for the observation specimen preparation

After the polish stages, OM observation can be done. SEM sample can be prepared based on the same making process. But surface metallization is required in our laboratory since the non-conductive nature of the composite makes it necessary to perform a gold deposit on the samples for observation. For this, the sample is placed in a vacuum chamber (Cressington Coater 208, see Fig. 2.6(b)) to receive the gold atoms. Then the gas metal (gold) is projected onto the substrate. A thin and very pure layer is thus deposited on the sample. The metallization of time and amperage are set at 120 sec and 40 mA respectively to obtain a layer of approximately 20 nm.

2.2.2 Methods for observations

Direct observation of flax ply gives the possibility to analyze the fiber organization (Fig. 2.7). For this observation, a USB CCD camera was used (Fig. 2.8(a)) with an installed software system named UEye. The UD flax ply reinforcements must be placed on an illuminating work plat. The acquisition of image of the reinforcement is done with a Melles Griot telecentric imaging optics connected to the camera and placed at a fixed distance – which means in the field of view of the object – with appropriate light illumination. The output numeric images (Fig. 2.7) made with the software system UEye consist of 1280 $pixels$ × 1024 $pixels$ corresponding to $25mm \times 20mm$ in the object plane.

Fig. 2.7 Typical unidirectional ply of flax (without matrix). Some of the fibers (elementary fibers or bundle of fibers) are not aligned in the longitudinal direction (UD70).

For the optical microscopy observations of cross sections, a Nikon ECLIPSE E600 (Fig. 2.8(b)) optical microscope were utilized, in which lens magnification can be selected as $5\times$, $10\times$, $20\times$, $50\times$ and $100\times$. This device is equipped with a CCD camera and homemade software is used in the microscopy system to process the images of optical microscopy samples. On the other hand, scanning electron microscopy has been done on Princeton Gamma-Tech Cambridge electron microscope (Fig. 2.8(c)). For the observation by scanning electron microscopy, samples are placed in specimen holder. Vacuum pressure was about $10^{-5}Pa$, magnification from $50\times$ to $800\times$ were used.

(a) CCD Camera (b) Optical microscope (c) Scanning electron microscope

Fig. 2.8 Observation tools

2.2.3 Specimen for tensile tests

The cuttings of test pieces are made by different processes determined by destination convenience and size and shape of laminated plates. For the rectangle shape cut by diamond cutting system (Fig. 2.9(a)), cutting steps include the following main contents:

- Using a diamond disk or mini diamond disk cooled with water.
- The high-speed machining center (HSC) is air-cooled.
- The size correction instrument with calibration line is fixed on the cutting platform.

The specimens are dried after cutting and then we remove all dust from these surfaces and clean them with acetone. If required, rub with abrasive paper or blast with suitable sand all the surfaces to which adhesive will not be applied. It is recommended that a film adhesive with a thin carrier be used. When necessary, tabs polished with shot blasting or sand paper are stuck on the test piece specimens under press in compliance with the ISO 527-5:2009 standards to prevent failure of the material in jaws[81].

(a) Diamond cutting system

(b) Laser cutting system

Fig. 2.9 Cutting tools

In order to avoid the use of water, and for specimens with different curvature radius in width size, we use laser machine (available in our laboratory since January 2016) to cut the composite laminated plates. The machine used to cut specimens is named Trotec Speedy 400 laser machine (Fig. 2.9(b)) with a CO_2 laser type. For our UD flax composite, the parameters are selected in accordance with the principle of reducing the burning range of the specimens as far as possible. And the cutting sequence should try to avoid stress concentration. Thus, we utilized the energy with a value of 80 W and cutting speed of 1.5 $mm\ s^{-1}$ to perform the operation through practice. The main parameters for tensile tests are given in Table 2.2.

Table 2.2 Parameters of unidirectional flax fiber composite plates for tensile tests

Plate	Product type	Flax density ($g\ m^{-2}$)	Length (mm)	Width (mm)	Thickness (mm)	Density ($kg\ m^{-3}$)	Nb of samples
UD70-6	70	78	320.7	235.6	1.13	1235	11
UD200-1	200	181	317.8	245.7	1.46	1204	15
UD110-1	110	125	324.0	249.0	1.70	1191	15
UD110-2	110	125	313.5	239.5	1.57	1225	20

For the aim of simplifying the making process of tensile test specimens, several types of composite specimens – which are UD flax composites and twill 2×2 flax fabric reinforced composites – have been manufactured with the shapes as showed as below in Fig. 2.10.

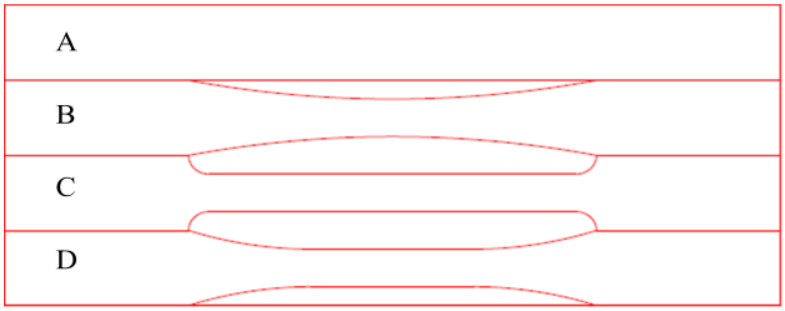

Fig. 2.10 Design of different specimen types for tensile tests (basic size $20\ mm \times 200\ mm$)

Therefore, four different shapes of test pieces consisting of textile flax fabric reinforcement were designed. Four samples for each shape have been tested (four plates, four specimens by plate), and then the influence of the shape on the tensile mechanical properties was analyzed. All the shapes on Fig. 2.10 were directly cut by the laser cutting system. After cutting, aluminum tabs were glued as usual to the end of the shape specimen *A*. For the monotonic tensile test, the extensometer is used on the specimens of shape *A*, *B* and *D*. However due to the shape used for specimen *B*, there is no region where strain could be considered as uniform, hence strain gauges have to be used in that case. The experiment procedures are carried out according the standard "Plastics: determination of tensile properties process", ISO 527-5:2009[81] which is suitable for composites with either thermoplastic or thermosetting matrices, including preimpregnated materials. The reinforcements covered include carbon fibers, glass fibers, aramid fibers and other similar fibers, in which the geometries covered

include unidirectional (*i.e.* completely aligned) fibers and rovings, and unidirectional fabrics and tapes. Effect of shape with textile composite at strain rate $10^{-4}s^{-1}$ and normal conditions are given in Fig. 2.11. Firstly, the effect of the plate is visible in Fig. 2.11(a). We do not note any influence of the plate, meaning that the repeatability of the tests is enough for our analysis. The effect of the different shapes is described in Fig. 2.11(b) and Fig. 2.11(c). We can see shape *A* (with aluminum tabs) and shape *D* (without any tab) are a little better in both ultimate stress and ultimate strain.

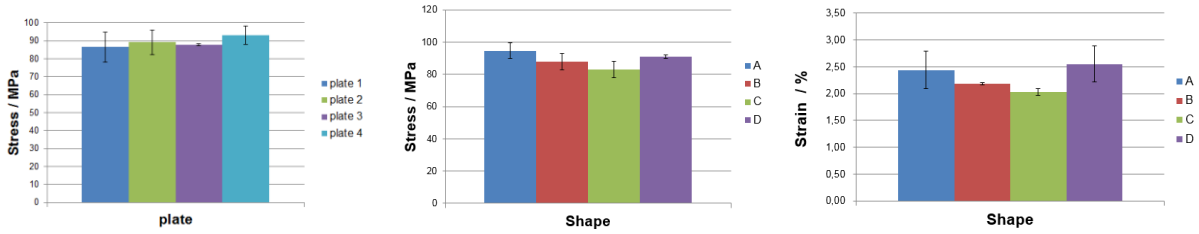

(a) Repeatability (b) Effect on ultimate stress (c) Effect on ultimate strain

Fig. 2.11 Effect of the shape of specimens on tensile mechanical properties (S300)

It is worth to note that the sample preparation for specimen shape *A* is really less convenient than the others. Indeed, on the one hand tabs need to be polished with shot blasting or sand paper before to be glued on each specimen, and on the other hand the use of glue is a drawback for high temperature tensile test. About the rupture position, it will always more easily break in the stress concentration position. For the shape *A*, the rupture happened in the place where is near the inside edges of metal tabs accounting for a large proportion. For the shape *B*, the rupture place is in the center of the sample near the strain gauge. For the shape *C*, it happens in the changing dimension of width or near the radium. In the shape *D*, the rupture is usually near the middle area of the test pieces near the extensometer. As a conclusion, combining the specimen making procedures, we determined shape D is a favorable way for us to making tensile test samples in the following UD reinforcement composite work.

Tensile tests of UD reinforcement composite have been tested using specimen with shape *D*. Unfortunately, the rupture is more likely to occur in fillet point due to longitudinal shear stresses between fibers. At this time, rectangular flax/epoxy tabs laminated with an orientation of $[-45°, 45°]$ are utilized to protect the end of *A*-shape specimens for the research work about mechanical properties of unidirectional composite (Chapter 3). And no tab are used for the behavior analysis of unidirectional composite (Chapter 4).

2.2.4 Methods for tensile tests

Tensile test is the main technique used to study the mechanical properties of our unidirectional composites. It allows determining the Young's modulus, yield stress, the stress and strain at rupture (Chapter 3), and the global mechanical behavior (Chapter 4) of the unidirectional flax composite. The mechanical test machine used here is a universal machine Instron (model 8800 Instron servo-hydraulic) with a cell force of $100\,kN$ and mechanical self-tightening jaw, allowing a good test behavior of the specimens (Fig. 2.12).

Fig. 2.12 Instron servo-hydraulic machine

The tests were conducted at selected temperatures and strain rates, depending to the specific aims. The test specimen is fixed by the two jaws. The experiment is carried out with a moving target in a certain rate, for instance $2\,mm/min$, or higher or lower speed in accordance with *ASTMD3039/D3039M* (Standard Test Method for Tensile Properties of Polymer Matrix Composite Materials). The force measurement is carried out in real time via a force transducer. The micro-measurements of deformations are carried out by using Vishay strain gauges or via an Instron extensometer, as showed in Fig. 2.13.

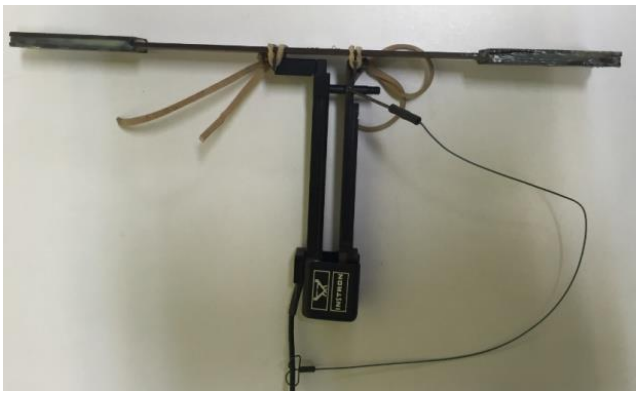

(a) Extensometer

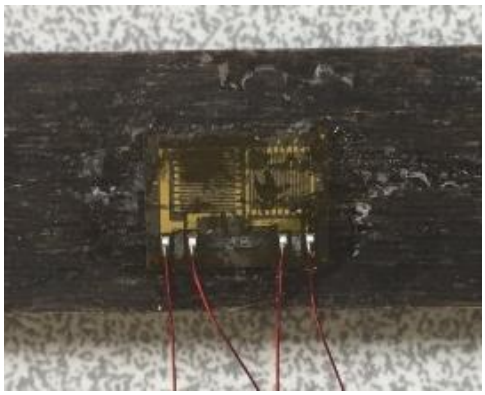

(b) Strain gauge on tensile test specimen

Fig. 2.13 Measurement deformation gauges for tensile tests

In the former case, the deformation sampling is synchronized to loading sampling by Vishay Controller and measured by the gauge resistivity. The output voltage is numerically transformed into deformation by the user. In the latter case – according to the small strain theory – the deformation is calculated from the elongation measurements according to the following relationship:

$$\varepsilon = \frac{l - l_0}{l_0} \tag{2.1}$$

where ε is the strain, $l$is the instantaneous length and l_0 is the initial gauge length ($50\ mm$ or $25\ mm$, here).

Knowing the tensile force and the cross section of the test specimen, the stress is determined according to the following equation:

$$\sigma = \frac{F}{A_0} \tag{2.2}$$

where F and A_0 are respectively the load and the initial cross section of the test specimen.

Young's modulus E is measured from the initial slope of the linear elastic portion of the tensile stress-strain curve. Poisson ratio ν in our UD flax composite is measured from the initial slope of the linear part of the transversal strain versus longitudinal strain curve.

Another case where we used the Instron tensile machine was to applied creep test in tensile configuration. Creep test involves a specimen under a constant load maintained at a constant

temperature. The creep test is used to observe the slow non-instantaneous deformation of a material mechanical properties occurred in the long-term constant temperature and constant stress. To the aim to understand the creep behavior of UD flax composite and investigate the mechanical behavior, different constant stresses were performed with a duration time of 30 min (Chapter 4).

2.2.5 Specimens for sorption tests

Sorption tests have been conducted here as a tool to analyze the quality of the composite (Chapter 5). Taking into account the mass and the dimensions of our laminated plates, the component ratios of UD composite specimens are listed in the Table 2.3. Silicon has been used to seal each edge of all the specimens, which designed to limit the effects of edges in the sorption test. It is thus considered that the distribution of water is one-way through the thickness of the specimen, and that the diffusion directly through the other two directions (length & width) is negligible. The choice of specimen size was 160 mm length and 110 mm width.

Table 2.3 Parameters of unidirectional flax fiber composite specimens for sorption (UD110-3)

	Specimen 1	Specimen 2	Specimen 3	Specimen 4
Length (mm)	159.5	160.5	159.5	159.5
Width (mm)	99	99.5	99	99
Thickness (mm)	1.52	1.50	1.55	1.54
Reinforcement ratio (%)	54	55	54	54
Porosity ratio (%)	11	10	9	10
Matrix ratio (%)	35	35	37	36

2.3 Preliminary analysis

2.3.1 Curing of flax/epoxy composite

Study of manufacturing parameters for characterizing properties of polymeric composite can be conducted by a number of methods. Among these, the follow up of the glass transition temperature T_g – which is defined as the transition between the entropy and the elastic state energy at its largest difference – can be an effective method of characterization of physicochemical changes induced by plasticization chain scission, evolution of the free

volume, etc. All the polymeric components of plant fiber composites exhibit a glass transition temperature above which the properties of the material could degrade significantly. The evolution of the glass transition temperature of the flax composite is an indicator which is important both as a measure of the degree of reticulation and to establish a maximal temperature for composite use, which defines the material operational limit. When the glass transition temperature of the composite is exceeded, certain mechanical properties may be compromised severely. Normally, it is necessary that the application temperature for a thermoset composite is below T_g in order to assure that the mechanical stiffness and creep resistance of the material is satisfactory. Here, the glass transition temperature was determined by a commercial dynamic analyzer apparatus called Kinetech on which T_g is deduced from torsion stiffness versus temperature curve. The operating of Kinetech is based on the principle as the automated ‘‘Torsion Pendulum’’ instrument shown in Fig. 2.14.

Fig. 2.14 Kinetech apparatus for glass transition measurement

The principle of measurement method involves applying a torsion loading with some time relaxations and measuring the instantaneous and the relaxed torques.

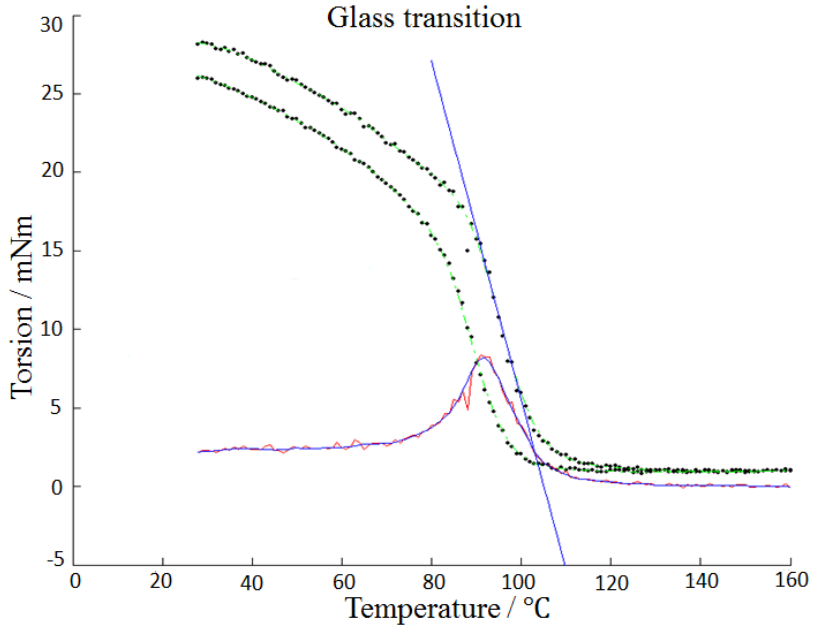

Fig. 2.15 Glass transition measurement of flax fiber composite, the plain curves are the fit of instantaneous torque, relaxed torque, and difference between them

This apparatus is widely used in laboratories and industries due to its relatively low cost and handiness. Generalizations on the cure and properties of thermosetting polymers, which have stemmed from development and application of the torsional braid analysis (TBA) technique, have been formulated in terms of cure relationships[82][83]. In our UD flax composite measurements, relations existing between T_g and the evolution of global properties of composites are expressed by the following parameters: temperature were set as $2°C\ min^{-1}$ speed growth until $160°C$ from room temperature, meanwhile the required torque is measured instantaneously and after two seconds of relaxation. T_g is determined on a sample of $48\ mm \times 8\ mm$ by length and width, respectively, with a small thicknesses (typically $1\ mm$) for different samples. The glass transition temperature can be measured at the maximum difference between the instantaneous and relaxed torques or at the inflection point of the instantaneous torque curves (Fig. 2.15). Herein, the first method is used as identity comparison results.

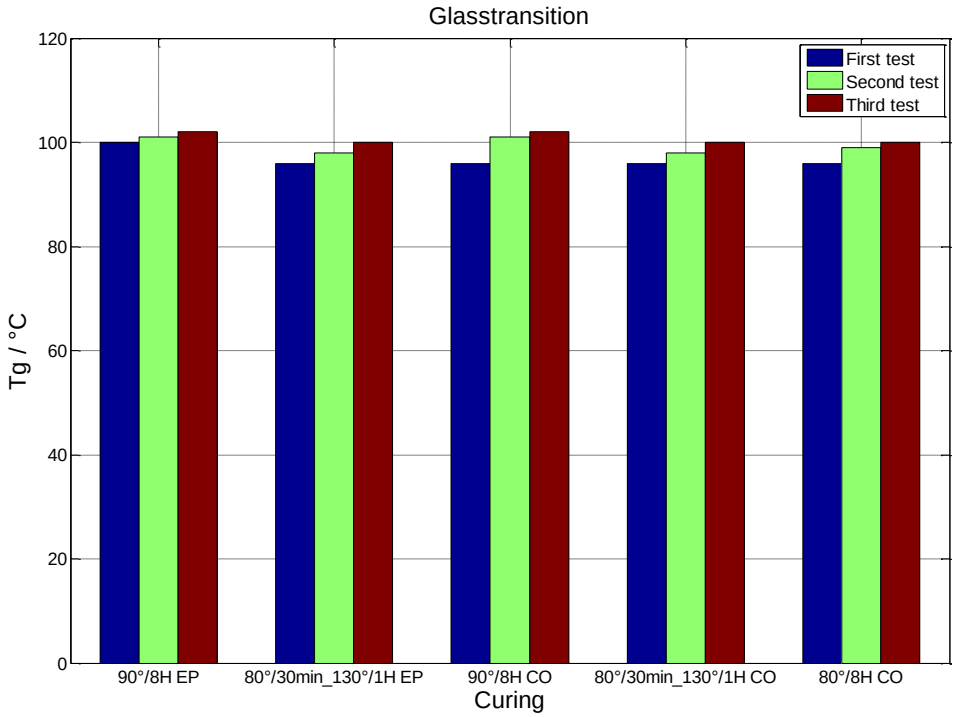

Fig. 2.16 Affection of curing process on T_g of pure resin, EP, and textile composite, CO (S300), three measurements for each specimen

Through a large number of test analysis, one conclusion is there is no visible difference amongst the curing process: $8h/80°C$, $0.5h/80°C + 1h/130°C$ and $8h/90°C$, whether it is epoxy resin only (EP) or flax textile reinforced epoxy composite (CO) with same reinforcement volume fraction, about 30% (Fig. 2.16). T_g ranged from 95 $°C$ to $100°C$. But the evolution of the T_g value after three successive measurements for each specimen shows that a post–curing is needed. Finally, the curing process which has been selected for unidirectional composite was $8h/80°C$ for first curing then $8h/80°C$ for post-curing.

The glass transition temperature of our unidirectional flax cured with epoxy resin 1564SP and hardener XB3486 as composite system is listed in Table 2.4. No visible relations have been found between the surface density of unidirectional flax plies and glass transition temperature of their composites. But T_g seems to be correlated to the ratios of different components of composite (Fig. 2.17). It is possibly due to the fact that not only the matrix but also flax fibers contain polymeric maters. Then the glass transition temperature of unidirectional composite appears as a non–linear response of a complex media.

Table 2.4 Glass transition temperature of unidirectional flax fiber composite

Plate	Flax density ($g\ m^{-2}$)	Fiber ratio (%)	Matrix ratio (%)	Porosity ratio (%)	T_g ($°C$)
UD70-1	78	18	79	3	87
UD70-2	78	16	81	3	85
UD70-3	78	18	76	6	82
UD70-4	78	18	80	2	81
UD70-5	78	15	81	4	84
UD110-1	125	48	40	12	88
UD110-2	125	47	44	9	96
UD110-3	125	54	31	15	97
UD200-1	181	49	40	11	89

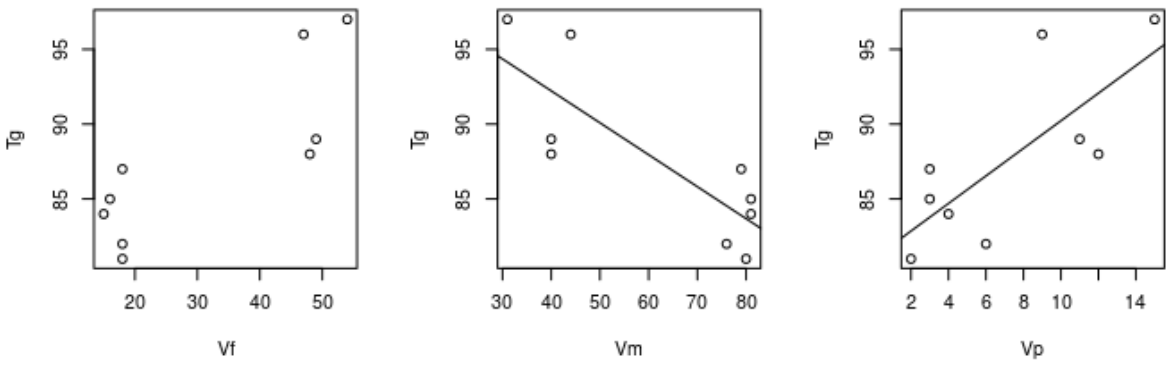

Fig. 2.17 Effect of composite component ratio and the glass transition temperature

2.3.2 Microstructure observation

Fig. 2.18 shows transverse sections of unidirectional flax composite observed by optical microscopy and scanning electron microscopy. In Fig. 2.18(a) we distinguish the flax fibers are mainly organized in bundle form inside composite. It is due to the mechanical process used to make the plies (see Fig. 2.1 and Fig. 2.2), using mainly technical fibers. Several flax fiber bundles are coated with resin, but problems of interface (porosities all along some bundles of fibers) can be identified. In Fig. 2.18(b) elementary fiber structure is more clearly visible. The transverse section of the flax fiber looks like pentagonal or hexagonal as usually observed.

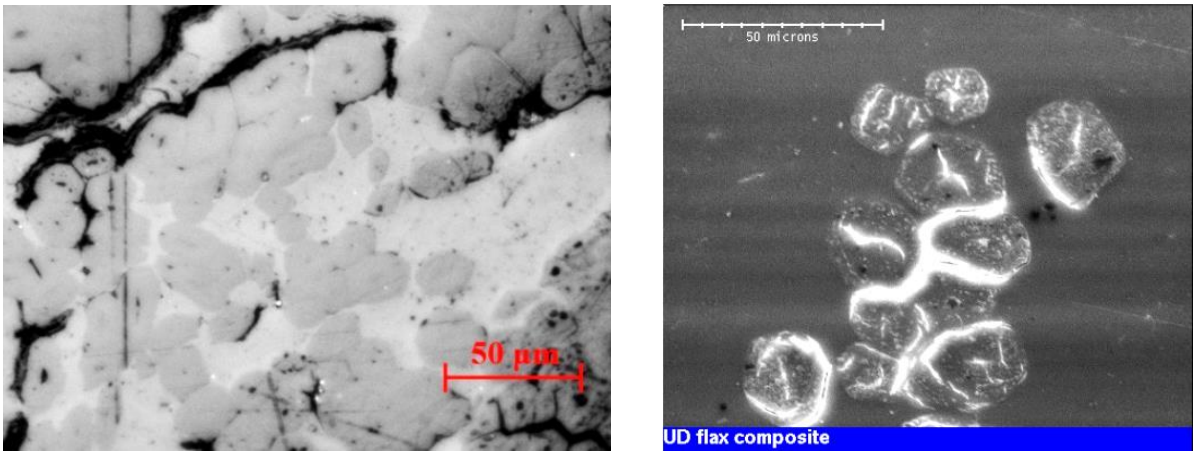

(a) Optical microscopy (b) Scanning electron microscopy

Fig. 2.18 Microstructure observations of unidirectional flax fiber composite

The transverse dimension of flax fibers could lie in the range of $10-30\ \mu m$ and hollow structure called the lumen in the center of fiber is compacted. Some of the elementary fibers (but not a lot) are separated from initial bundle in the unidirectional composite. We conclude that the used flax reinforcement is not only constituted by flax bundle but also by a low certain proportion of elementary flax fibers.

2.3.3 Ratio of different composite components

Porosity, which is defined as air-filled cavities inside an otherwise continuous material, is a most often unavoidable component in all composite materials, caused by the mixing and consolidation of two discrete material components. The fiber and matrix components of long fiber composites are primarily concerned in studies of most composites whether artificial or biobased. However, existence of the porosity as third component should not be ignored, especially for plant fiber reinforced polymer. Plant fibers are relatively more difficult to impregnate by resin than artificial fibers such as glass or carbon fiber[46]. In addition, the presence of porosity in the composite is known to dramatically reduce the mechanical and sorption properties of these materials[31][84][85]. For this, the porosity ratio V_p cannot be neglected and should be taken into account when analyzing the mechanical performances of the plant fiber composites.

For fraction measurement, input dimension parameters of experiment specimens are usually gained from the measurements (or the manufacturer data). We conducted a measurement by a direct method. The obtained data: length, width, thickness, mass of the flax plies, mass of the

composite plates, fiber density, matrix density. Reinforcement, matrix and porosity fractions have been allowed to be calculated combining basic input parameters as the method as showed below.

Volume ratio of reinforcement:

$$V_f = \frac{v_f}{v_c} \tag{2.3}$$

$$= \frac{m_f/\rho_f}{v_c} \tag{2.4}$$

$$= \frac{n_l \rho_l^s \, L \, W/\rho_f}{L \, W \, h} \tag{2.5}$$

$$= \frac{n_l \rho_l^s}{h \, \rho_f}. \tag{2.6}$$

Volume ratio of matrix:

$$V_m = \frac{v_m}{v_c} \tag{2.7}$$

$$= \frac{m_m/\rho_m}{v_c} \tag{2.8}$$

$$= \frac{(m_c - m_f)/\rho_m}{L \, W \, h} \tag{2.9}$$

$$= \frac{m_c - m_f}{\rho_m \, L \, W \, h}. \tag{2.10}$$

Volume ratio of porosity:

$$V_p = 1 - V_f - V_m \tag{2.11}$$

$$= 1 - \frac{m_c}{\rho_m \, L \, W \, h} + \frac{n_l \rho_l^s}{h} \left(\frac{1}{\rho_m} + \frac{1}{\rho_f} \right). \tag{2.12}$$

In these relations, the basic input parameters are v for volume, m for mass, L, W and h for length, width and thickness, respectively, ρ^s and ρ for surface and volume density, respectively, and n for the ply numbering. The subscripts$f$, m, p, and $l$stand for fiber, matrix, porosity, and layer, respectively.

The propagation of uncertainty method delimits the uncertainty on V_f, V_m, and V_p values, utilizing the accuracy of apparatuses. The current methods offered here make us suitable and

easy to use common technique to analyze the ratios of reinforcement, matrix and porosity. In this work, special care has been taken in the measurement of the volume v_c of plates developed by thermo-compression. For better accuracy, the volume is calculated by a fitting solution in which the procedure is to recalculate the thickness evolution of the composite material, upper surface being not absolutely parallel to bottom surface in the one hand, and slightly curved in both directions in the other hand (see Fig. 2.19). The plate thickness was reconstructed through polynomial fitting method in two directions of length and width with two-free degrees. More than twenty fitting points were used at the thickness directions each time. Finally, the reconstructed composite volume was used for component ratio calculation based on relations (2.5), (2.9) and (2.11). There is a small difference in component fraction results between the thickness fitting solution and the measurement of mean thickness.

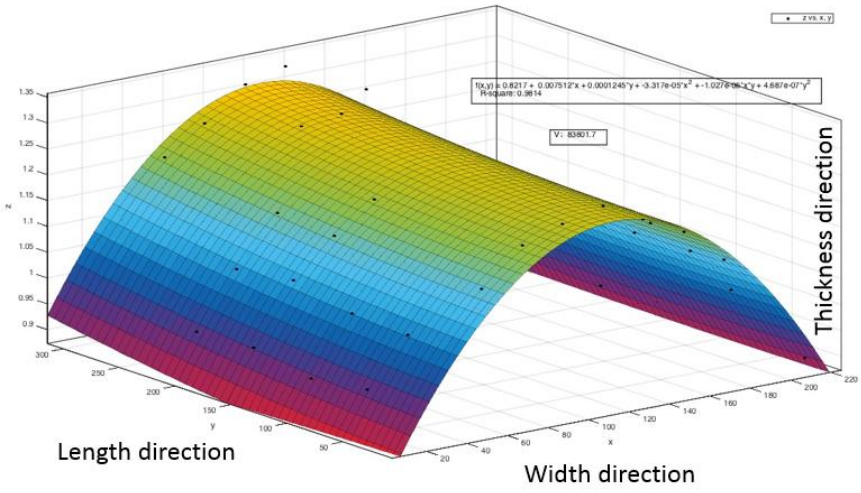

Fig. 2.19 Typical reconstruction of composite thickness evolution

At last in our unidirectional flax composite, the mean final mass density of composite ρ_c is close to 1.25 and the mean final volume percentage of porosity is close to 10% when the reinforcement ratio is 55% (see Table 2.3). The fulfillment of component percentage calculation is consistent with description above by measuring the dimensions and the mass of composite firstly while knowing the density of matrix and reinforcement. The fiber density (lumen cut, no humidity) deemed to be $1540\ kg\ m^{-3}$ [47]. The surface density of reinforcement is measured for each product (see Table 2.2 and Table 2.4). The matrix density measured in the laboratory is $1140\ kg\ m^{-3}$.

2.4 Conclusion

In this chapter, various efforts were carried out to improve the preparation of specimens and characterize basic properties of flax fiber composite. First of all, considering the stabilities and features of the UD composite products, flax fiber composite has been made by hot platen method with detailed steps to prevent non necessary mistakes in the preparation progress. UD flax composite was made with good surface condition. Specimens for microstructure observation of OM and SEM were also prepared by optimized polishing process combining extensive testing offered practical polish process parameters. As a result, microstructure of UD flax composite was found. What is important to us is the tensile specimens should have a good test condition. Based on this goal, laser cutting system was introduced into the tensile specimen preparation and four different shapes taking into account facilitation and practicality have been developed. For better performing tensile tests, stain gage and extensometer are often used together. T_g as an indicator for utilization of our UD flax composite has been investigated in detail. Due to the porosity is always exist in the composite material, a global measurement of different component ratios in the composite is developed considering that the plane in the upper part is not absolutely parallel to the opposite part.

Chapter 3 EFFECTIVE MECHANICAL PROPERTIES OF REINFORCEMENT

As said in Chapter 2, the reinforcement used in that study is a purely unidirectional ply of flax reinforcement. Nevertheless, the fibers cannot be considered as perfectly aligned in one direction, as shown in Fig. 3.1 an amount of fibers appear as “disoriented”. This word “disorientation” used in that study refers to that phenomenon. As it is well known, the orientation of fiber inside the composite has significant affection on the performance of mechanical properties[86]. Effort was made to modify previous composite theory[49] to take into account the complex orientation of our reinforcement. The aim was to evaluate the effective mechanical properties of flax fiber in the composite laminates. Therefore, this chapter will start by a presentation of a suitable method to analyze the orientation of dry ply, with a nominal surface density 70 g/m^2, 110 g/m^2 and 200 g/m^2. Then, the mathematical formulation of our theory is presented. Hence we will discuss the results we get.

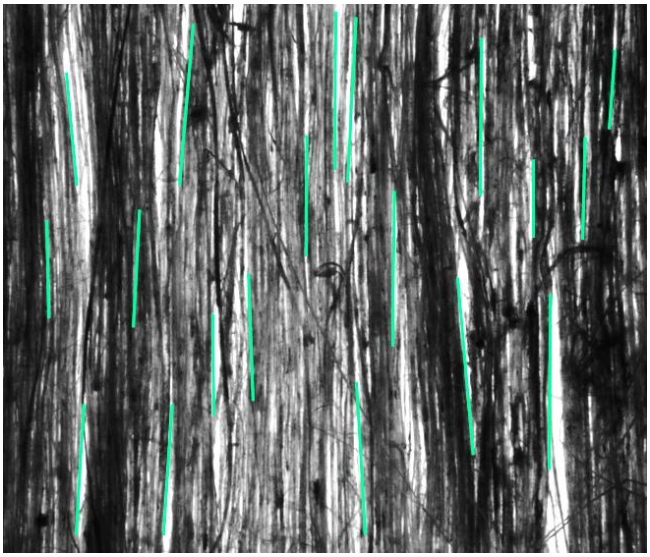

Fig. 3.1 Example of fiber disorientation into a flax ply (UD70)

3.1 Analyses of the orientation using structure tensor

3.1.1 Structure tensor theory

Structure tensors are matrix representations of partial derivatives. In the field of image processing and computer vision, they are typically used to represent gradients, edges or similar information. Structure tensors also provide a more powerful description of local

patterns and allow obtaining local orientation[87][88]. For instance, Nouar et al. presents a direct method using computed tomography to determine finite element models based on the real geometry of the reinforcement[88]. They used a structure tensors method on X-ray tomography image analysis to separate warp and weft yarns of a 2×2 carbon twill weave according their orientation. The orientations are computed thanks to the calculation of the structure tensor[87]. This tensor is defined for each pixel as a 2×2 symmetric positive matrix J, where f_x and f_y are the partial spatial derivatives of the image $f(x, y)$, along the principal directions x and y, respectively. Since the tensor is symmetric we have only three independent components in the matrix J, written here as in operator notation:

$$J = \begin{bmatrix} \langle f_x, f_x \rangle_w & \langle f_x, f_y \rangle_w \\ \langle f_x, f_y \rangle_w & \langle f_y, f_y \rangle_w \end{bmatrix}. \tag{3.1}$$

Otherwise, the weighted inner product between two arbitrary images g and h is defined as:

$$\langle g, h \rangle_w = \iint_{R^2} w(x, y) g(x, y) h(x, y) dx dy. \tag{3.2}$$

The window function $w(x, y)$ has important influence on the orientation calculation and determines the spatial resolution of the representation specifying the region of interest (ROI)[88]. The local predominant orientation corresponds to the direction of the largest eigenvector of the structure tensor. In the two-dimensional space, we can readily solve the eigenvalue problem that every symmetric matrix reduces to a diagonal matrix by a suitable coordinate transformation. However, the solution is not reached in the standard way by solving the polynomial characteristic to determine the eigenvalues. It turns out that it is easier to rotate the inertia tensor to the principal axes coordinate system. Then the rotation angle θ in the considered region corresponds to the angle of local orientation:

$$\begin{bmatrix} J_1 & 0 \\ 0 & J_2 \end{bmatrix} = \begin{bmatrix} \cos\theta & \sin\theta \\ -\sin\theta & \cos\theta \end{bmatrix} \begin{bmatrix} \langle f_x, f_x \rangle_w & \langle f_x, f_y \rangle_w \\ \langle f_x, f_y \rangle_w & \langle f_y, f_y \rangle_w \end{bmatrix} \begin{bmatrix} \cos\theta & -\sin\theta \\ -\sin\theta & \cos\theta \end{bmatrix}. \tag{3.3}$$

Subtraction of the diagonal elements results in:

$$J_1 - J_2 = \left(\langle f_x, f_x \rangle_w + \langle f_y, f_y \rangle_w \right) \cos 2\theta + 2 \langle f_x, f_y \rangle_w \sin 2\theta \tag{3.4}$$

while from the off-diagonal element:

$$\frac{1}{2}\left(\langle f_y, f_y\rangle_w - \langle f_x, f_x\rangle_w\right)\sin 2\theta + \langle f_x, f_y\rangle_w \cos 2\theta = 0. \tag{3.5}$$

The orientation angle is thus given by:

$$\theta = \frac{1}{2}\arctan\left(2\frac{\langle f_x, f_y\rangle_w}{\langle f_x, f_x\rangle_w - \langle f_y, f_y\rangle_w}\right). \tag{3.6}$$

These orientation measures are arrays termed angular nearest-neighbor gray-tone spatial-dependence matrices. For instance, we consider a resolution cell (ROI), to have at least eight nearest-neighbor resolution pixels, at window size value 3 for each pixel itself standing for an orientation needed to be calculated with image as in Fig. 3.2.

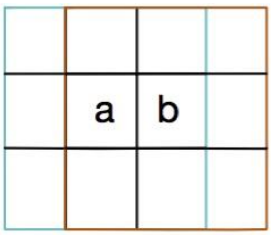

Fig. 3.2 “a” and “b” are calculated by nearest eight neighbors at window size three

As already said, the windows function is a key parameter to determine the final calculation results. According Fig. 3.2, the window was set as a square with a length of several pixels.

3.1.2 Analyses of orientation of dry flax ply

First, the method describe in the above section was used to obtain the orientation of an image created numerically. The picture is composed by horizontal lines. Each line has a one unique grey-level. The grey-level of each line is obtained with a one-dimensional sine function with a pulsation of 0.01. Then, the whole image is rotated by a known angle. Fig. 3.3 presents an image where the rotation angle was 160 deg. Using a square window of size 21 $pixels$, an average orientation value of 159.89 deg was obtained. This method is hence suitable to obtain local orientation of a pattern in an image with correct accuracy.

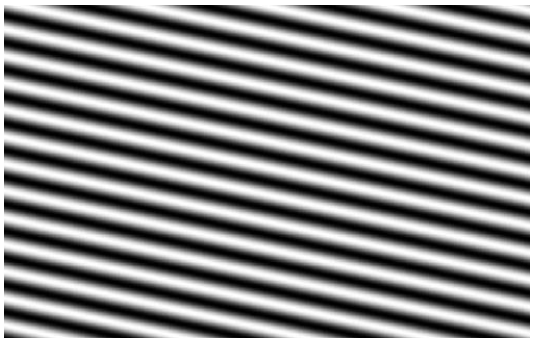

Fig. 3.3 Picture obtained with a rotated sine signal used to determine the calculation accuracy

However, the analysis of UD flax plies is much more complex (see Fig. 3.1) and the effect of the square window size need to be evaluated. Image of flax reinforcement get using method described in Section 2.2.2 could be analyzing using structure tensor, and an orientation maps could be plotted. These maps represent the local orientation of each pixel. Window sizes from 3 to 201 $pixels$ with two-pixel intervals have been designed to analyze the orientations of flax reinforcement. As an example, Fig. 3.4 shows two results obtained with the same image and two different sizes.

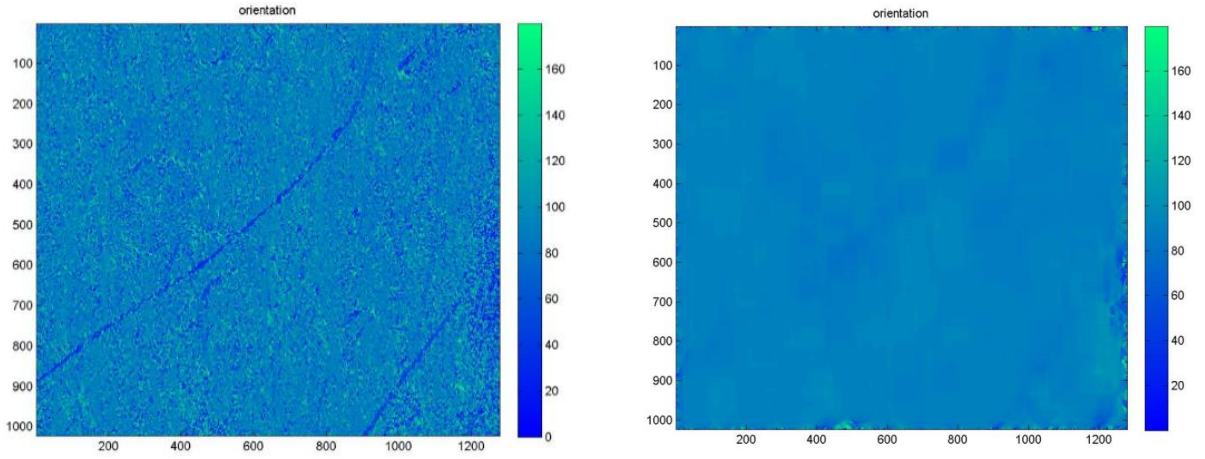

(a) ROI of 3 $pixels$ (b) ROI of 91 $pixels$

Fig. 3.4 Orientation map obtained with two different sizes of window

Fig. 3.4(a) shows a noisy orientation maps but as the size of the ROI increase, as for Fig. 3.4(b), the orientation is averaged and all the pixels have an average orientation (here around 90 deg). This idea is confirmed by Fig. 3.5, where the maximal and the minimal angles found in the maps was plotted versus the ROI size. These results confirmed that if the ROI size is too large, some information about the local orientation of fiber inside flax ply will be lost.

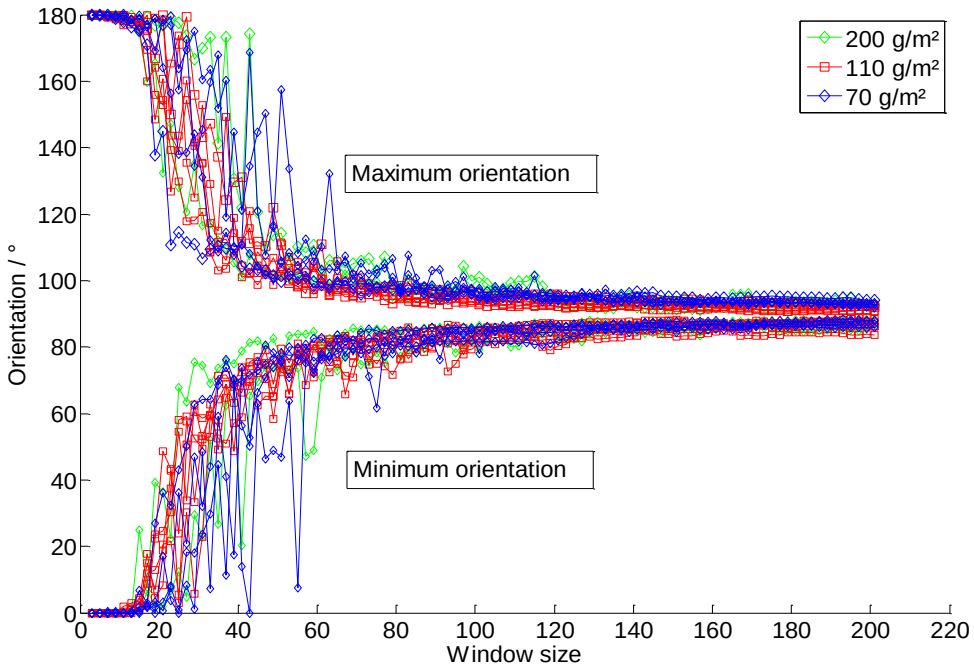

Fig. 3.5 Relationship between the maximal and minimal angle and window size (ROI)

Consequently, the orientation should be described using statistical distribution. Histograms of the number of pixel with a certain orientation are plotted on Fig. 3.6. As displayed on Fig. 3.6(c), when the ROI size is large ($31 \times 31\ pixels$) the statistical distribution is highly narrow and mainly the average value ($90\ deg$) is computed. But when the ROI size is small ($3 \times 3\ pixels$), some artifacts appear on the distribution, see Fig. 3.6(a) where the fiber local orientation values of $0\ deg$ and $90\ deg$ are overestimated. This phenomenon could be due to the fact that the ROI size is small compared the technical fiber size on the image, leading to some regions with almost uniform grey level. In that case it could be difficult to correctly compute the gradient and therefore the calculation of the orientation is difficult. Thus as a conclusion, the ROI has to be large enough to remove artifacts on the distribution of orientation and small enough to get sufficient information on the distribution. Fig. 3.6(e) shows the best compromise in term of ROI size, the quantile-quantile plot being neither biased for low angles nor for high angles. In this work, considering filtering artifacts and not missing too much information the ROI sizes $11 \times 11\ pixels$ or $13 \times 13\ pixels$ have been selected ($214\ \mu m$ and $253\ \mu m$, respectively), depending to the tested plies.

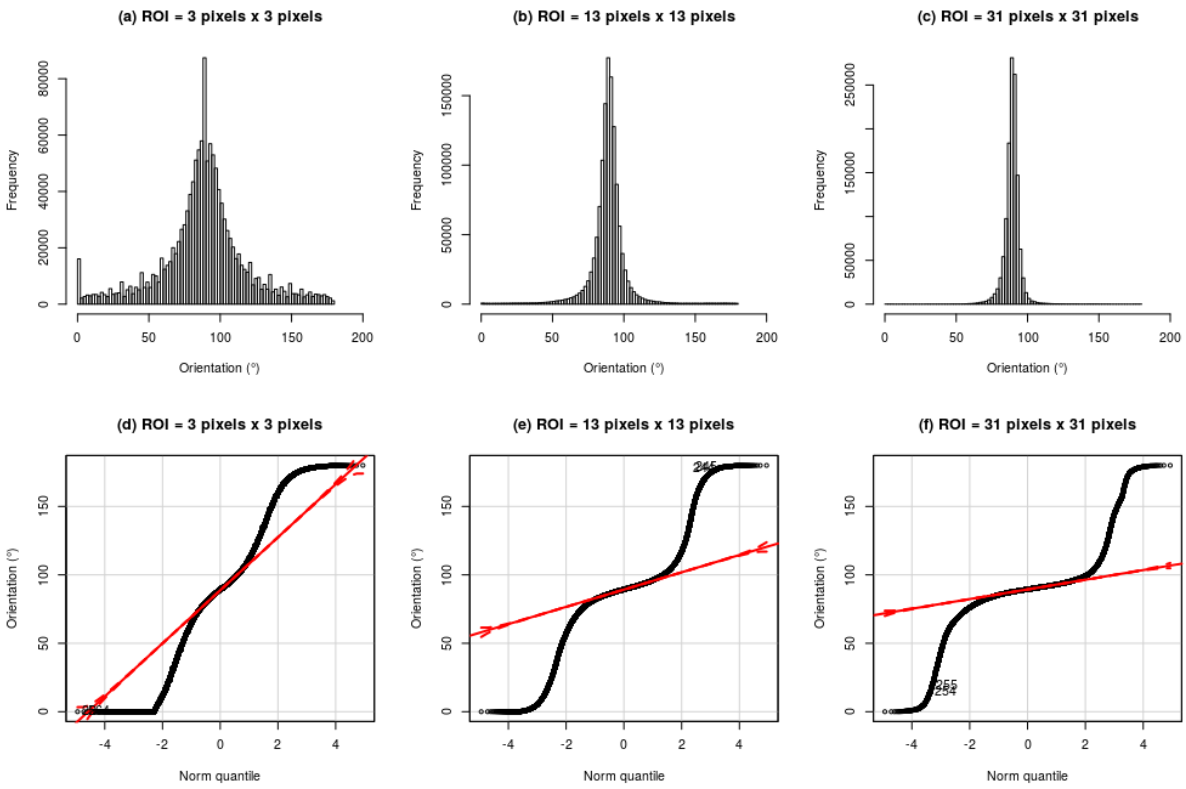

Fig. 3.6 Relationship between orientation distribution and window size, top: histogram, bottom: Q-Q plot

A smooth distribution from experiment data is considered as suitable in the following analyzes. For instance, using this guideline, an acceptable orientation distribution function of UD flax ply with a surface density of 200 g/m^2 is plotted on Fig. 3.7 where the average value has been shifted to 0 deg for convenience. The width of the orientation distribution function is narrow indicating that the most probable orientation is coincident with the loading direction.

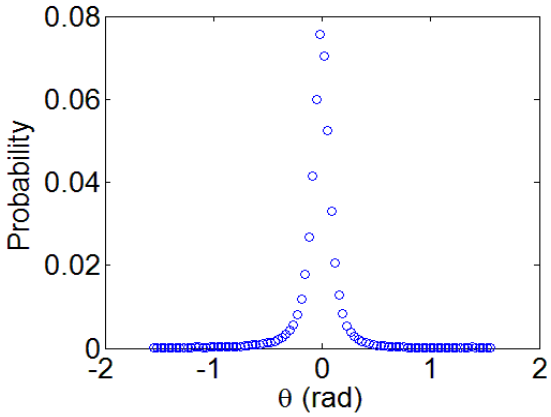

Fig. 3.7 Suitable orientation distribution function of UD flax ply with a density of 200 $g\ m^{-2}$

3.2 Composite theory

3.2.1 Classical model for mechanical properties of composite

The traditional model for predicting the longitudinal or transversal stiffness and strength of a composite is based on the application of the classic "rule of mixtures". This rule of mixtures can be illustrated in Fig. 3.8. The variation of the modulus is linear between the values E_m of the modulus of the matrix and E_f of the modulus of the fibers, when the volume fraction V_f of the fibers varies from 0 to 1.

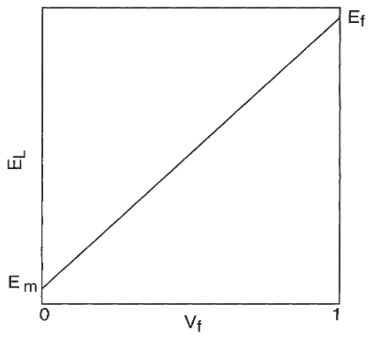

Fig. 3.8 Evolution of the Young's modulus caused by composition ratio in the composite[86]

Composite stiffness and stress can be predicted using a micro-mechanics approach termed the rule of mixtures. This model is based on assumptions of uniform and identical deformation in the longitudinal direction (Fig. 3.9) and the same constraint in the transverse direction in the fiber and in the matrix.

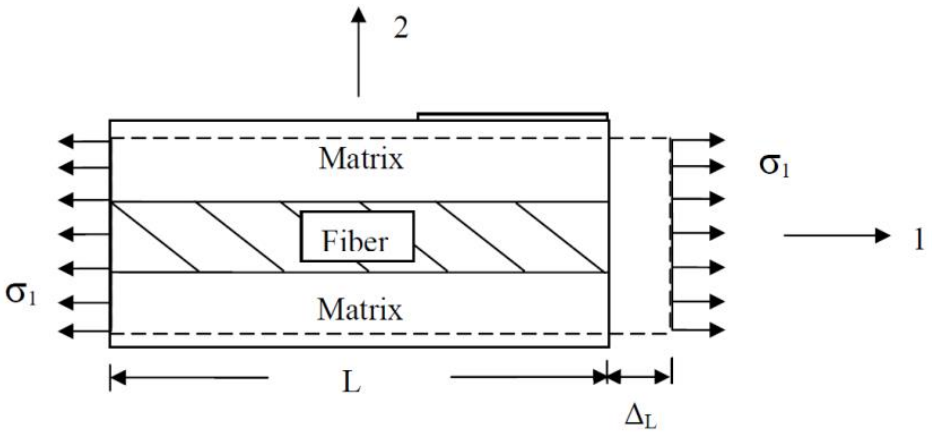

Fig. 3.9 Representative volume element (RVE) in the composite

In the longitudinal direction, the total resultant force on the element equals the sum of the forces acting on the fiber and matrix shown as below:

$$\sigma_L A_c = \sigma_f A_f + \sigma_m A_m$$
$$\sigma_L = \sigma_f \frac{A_f}{A_c} + \sigma_m \frac{A_m}{A_c} \tag{3.7}$$

where A_c, A_f and A_m are composite, fiber and matrix cross sections, respectively and σ_L, σ_f and σ_m are the longitudinal stress of composite, the fiber stress and the matrix stress. Considering unit length and introducing the volume fraction V as $V_i = A_i/A_c$ for $i = m$ and f, we can obtain:

$$\sigma_L = \sigma_f V_f + \sigma_m V_m. \tag{3.8}$$

Using Hooke's law and assuming that the average strains in the composite, fiber, and matrix along the longitudinal direction are equal (strain compatibility), the Young's modulus in longitudinal direction can be computed according (Equation (3.9)):

$$E_L = E_f V_f + E_m V_m \tag{3.9}$$
$$= E_f V_f + E_m(1 - V_f) \tag{3.10}$$

where E, σ and V are the modulus, stress and volume fraction, subscript L, m and f stand for longitudinal direction, matrix and fiber.

In the transverse direction, the total composite displacement equals the sum of the corresponding transverse displacements in the fiber and the matrix according to geometric compatibility. Using the same approach considering the strain, the transverse properties could be expressed as following[89][90]:

$$E_T = \frac{E_f E_m}{E_f V_m + E_m V_f} \tag{3.11}$$
$$\sigma_T = \frac{\sigma_f \sigma_m}{\sigma_f V_m + \sigma_m V_f}. \tag{3.12}$$

Due to the important affection on mechanical properties of porosity existing in our UD flax composite, porosity volume fraction is also taken into account by introducing a multiplicative factor $(1 - V_p)^x$ in the rule of mixture. V_p is the porosity volume ratio and x is an efficiency porosity exponent that quantify how V_p affect the mechanical properties. The complete and improved porosity corrected rule of mixtures model is described by following equations[49]:

$$E_L = \left(E_f V_f + E_m V_m\right)\left(1 - \mathrm{V_p}\right)^{\mathrm{x}} \tag{3.13}$$

$$\sigma_L = \left(\sigma_f V_f + \sigma_m V_m\right)\left(1 - \mathrm{V_p}\right)^{\mathrm{x}} \tag{3.14}$$

$$E_T = \frac{E_f E_m}{E_f V_m + E_m V_f}\left(1 - \mathrm{V_p}\right)^{\mathrm{x}} \tag{3.15}$$

$$\sigma_T = \frac{\sigma_f \sigma_m}{\sigma_f V_m + \sigma_m V_f}\left(1 - \mathrm{V_p}\right)^{\mathrm{x}}. \tag{3.16}$$

Considering the porosity effect, some research work proposed $x = 2$ gives a fitting resultfor the experimental data in expression of composite mechanical behavior[31][91]. We retain this value for the unidirectional reinforcement.

In the case of unidirectional composite subjected to axial tension, the deformations of the fiber and the matrix are assumed to be identical as an isotropic material. If we consider that the matrix deformation at rupture (8.2% for our matrix according to the manufacture data by Huntsman) is greater than that of fiber (3.2% maximum according to the literature[92]. Then matrix does not reach its breaking strain, and the tensile rupture of fibers will determine the rupture in the composite. Therefore, σ_m in Equation (3.14) should reflect the constraint of matrix at the time of rupture of the composite. Hence for correction, σ_m^r which is the stress of matrix at fiber failure strain is used. In the case of a transverse load to the direction of the fiber, the rule of mixture variables is also based on the isotropy of the tensile properties of the fibers and the matrix. However, the matrix could be strained non-uniformly within composites tested in the transverse direction. Moreover, rupture of the composite occurs either by disruption of the matrix or by debonding the fiber/matrix interface or possibly by transverse rupture of the reinforcement due that although this isotropy assumption is acceptable for the matrix, the longitudinal tensile properties of most plant fibers (flax, jute…) and artificial (carbon, aramid) are widely greater than in the transverse properties. It should be more

complicate and also adjusted, for simplicity, the same σ_m^r is considered to value the breaking stress of the matrix at point of composite failure in Equation (3.16). Considering the strain compatibility, the linear behavior of σ_m^r is estimated using the following equation:

$$\sigma_m^r = E_m \frac{\sigma_f}{E_f} \tag{3.17}$$

The final equations are:

$$E_L = \left(E_f V_f + E_m V_m\right)\left(1 - \mathrm{V_p}\right)^{\mathrm{x}} \tag{3.18}$$

$$\sigma_L = \left(\sigma_f V_f + E_m \frac{\sigma_f}{E_f} V_m\right)\left(1 - \mathrm{V_p}\right)^{\mathrm{x}} \tag{3.19}$$

$$E_T = \frac{E_f E_m}{E_f V_m + E_m V_f}\left(1 - \mathrm{V_p}\right)^{\mathrm{x}} \tag{3.20}$$

$$\sigma_T = \frac{\sigma_f E_m}{E_f V_m + E_m V_f}\left(1 - \mathrm{V_p}\right)^{\mathrm{x}}. \tag{3.21}$$

A similar approach could be used to compute all the elastic properties of the composite, such as longitudinal Poisson's ratio (ν_{LT}) and the longitudinal shear modulus (G_{LT}), see Berthelot[86] for more details.

$$G_{LT} = \frac{G_f G_m}{G_f V_m + G_m V_f}\left(1 - \mathrm{V_p}\right)^{\mathrm{x}} \tag{3.22}$$

$$\nu_{LT} = \nu_f V_f + \nu_m V_m \tag{3.23}$$

3.2.2 Taking into account a statistical distribution of fiber orientation

Several models could be found in literature to give a probabilistic assessment to the orientation of fibers in fiber reinforced composites[93]. These works are usually done for discontinuous fiber reinforced thermoplastics composites[94][95]. The model is proposed here to predict effective elastic properties of continuous fiber composite taking into account a statistical distribution of orientation. The approach consisted in a modification of the equations of composite theory (Equation (3.18) to Equation (3.23)) by adding statistical

orientation distribution function. It is assumed that all materials that are matrix and flax fiber are isotropic and elastic materials. All plies in the composite manufactured for this study have the same orientation (see Section 2.1.3), therefore the elastic behavior of composite materials could be assumed as orthotropic. The linear elasticity relation can be written in the following matrix form[86][96]:

$$\varepsilon = \mathbf{S}\sigma \tag{3.24}$$

where **S** is the compliance matrix and is defined as follow:

$$\boldsymbol{S} = \begin{bmatrix} \frac{1}{E_1} & -\frac{\nu_{12}}{E_1} & -\frac{\nu_{13}}{E_1} & 0 & 0 & 0 \\ -\frac{\nu_{12}}{E_1} & \frac{1}{E_2} & -\frac{\nu_{23}}{E_2} & 0 & 0 & 0 \\ -\frac{\nu_{13}}{E_1} & -\frac{\nu_{23}}{E_2} & \frac{1}{E_3} & 0 & 0 & 0 \\ 0 & 0 & 0 & \frac{1}{G_{23}} & 0 & 0 \\ 0 & 0 & 0 & 0 & \frac{1}{G_{13}} & 0 \\ 0 & 0 & 0 & 0 & 0 & \frac{1}{G_{12}} \end{bmatrix}. \tag{3.25}$$

This compliance matrix **S** in Equation (3.25) is expressed in the principal directions of material. In other words, the loading direction is parallel (or perpendicular) to the direction of the fibers. We have shown in Section 3.1.2 that some fibers in one ply are not aligned in the tensile direction; hence, we need to choose a reference axis system for all the fibers in one ply and to calculate the elastic behavior of all the fibers in that coordinate system (Fig. 3.10). It was done by using rotation operator on the compliance matrix.

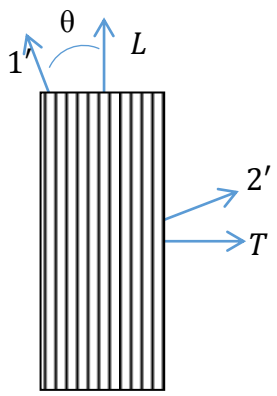

Fig. 3.10 Rotation by angle θ of the principal direction (L-T)

Adopting the usual Voigt's notation for stress and strain, and following the work of Berthelot[86], the compliance matrix $\mathbf{S}'$ in the coordinate system ($1'$-$2'$) can be expressed as follow:

$$\mathbf{S}' = \mathbf{T}_\varepsilon \mathbf{S} \mathbf{T}_\sigma^{-1} \tag{3.26}$$

where $\mathbf{T}_\varepsilon$ and $\mathbf{T}_\sigma$ are the rotation operator in Voigt notation for the strain and stress respectively and are expressed according Berthelot[86].

$$\mathbf{T}_\varepsilon = \begin{bmatrix} \cos^2\theta & \sin^2\theta & 0 & 0 & 0 & \sin\theta\cos\theta \\ \sin^2\theta & \cos^2\theta & 0 & 0 & 0 & -\sin\theta\cos\theta \\ 0 & 0 & 1 & 0 & 0 & 0 \\ 0 & 0 & 0 & \cos\theta & -\sin\theta & 0 \\ 0 & 0 & 0 & \sin\theta & \cos\theta & 0 \\ -2\sin\theta\cos\theta & 2\sin\theta\cos\theta & 0 & 0 & 0 & \cos^2\theta - \sin^2\theta \end{bmatrix} \tag{3.27}$$

$$\mathbf{T}_\sigma = \begin{bmatrix} \cos^2\theta & \sin^2\theta & 0 & 0 & 0 & 2\sin\theta\cos\theta \\ \sin^2\theta & \cos^2\theta & 0 & 0 & 0 & -2\sin\theta\cos\theta \\ 0 & 0 & 1 & 0 & 0 & 0 \\ 0 & 0 & 0 & \cos\theta & -\sin\theta & 0 \\ 0 & 0 & 0 & \sin\theta & \cos\theta & 0 \\ -\sin\theta\cos\theta & \sin\theta\cos\theta & 0 & 0 & 0 & \cos^2\theta - \sin^2\theta \end{bmatrix}. \tag{3.28}$$

Combining the equations (3.25), (3.26), (3.27) and (3.28), the mechanical properties of the laminate in the new coordinate system can be expressed as a function of the composite properties in main directions (L-T). For instance the Young's modulus in the direction $1'$ can be computed as below:

$$S_{1'1'} = \frac{1}{E_{1'}} = \frac{1}{E_L}\cos^4\theta + \frac{1}{E_T}\sin^4\theta + \left(\frac{1}{G_{LT}} - \frac{2\nu_{LT}}{E_L}\right)\sin^2\theta \cdot \cos^2\theta \tag{3.29}$$

where E_L, E_T, G_{LT} and ν_{LT} are the elastic properties of the composite compute using rules of mixture presented in equations (3.18), (3.20), (3.22) and (3.23) respectively.

The idea of the model is to compute elastic properties of composite ply taking into account all fiber orientations in a ply. Let's suppose that $f(\theta)$ is the probability to find a continuous fiber with an orientation of $d\theta$. Moreover we considered that several orientations of fiber could be found in a ply. Therefore assuming that statistical orientation distribution function f exists, the properties of ply could be defined as:

$$\langle S_{ij} \rangle = \int_{-\frac{\pi}{2}}^{\frac{\pi}{2}} S_{ij}(\theta) f(\theta) d\theta \tag{3.30}$$

Equation (3.30) defines the effective compliance properties as average operation. The integration range is defined by the interval $[-\pi/2\,, \pi/2]$ rather than the usual range $[-\infty, \infty]$ due to the π-periodicity of the problem. The orientation distribution function f is then evaluated by the method described in Section 3.1.2 in a discontinuous form (Fig. 3.11). The final expression of the effective compliance properties $\langle S_{ij} \rangle$ is therefore:

$$\langle S_{ij} \rangle = \sum_{Nb\ bins} S_{ij}(\theta) \cdot F(\theta) \tag{3.31}$$

where $F(\theta)$ is the probability to find a fiber with an orientation between $\theta - \Delta\theta$ and $\theta + \Delta\theta$.

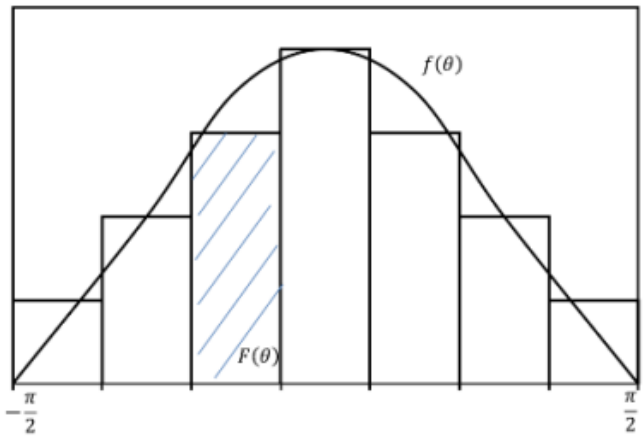

Fig. 3.11 Evaluation of the orientation distribution function f by a discontinuous approach

The validation of this model was conducted by analyzing the effect of several orientation distribution functions f on the value of longitudinal modulus of the composite for Young's modulus of fiber ranging from 0 GPa to 50 GPa. The two limit cases were selected as purely UD fiber and as totally randomly oriented fiber in a ply. The first was modeled using a Dirac function (purely UD) and the latter by a uniform distribution. Moreover five Gaussian distributions were selected with increasing standard deviation (5 deg, 10 deg, 20 deg, 30 deg, 100 deg) as plotted on Fig. 3.12.

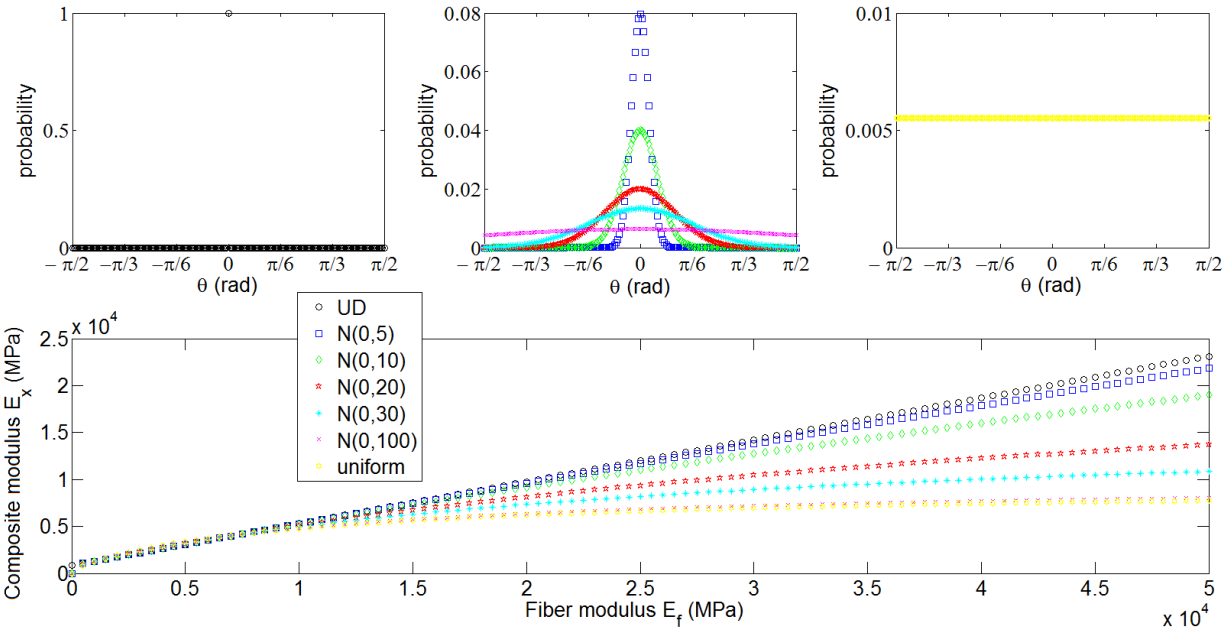

Fig. 3.12 Sensibility to orientation distribution of fibers, from the top left to right: purely unidirectional, normalized at 0 deg with standard deviation from 5 deg to 100 deg, and randomly distributed.

As shown on Fig. 3.12, the results obtained for purely UD (black curve) is equivalent to that obtain with classical rules of mixture (Equation (3.18)). Indeed, the longitudinal modulus of composite increases linearly as the Young's modulus of fiber increases. Furthermore, the increase of the standard deviation of the Gaussian distribution was used to model the increase of amount of fiber disoriented in the flax ply. The performance of the composite, evaluated here only by the longitudinal modulus, decreases as the standard deviation increase. For example, considering a flax modulus of 40 GPa, the composite modulus is 18.7 GPa if the reinforcement is purely UD and if the standard deviation of the Gaussian distribution is set at 10 deg, the composite modulus drops to 12.2 GPa. The composite modulus is reduced by almost a third. The trends obtained here confirmed that this model could be used as a first approximation to take into account the orientation distribution function in composite laminate theory and will be used to assess the properties of UD flax fiber inside our composite.

3.2.3 Model sensitivity to input parameters

The sensitivity of the model to the input parameters has been assessed. We focus on that section to the evaluation of the effective modulus of flax fiber inside the composite laminate, and only the Young's modulus of the composite in the loading direction are required. Then, only the component S_{11} has to be evaluated. The properties of the matrix (E_m, ν_m), the Poison's ratio of the fibers (ν_f) and the volume fractions (V_p,V_m and V_f) are the input parameters. The nominal value of each parameter is given in Table 3.1. Deviations of the parameters are applied and of which the effect on the response is evaluated. One orientation distribution function f was selected from one measurement for all the calculations and it is the one plotted on Fig. 3.7.

Table 3.1 Nominal material parameters required for the model

Matrix modulus E_m(GPa)	Matrix Poisson's ratio ν_m	Fiber Poisson's ratio ν_f
3	0.45	0.38

Assuming that the fiber modulus range from 0 to 80 GPa, the longitudinal modulus of composite was computed (Fig. 3.13). First the volume fractions of fiber are supposed to range from 15% to 55% and the volume fraction of porosity was kept constant at 10%

(Fig. 3.13(a)). Another parameter which is very important on the composite behavior is the porosity, hence, the volume fractions of fiber are supposed to range from 0% to 20% and the volume fraction of fiber was kept constant at 30% (Fig. 3.13(b)).

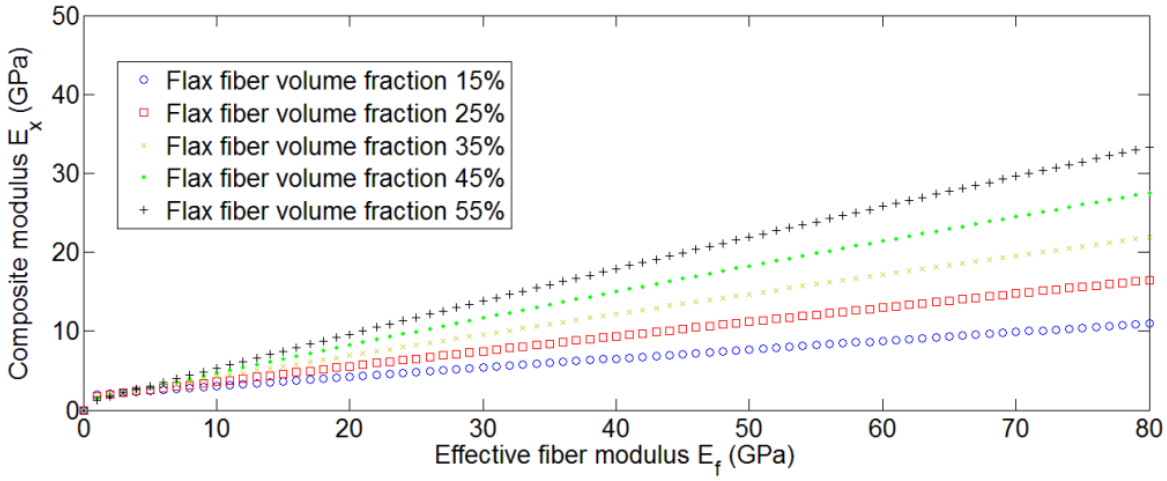

(a) Effect on the volume ratio of fiber on the composite longitudinal modulus

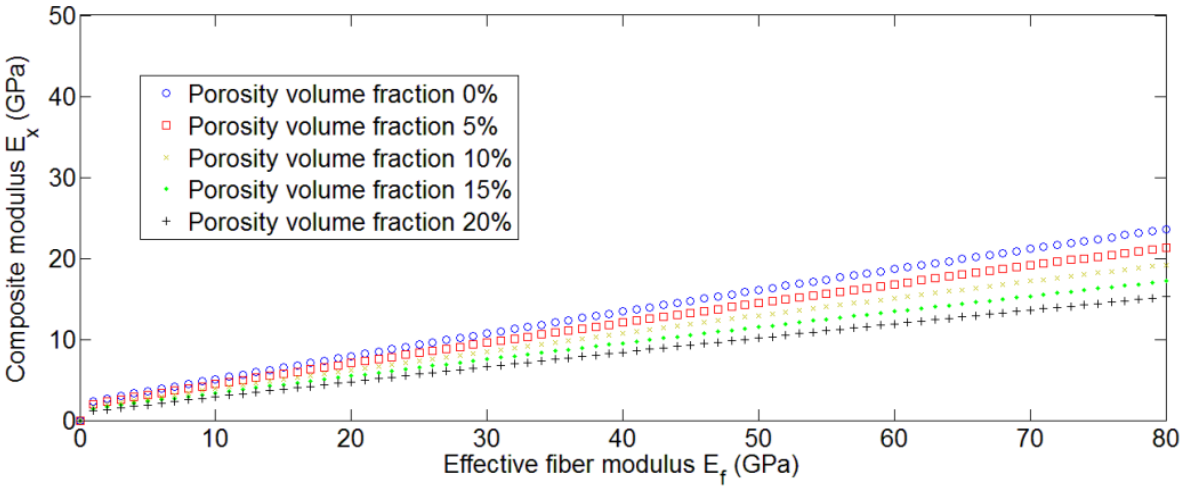

(b) Effect on the volume ratio of porosity on the composite longitudinal modulus

Fig. 3.13 Effect of the volume ratio on the computed longitudinal composite modulus

From both results in Fig. 3.13, general conclusions could be drawn. Flax fiber volume fraction has huge influence on the composite mechanical behavior. The composite modulus increases with the increase of flax fiber volume fraction. Moreover, as shown in Fig. 3.13(b), porosity volume fraction has evident influence on the mechanical behavior of composite. For the same level of composite modulus, flax fiber need to exhibit higher effective mechanical modulus when the volume fraction of porosity is higher in the composite, and generally, the composite

mechanical behavior decreases with the increase of porosity volume fraction. These trends encourage us to improve the volume ratio measurement as described in Section 2.3.3.

The behavior of the flax fiber inside the composite is still unknown. By the elastic model developed in this PhD, an estimation of the Young's modulus of fiber in composite could be computed. However, these computations required the use of the Poisson's ratio of UD flax fiber. Here, five different Poisson's ratios of flax fiber has been used (0.05, 0.15, 0.25, 0.35 and 0.45) to analyze its influence on the longitudinal modulus of composite with volume fraction of flax fiber 55% and porosity 10%, the other parameters are set according Table 3.1. A straight forward result shown in Fig. 3.14 reflect Poisson's ratio of flax fiber does not behave influence on the composite behavior as far as only the longitudinal behavior of composite is concerned.

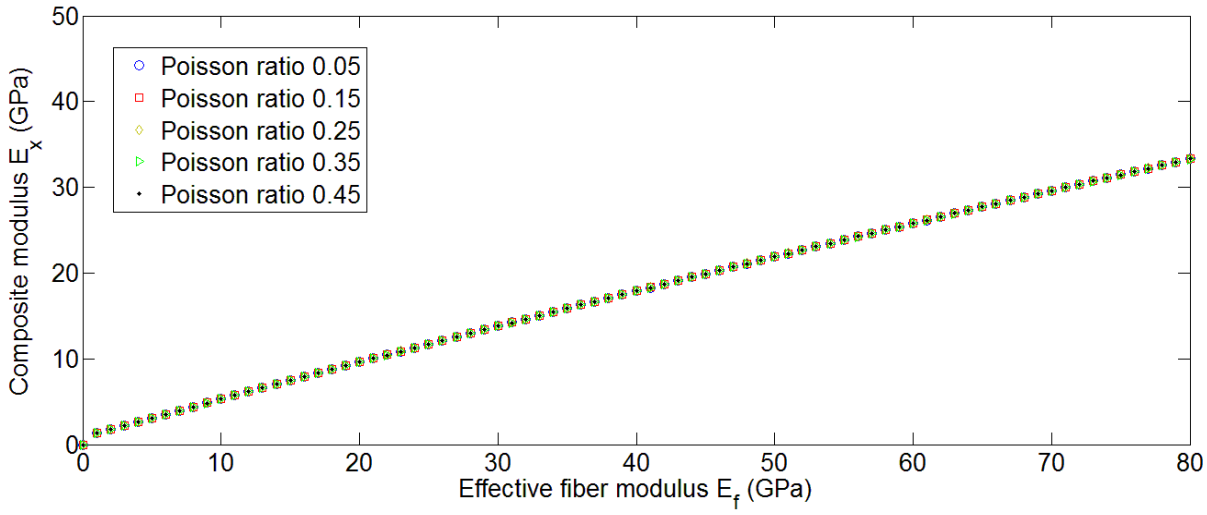

Fig. 3.14 Effect of flax fiber Poisson's ratio on the computed longitudinal composite modulus

Similar analyses could be done with the elastic properties of the matrix (E_m and ν_m). Worth to point out that the Poisson's ratio have less effect on longitudinal modulus of composite than the matrix Young's modulus. Therefore only the effect on the latter is plotted on Fig. 3.15. Comparing the results of Fig. 3.13 to Fig. 3.15, it appeared that the most important parameter seems to be the volume ratio of components.

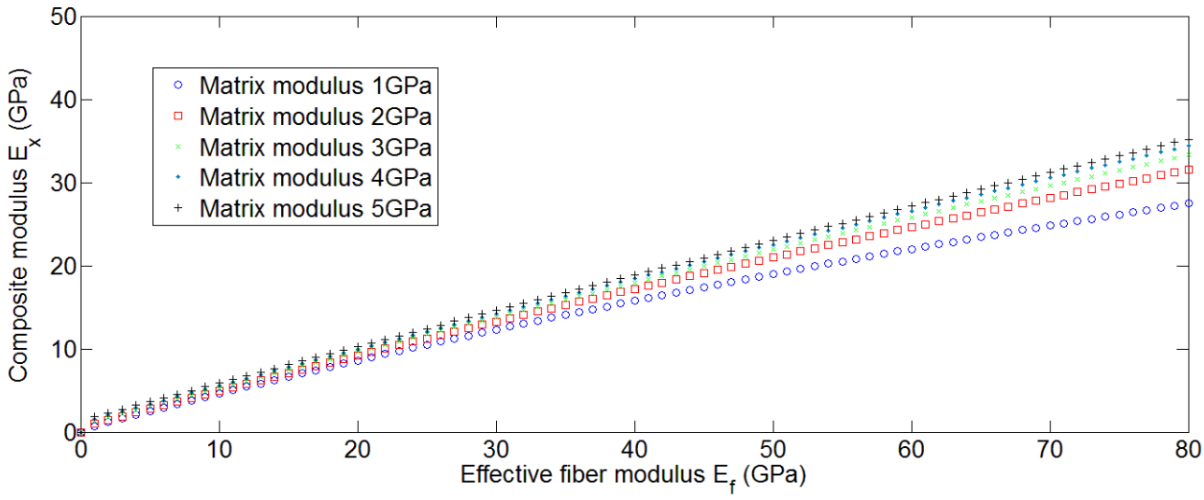

Fig. 3.15 Effect of matrix modulus on the computed longitudinal composite modulus

3.3 Performance of UD flax composites

3.3.1 Experimental test on UD laminate

The mechanical properties of composite were acquired from the monotonic tensile tests done on Instron 8800. Experiment details are described in Section 2.2.4. Seven specimens have been prepared for monotonic tensile experiments at the same strain rate about $10^{-4}s^{-1}$. UD flax fiber composites have been made according the method detailed in Section 2.1.3. Volume fractions of composite phases (matrix, fiber and porosity) have been computed as described in the Section 2.3.3. From Fig. 3.16, we can see the fiber, matrix and porosity volume fraction is about 48%, 42% and 10%, respectively. For the sake of clarity, details of the plate parameters are listed in Table 3.2. The UD plates have similar volume fractions taking in account error bars.

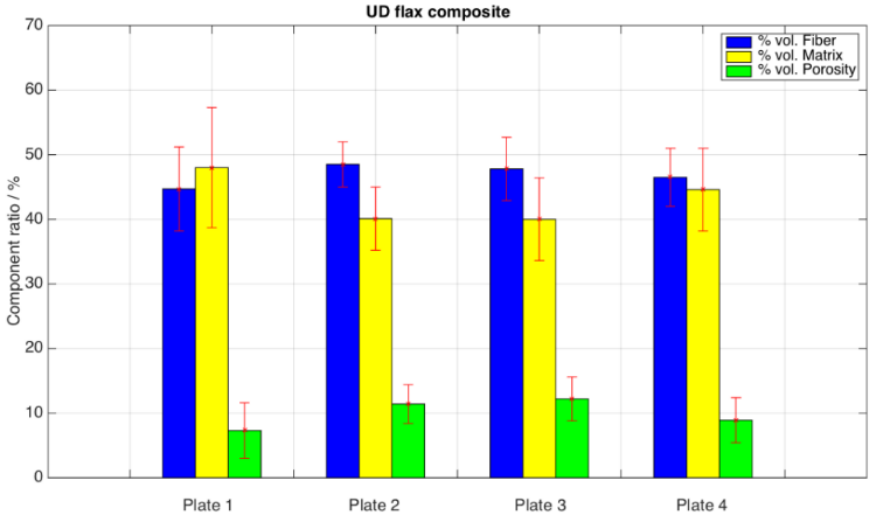

Fig. 3.16 Volume fraction of matrix, fiber, and porosity in UD flax composite plates

Table 3.2 Volume fractions of UD flax composite prepared for mechanical properties analysis.

	UD70-6 (Plate 1)	UD200-1 (Plate 2)	UD110-1 (Plate 3)	UD110-2 (Plate 4)
V_f (%)	44.7 ± 6.5	48.5 ± 3.5	47.8 ± 4.9	46.5 ± 4.5
V_m (%)	48.0 ± 9.3	40.1 ± 4.9	40.0 ± 6.4	44.6 ± 6.4
V_p (%)	7.3 ± 4.3	11.4 ± 3.0	12.2 ± 3.4	8.9 ± 3.5

Typical tensile stress-strain curves for UD flax fiber composite loaded until failure are shown in Fig. 3.17.

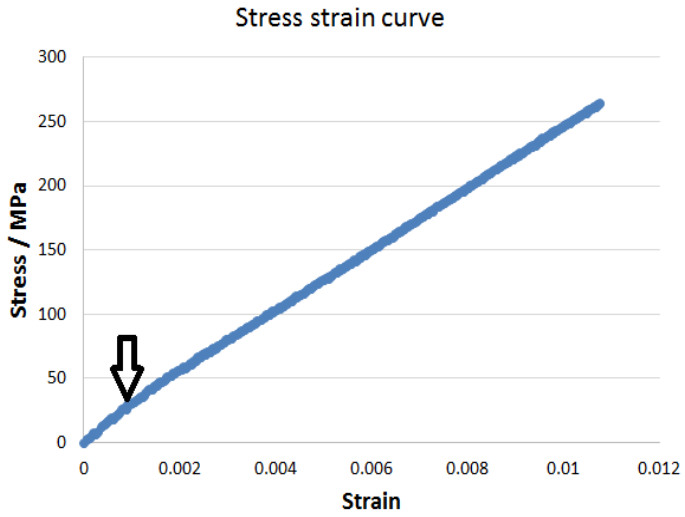

Fig. 3.17 Typical monotonic tensile behavior of UD flax fiber reinforced composite at ambient temperature at $\dot{\varepsilon} = 10^{-4}s^{-1}$

It is clear to see there are at least two regions in the monotonic tensile test at ambient temperature and normal strain rate divided by a threshold value (Fig. 3.17 arrow). The stress is proportional to the load while smaller than threshold value in agreement with Hooke's behavior. In the following, the first region will be used to calculate the Young's modulus of the composite from the slope of the initial linear part of the typical curve. The mechanical properties such as longitudinal Young's modulus E_L and ultimate stress σ_L of UD flax composites can be deduced from monotonic tensile tests at ambient temperature and at a strain rate $10^{-4}s^{-1}$. The mechanical properties of our UD flax fiber composite are summarized in Table 3.3.

Table 3.3 Properties of UD composites obtained from tensile test at $\dot{\varepsilon} = 10 - 4\ s^{-1}$.

Parameters	UD70-6 (Plate 1)	UD200-1 (Plate 2)	UD110-1 (Plate 3)	UD110-2 (Plate 4)
$V_f(\%)$	44.7 ± 6.5	48.5 ± 3.5	47.8 ± 4.9	46.5 ± 4.5
$E_L(GPa)$	27.8 ± 1.7	28.7 ± 2.5	–	28.7 ± 1.2
$\sigma_L(MPa)$	275.6 ± 5.5	255.3 ± 16.3	–	312.0 ± 22.0

These values will be considered as input parameters in the next section in order to compute the effective properties of flax fiber inside the composite.

3.3.2 Flax fiber properties using statistical distribution function

To apply the model described in Section 3.2.2 to estimate the properties of present UD flax reinforcement the properties of the matrix need to be evaluated. The properties have been chosen according manufacturer datasheet given in Table 3.4. The other mechanical properties, namely the Poisson's ratio of fiber and the Poisson ratio of matrix have been chose according Table 3.1. Furthermore, the volume fraction of fiber and the volume fraction of porosity have been set at 46.9% and 10.0% corresponding to the average value obtained experimentally. The volume fraction of matrix is then 43.1%.

According the work described in Section 3.1.2, suitable statistical distribution function to describe the orientation of fibers in a ply is remembered in Fig. 3.18.

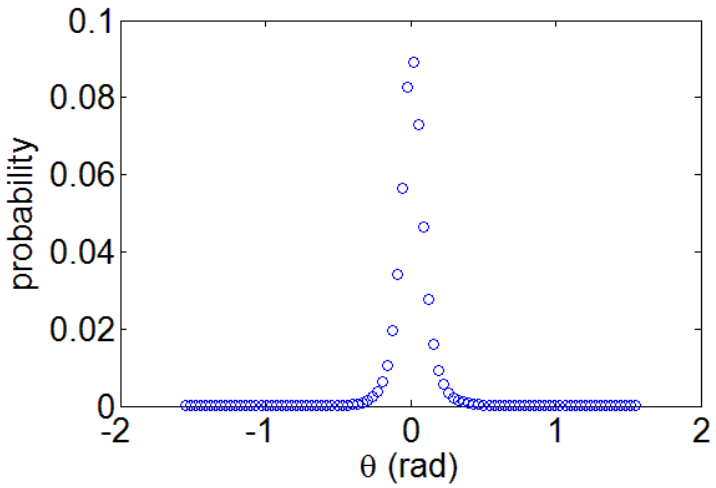

Fig. 3.18 Best orientation distribution function of UD flax ply with a surface density of $78\ g\ m^{-2}$

Table 3.4 Key data of the used epoxy matrix (by Huntsman)

$E_m(GPa)$	$\sigma^u(MPa)$	$\varepsilon^u(\%)$
2.93 ± 0.07	62 ± 2	8.2 ± 0.2

Following the same approach that in Section 3.2.3, taking into account the statistical distribution function that describes the orientations of flax fiber in flax ply, the effect of the Young's modulus of fiber (ranged from 0 GPa to 100 GPa) on the composite modulus in the loading direction can be evaluated and are plotted, see Fig. 3.19. Such diagram allows computing the effective properties of flax according the Young's modulus of composite that have been measured in Section 3.3.1. The effective Young's modulus of the unidirectional reinforcement was finally measured as 86 GPa.

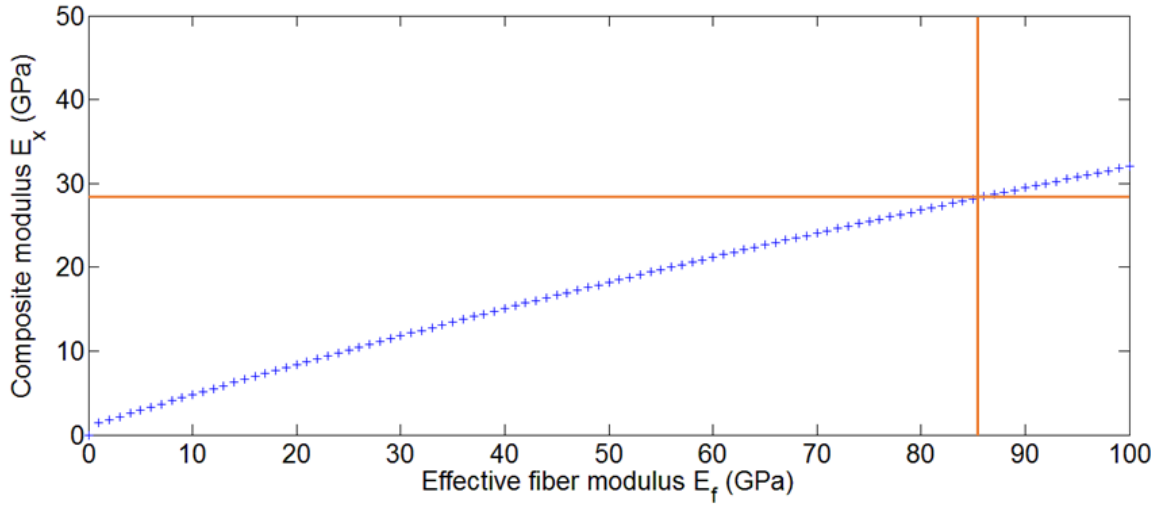

Fig. 3.19 Effect of the effective flax Young's modulus on the longitudinal composite modulus taking into account the orientation distribution function of UD flax fiber ply

It could be compared to previous flax composite studied in our laboratory (Fig. 3.20). The abbreviations QUD and S respectively correspond to yarn reinforcement and balanced textile twill $2/2$ reinforcement (see Appendix). The associated number is the basic unit area weight of fabrics by manufacturer ($g\ m^{-2}$). Worth to point out that the effective modulus of both kinds of flax reinforcement (balanced or QUD) shows an ultimate value to approximately 72 GPa. However, the fiber orientation was not considered in the previous study[49]. As expected, UD and QUD flax fiber reinforcements have better mechanical efficiency than

textile reinforcements under the longitude tension.

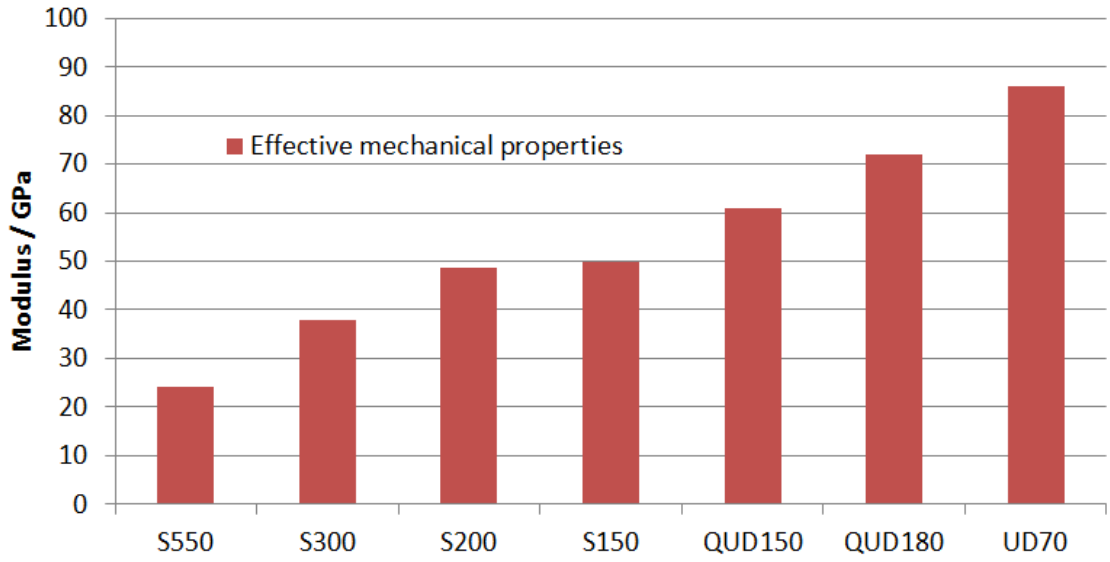

Fig. 3.20 Effective mechanical properties of flax reinforcement studied in our team

3.4 Conclusion

In this chapter, unidirectional flax composite has been made by the hot platen press method. Mechanical properties of the composite have been analyzed. A new model of the theory not only taking into account porosity efficiency and priority rupture of fibers but also taking flax fiber orientation into account in standard experiment situations has been established and applied. UD flax ply exhibits the highest effective mechanical properties compared to the previous flax reinforcement (balanced or quasi-unidirectional) used in our laboratory. However, worth to point out those strong assumptions has been done concerning the material (elastic isotropic for matrix and fibers, elastic orthotropic for composite). Nevertheless, our new approach paves the way to replace the shrinkage used in Cherif et al.[49] by the in-situ fiber orientation as a key parameter to analyze the efficiency of polymer reinforcement by plant fibers. The elasticity of flax composite will be discussed in the next chapter.

Chapter 4 PHENOMENOLOGICAL ANALYSIS

Chapter 3 has presented a model to predict the main mechanical parameters of unidirectional plant fiber composites based on the rule of mixture and the distribution of both the reinforcement orientation. This approach cannot predict the evolution of the mechanical response of the material between initial loading (purely elastic) and failure loading. What is the interest is that one of the major practical problems that we have to face is some changes of the mechanical behavior for different regions (including the elastic region) depend upon thermodynamic and kinetic factors. Indeed, plant-based reinforced polymers often present nonlinear behavior under tensile loading. In order to study this general behavior here, the mechanical characteristics of UD flax composite are studied in a variety of practical conditions. Moreover, plant fibers have significant variations in the diameter, defects content, and maturity which will pass to the finished UD composite product and which makes a study on the impact on the rigidity and strength a challenge. The aim of Chapter 4 is to analyze the mechanical behavior with a phenomenological point of view. The analysis is based on a previous phenomenological model developed in our team.

4.1 Effect of thermodynamic and kinetic factors

4.1.1 Global view of UD flax composite at tension condition

Typical stress-strain tensile test curves for UD flax fiber composite loaded to the point of breaking are shown in Fig. 4.1 and Fig. 4.2. The later gives a value of aspect ratio in transverse and longitudinal strain. Here firstly, typically monotonic and repetitive progressive load (RPL) curves are presented in Fig. 4.1. It is clear to see there are at least two regions in the monotonic tensile test at high speed and ambient temperature which divided by a threshold value (arrows in Fig. 4.1(c) and Fig. 4.1(d)). The stress is linearly proportional to the load while smaller than threshold value in agreement with Hooke's behavior. Here in our UD composite, the first region will be used to calculate the Young's modulus of the composite. Taking into account the cross section dimensions of the specimens, the Young's modulus is calculated from the slope of the initial linear part of the typical curve. In this work, all the tests have been done several times when possible (generally three) in order keeping the mean curve for each tested set of parameters. The stress-strain curve is strongly influenced by any of the following conditions such as temperature, the rate of loading, constituents

construction, specimen moisture content and reinforcement morphological characteristics i.e. orientation and length in the specimen. Thus, a large spread in the mechanical behavior values can be observed from one to another. Before tensile test, the cross section (width and thickness) of each specimen is measured with a micrometer.

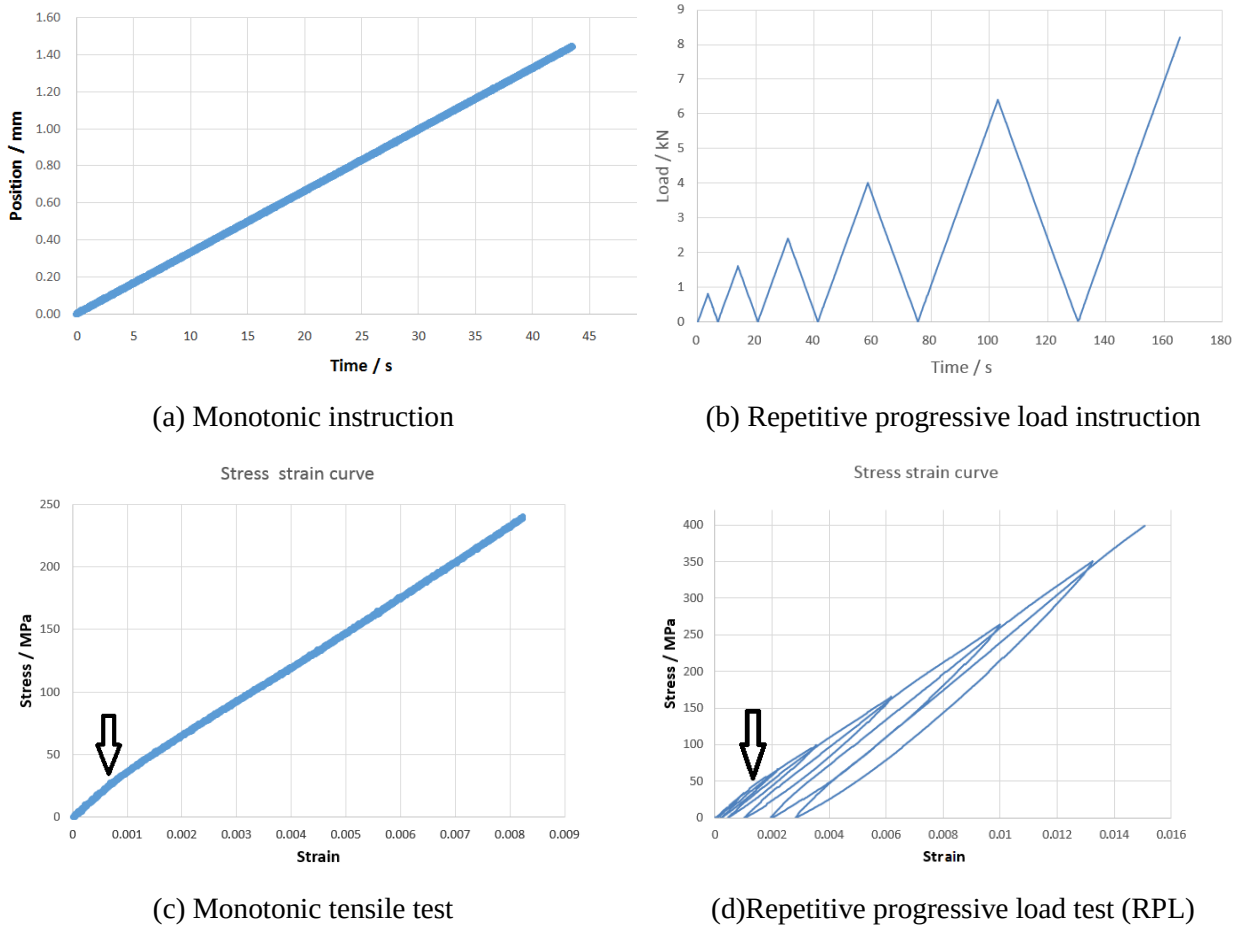

(a) Monotonic instruction

(b) Repetitive progressive load instruction

(c) Monotonic tensile test

(d)Repetitive progressive load test (RPL)

Fig. 4.1 Typical tensile experiment curve at normal speed and ambient temperature.

From the Fig. 4.1(d), we can see that not only the Hooke's (elastic) behavior but also nonlinear behavior appears visibly when the load is cycled with a nominal value above the threshold load. Besides, three regions divided by obvious change in rigidity will be discovered and analyzed due that the non-elastic deformation appearance determined by the cycle value we set considering test environment especially when it is above the threshold transition.

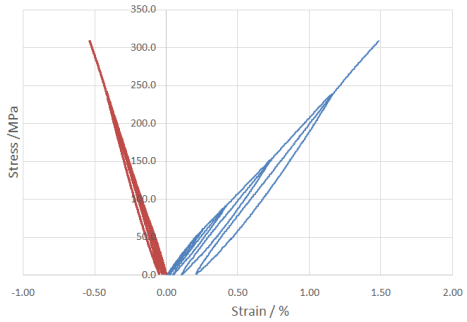

(a) Stress vs transverse and longitudinal strain

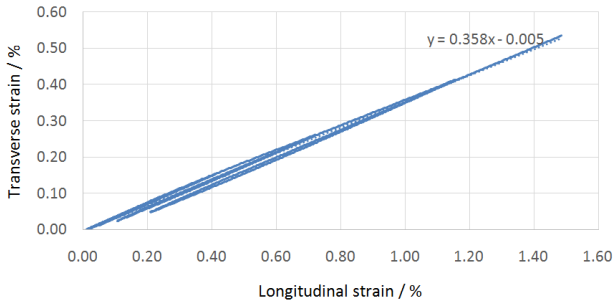

(b) Transverse strain vs longitudinal strain

Fig. 4.2 Typical transverse response to tensile loading (UD110)

4.1.2 Apparent effect of temperature

Each composite material has a temperature range suitable for its utilization. The UD flax composite has an average T_g value of $92°C$ (see Section 2.3.1). We use this value as an indicator to design different loading conditions, especially in relation to the temperature factor. Three temperature conditions, $20°C$, $50°C$, and $80°C$ respectively, are designed for UD composite within tensile test, taking in account the same order of magnitude of strain rate. Repetitive progressive loading (RPL) tests can represent us viscous information during the tensile experiments. Viscoelastic effects can be captured during different loading cycles. Fig. 4.3 – based on RPL test – illustrates the overall impacts caused by temperature on the mechanical properties of UD composite. There is a large change in the non-elastic deformation between cycles which is more obvious at high temperature as shown in Fig. 4.3(a) showing higher strains for the same load at $80°C$. In Fig. 4.3(b), it tells us the composite ultimate stress deceases while the temperature increases. The failure strain which is determined by the point of the breaking stress is also affected by the temperature effect. In general, the Young's modulus of UD flax composite decreases while the temperature is raised, as shown in Fig. 4.3(c).

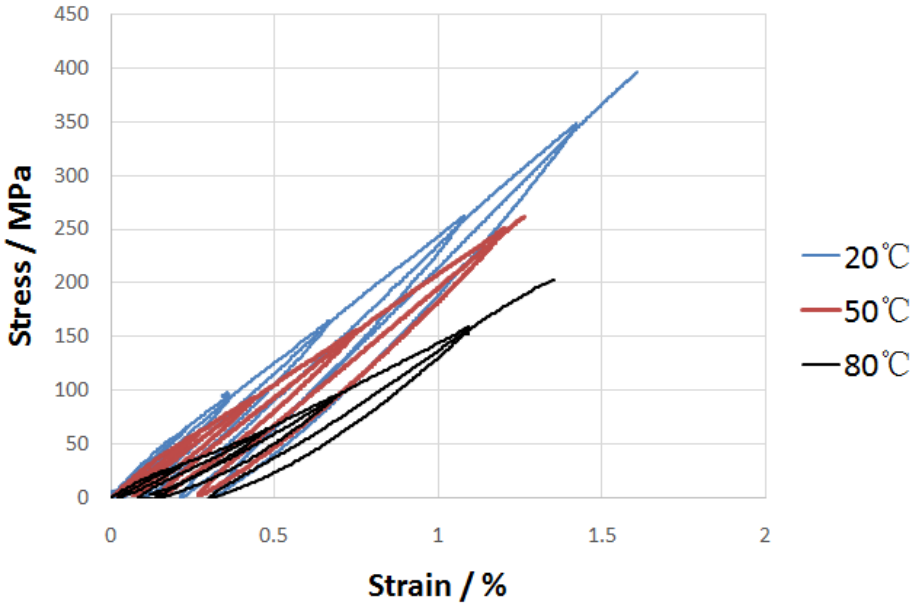

(a) RPL tests at different temperature conditions

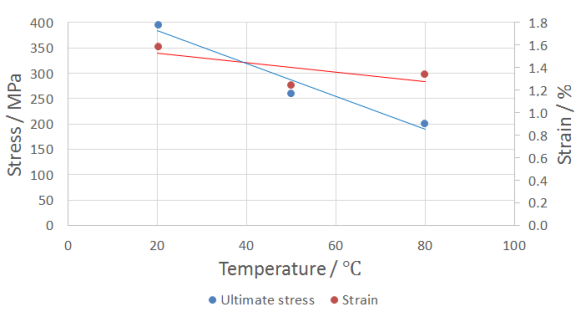

(b) Evolution of ultimate stress and strain

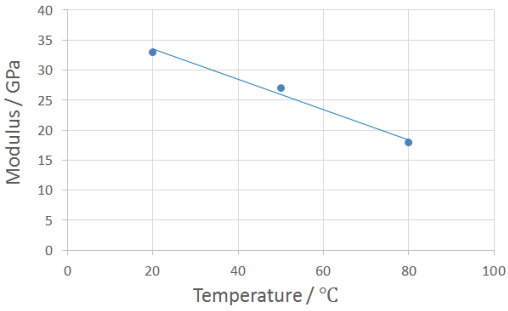

(c) Evolution of Young's modulus

Fig. 4.3 Effect of temperature on UD flax composite (UD110)

4.1.3 Apparent effect of strain rate

Effect of strain rate is synthetized on Fig. 4.4. As we can see in Fig. 4.4(b) where strain rate $5 \times 10^{-4} s^{-1}$ is corresponding to $10\, MPa\, s^{-1}$, lower stain rate when the tensile test performed shows a lower ultimate stress. In Fig. 4.4(c), the ultimate strain has a tendency to decrease when decrease the stain rate of test sample. However, the Young's modulus decreases comparing order of magnitude $10^{-4} s^{-1}$ with $10^{-5} s^{-1}$ and for the lower strain rates $10^{-7} s^{-1}$ (Fig. 4.4(d)).

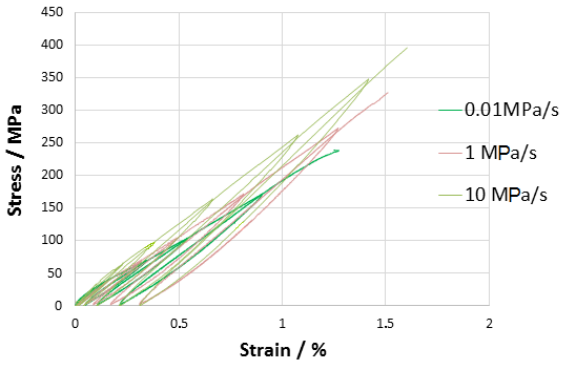

(a) RPL curves

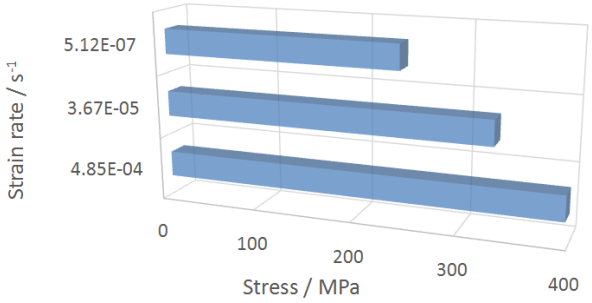

(b) Ultimate stress

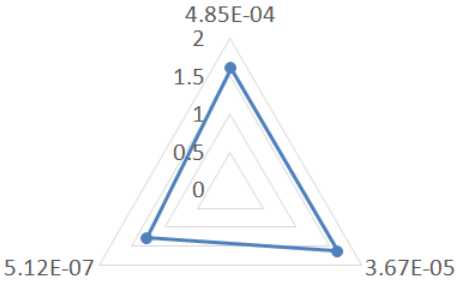

(c) Ultimate strain

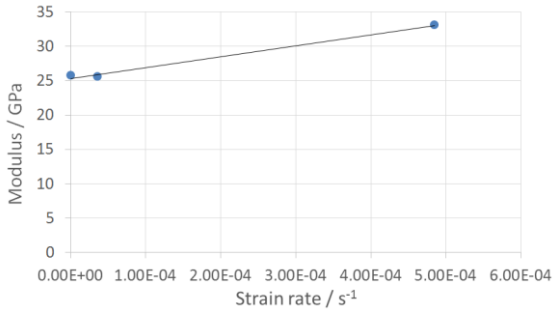

(d) Young's modulus

Fig. 4.4 Effect of strain rate on UD flax composite (UD110)

Behavior of UD flax composite are also represented in Fig. 4.5 where we can see that not only two regions but three emerge when the tensile test performed at high temperature $80°C$ or very low test speed $0.01\ MPa\ s^{-1}$. These three regions will be conformed in the next sections.

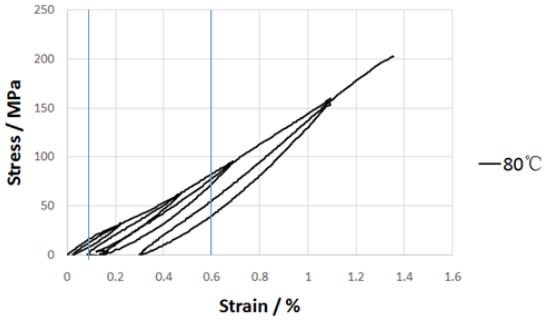

(a) With high temperature test

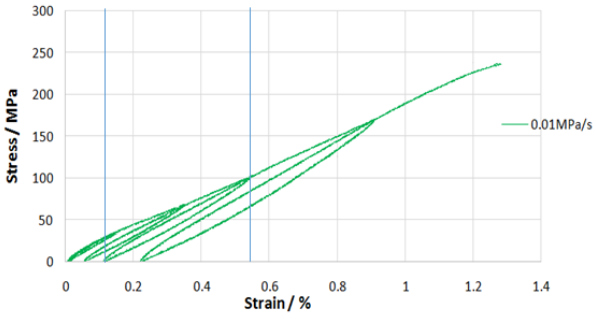

(b) With low strain rate

Fig. 4.5 Appearance of three-region behavior for unidirectional flax composite (UD110)

4.1.4 Evolution of apparent rigidity

Just as the case of humidity increases, it is shown that as the temperature increases or loading

speed decreases, the ultimate stress of UD flax fiber composite decreases. There is a big decline in ultimate stress of both more than 100 MPa in the highest temperature 80 $°C$ or lowest loading speed 0.01 $MPa\ s^{-1}$. Meanwhile the global behavior of composite is also clearly impacted by such factor (loading environment of temperature/strain rate), especially at high temperature of 80$°C$ shown in Fig. 4.5(a) and at loading speed of 0.01 $MPas^{-1}$ shown in Fig. 4.5(b). It intended to indicate three regions in the deformation behavior.

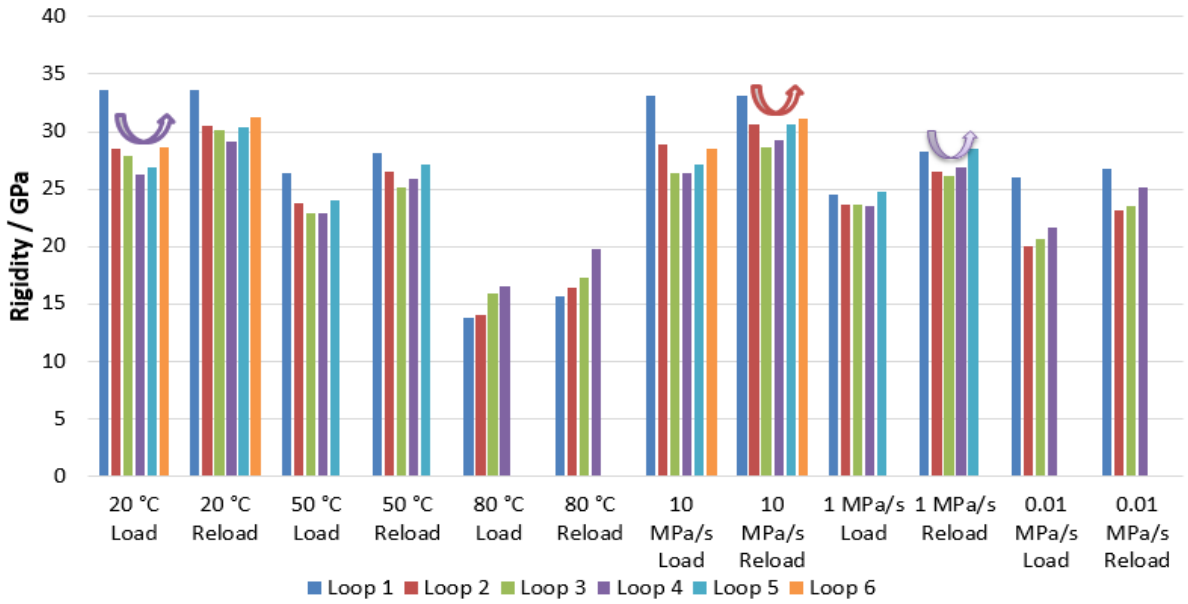

(a) Secant modulus in load and reload cycles in all cases

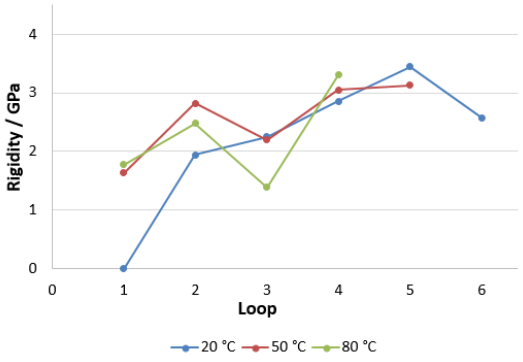

(b) Difference of secant modulus between load and reload at different temperature

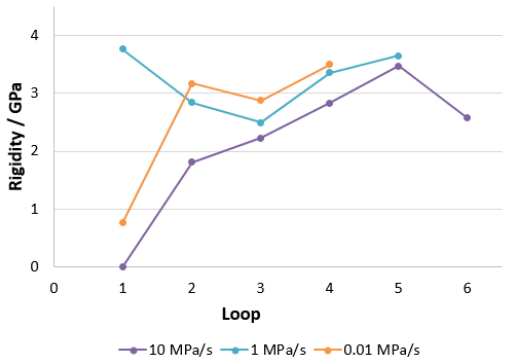

(c) Difference of secant modulus between load and reload at different strain rate

Fig. 4.6 Evolution of modulus of UD composite during RPL test in different conditions (UD110)

As shown in the Fig. 4.5, it is clear to see the unload curves and reload curves do not overlap. The evolution of the rigidity is studied on Fig. 4.6. For each loop l, the secant modulus is

calculated for the maximal stress level $\widehat{\sigma_l}$; for each following loop $l+1$, the secant modulus is also calculated for the same stress level $\widehat{\sigma_l}$. Let us call the first value "rigidity during load" and the second value "rigidity during reload". From Fig. 4.6(a), we can see that the secant rigidity firstly decreases then increases for all RPL tests, except at the test condition at 80°C. For that temperature, the experiment condition is close to the glass transition temperature of UD flax composite (T_g: $92°C$). This could be the main reason which could account for why there is no increase in rigidity for $80°C$ condition in the initial region at tensile deformation, in addition, the maximal stress level of first loop, $\widehat{\sigma_1}$, could exceed the yield stress. Obviously, the rigidity increases undergo reload for each cycle. The increase of rigidity amongst cycles after reload is higher in the low temperature interval of $20°C$ than that of $50°C$ and $80°C$, as shown in Fig. 4.6(b). For loading speed conditions, inversely, the increase rate of rigidity is higher at high strain rate which is $5 \times 10^{-4}\ s^{-1}$(corresponding to $10\ MPa\ s^{-1}$) than at the other two situations ($1\ MPa\ s^{-1}$ and $0.01\ MPa\ s^{-1}$) shown in Fig. 4.6(c). Furthermore, we can see that there is a clear decrease of secant modulus at loop 3 (Fig. 4.6(b) and Fig. 4.6(c)) for conditions of higher temperatures ($50°C$and $80°C$) and lower loading speeds ($1\ MPa\ s^{-1}$ and $0.01\ MPa\ s^{-1}$). After reload, rigidity has a visible increase, which shows us three apparent regions exist for mechanical behavior of UD flax composite in general case.

4.1.5 Evidence of permanent strain in second and third regions

Creep tests are effective measures for slow plastic deformation. Creep behavior at each region of UD flax composite expected in our work has been investigated. Constant stress $25\ MPa$, $130\ MPa$ and $200\ MPa$, respectively, following with a $0\ MPa$ were performed on each region with a duration time of $30\ min$ at an ambient temperature.

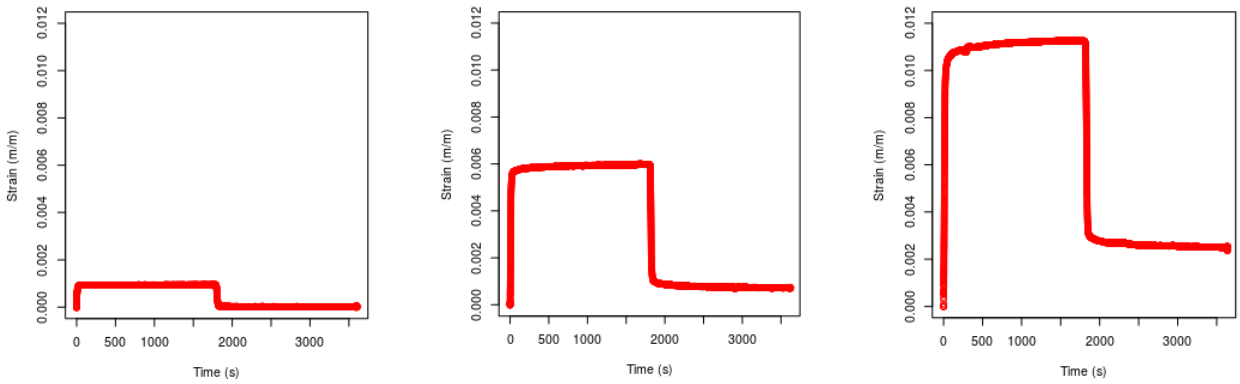

(a) 25 MPa (first region) (b) 130 MPa (second region) (c) 200 MPa (third region)

Fig. 4.7 Creep test at three levels of load corresponding to expected regions of UD110

Fig. 4.7 shows the obvious changes of strain at constant stress in the three expected regions in stress strain curve (see Fig. 4.5). In Fig. 4.7(a), when the constant stress 25 MPa was loaded on the specimen, the initial strain of the plateau increased a little fast firstly, and then with a slow increase until reached about 0.106 % from 0.098 % with an average increase rate $10^{-8}s^{-1}$. In Fig. 4.7(b), the same test with 130 MPa was carried on the second region, clearly, a bigger deformation come out which is approximate 0.59 % from the start point, meanwhile, with an average increase rate $10^{-7}s^{-1}$ reached about 0.65 %. The same observation can be done in the third region Fig. 4.7(c) which is from 1.02 % to 1.11 % with an average increase rate $10^{-5}s^{-1}$. In addition, when we performed unload to 0 MPa with a following duration 30 min, it is apparent that the UD composite restored to the initial state for 25 MPa creep test. Oppositely, the creep tests at 130 MPa and 200 MPa show irreversible deformation at about 0.07 % and 0.23 %, respectively. These observations show the evidence of viscous effects in the supposed elastic region and other viscous effects in the non-elastic regions.

Finally, it is necessary to note that there is distinctive changes in behavior between the first and the second or third region. The evolutions between the different regions could be caused by the microstructural properties where the tilt angles of the microfibrils adjust (reorientation) when the load is added on the composite and which could have an important influence on the mechanical properties[97]. In particular, the tensile deformation beyond the yield point does not deteriorate the stiffness of either individual cells or foils[98]. This indicates that there is a dominant recovery mechanism that reforms the amorphous matrix between the cellulose microfibrils within the cell wall, maintaining its mechanical properties. This “stick-slip” mechanism provides a plastic response similar to that effected by moving dislocations in

metals[98]. For lots of plant fiber composites, such behavior evolution could also be due to macroscopic adjustment at the scale of fibers, or other phenomena arising from the different components. In order to help understand the elastic phenomena that govern the mechanics of plant fiber composites, a phenomenological study is proposed later.

4.2 Previous phenomenological model

A viscoelastoplastic model about flax fiber composite behavior at 20℃ has been developed in our team with the help of the specialist Fabrice Richard[47]. The parameters of this model have been identified on quasi-UD flax yarn and quasi-UD flax textile reinforcements based on twisted yarn[47]. quasi-UD flax yarn are constituted by "big" non-woven yarns (more than $20\ tex$) aligned in one direction only. Quasi-UD flax textile is constituted by "small" woven yarns ($24\ tex$), aligned in two perpendicular directions: warp and weft. The weft yarns – which are ten times fewer than warp yarns - are necessary for the ply handiness.

The total strain ε is partitioned in an elastic part ε^{e} (instantaneous reversible strain) and an inelastic part ε^{in} which is the sum of viscoelastic contribution ε^{ve} (time-dependent reversiblestrain) and viscoplastic contribution ε^{vp}(time-dependent irreversiblestrain):

$$\varepsilon = \varepsilon^{e}+\varepsilon^{ve}+\varepsilon^{vp}. \tag{4.1}$$

In the context of thermodynamics, physical phenomena can be described with a precision which depends on the choice of the nature and the number of state variables. The state variables, also called thermodynamic or independent variables, are the observable variables and the internal variables. The standardized framework[47] assumes that mechanical behavior is obtained when two potentials are defined: a free energy density ψ to define state laws and a dissipation potential Ω to determine flow direction. Based on experimental results of ultimate stress, ultimate strain and Young's modulus, and that elasticity and inelastic behaviors are uncoupled, the two potentials are proposed. The state laws can then be written as:

$$\sigma = \rho\frac{\partial\psi}{\partial\varepsilon^{e}} \tag{4.2}$$

$$X_i = \rho\frac{\partial\psi}{\alpha_i} \tag{4.3}$$

where α_i and X_i variables stand for inelastic phenomena, ρ is the mass density, and σ is the Cauchy's stress.

The evolution of internal variables is expressed as:

$$\dot{\varepsilon}^{in} = \frac{\partial \Omega}{\partial \sigma} = \dot{\varepsilon}^{ve} + \dot{\varepsilon}^{vp} \tag{4.4}$$

$$\dot{\alpha}_i = -\frac{\partial \Omega}{\partial X_i}. \tag{4.5}$$

The system of ordinary differential equations has been solved with a homemade simulation software, MIC2M[47], using an algorithm based on the Runge-Kutta method. An inverse approach is used to extract the parameters from the experimental strain measurements. This approach consists of an optimization problem where the objective is to minimize the gap between the experimental strain ε_m (m "measured") and the numerical result ε_c (c "calculated"), which can be defined as:

$$\Theta^* = argmin\, f(\Theta) \tag{4.6}$$

$$f(\Theta) = \sum_{i=1}^{N} \left(\frac{\varepsilon_c(\Theta, t_i) - \varepsilon_m(t_i)}{N \varepsilon_{max}} \right)^2 \tag{4.7}$$

where the vector $\Theta = [\Theta_1, \dots, \Theta_n]$ collects the unknown parameters to be identified and $f(\Theta)$ is the cost function. The ith data point corresponds to the acquisition timet_i. N is the number of the acquisition times in the experimental test. ε_{max} is a weighting coefficient defined as the maximum strain values. The minimization problem was solved using an algorithm based on the Levenberg-Marquardt method coupled with genetic approach implemented in MIC2M software[47].

To determine if the information is suitable for reliable parameter estimation Θ^*, a practical identifiability analysis was performed on results[47]. This identifiability analysis is based on local sensitivity functions. Such functions quantify the relationship between the outputs and the parameters of the model. Poor identifiability of the model parameters can be due to a small sensitivity of the model results to a parameter, or by a linear approximation dependence of sensitivity functions on the results with respect to the parameters. High collinearity index indicates correlation among the parameters. Parameter subsets with collinearity index smaller than five are considered as good and experiment values above twenty are critical (see Poilâne et al.[47] for detail). This approach led our team to model the mechanical behavior of the flax fiber composite by a phenomenological model with kinematic hardening taking viscosity into account. The viscoelastoplastic model was identified in the case of uniaxial test of UD flax

yarn/epoxy composite at 20°C [47]. The particularity of the reinforcement is the disorientation of constitutive fibers due to the use of twisted yarns.

Based on experimental results, the free energy and dissipation potential are proposed in the following equations:

$$\psi(\varepsilon^{e}, \alpha_i) = \frac{1}{2\rho} E(\varepsilon^{e})^2 + \frac{1}{2\rho} \sum_{i=1}^{3} C_i \alpha_i^2 \tag{4.8}$$

$$\Omega = \Omega^{ve} + \Omega^{vp} = \frac{1}{2n} (\sigma - X_1)^2 + \frac{1}{2K} < f >^2 \tag{4.9}$$

$$f = |\sigma - X_1 - X_2 - X_3| - \sigma_Y + \frac{\gamma_3}{2C_3} {X_3}^2 \tag{4.10}$$

where ρ is the mass density, E and σ_Y are the Young's modulus and the initial yield stress, respectively, n and K are viscosity coefficients corresponding to elastic and plastic phenomena, respectively. C_1 is the viscoelastic stiffness. C_2 , C_3 and γ_3 are hardening coefficients. C_2 characterizes linear kinematic hardening. C_3 and γ_3 refer to nonlinear kinematic hardening coupled to a contraction of elastic region in order to imporove the unloading modeling in RPL tests. The symbols <> denote Macauley's brackets such as $< x > = x$ if $x \geq 0$ and $< x > = 0$ in other cases. The state laws for mechanical behavior become:

$$\sigma = E\, \varepsilon^{e} \tag{4.11}$$

$$X_i = C_i \alpha_i \tag{4.12}$$

and the evolution of internal variables defined becomes:

$$\dot{\varepsilon}^{ve} + \dot{\varepsilon}^{vp} = \frac{1}{\eta} (\sigma - X_1) + \frac{< f >}{K} sign(\sigma - X_2 - X_3) \tag{4.13}$$

$$\dot{\alpha}_1 = \frac{1}{\eta} (\sigma - X_1) \tag{4.14}$$

$$\dot{\alpha}_2 = \frac{< f >}{K} sign(\sigma - X_2 - X_3) \tag{4.15}$$

$$\dot{\alpha}_3 = \frac{< f >}{K} \left[sign(\sigma - X_2 - X_3) - \frac{\gamma_3}{C_3} X_3 \right]. \tag{4.16}$$

From a rheological point of view the model proposed in Poilâne et al.[47] is for elastic contribution a linear spring E, and for viscoelastic contribution a classical Kelvin-Voigt model which comprises a linear viscous damper and a linear spring connected in parallel. A more complex model is required for viscoplastic contribution, it consists in adding two-kinematic

hardenings: a linear kinematic hardening and a non-linear kinematic hardening. In addition, a coupling between translation and contraction of the elastic region during loading is added. Finally, seven inelastic parameters have to be identified: viscosity coefficient in elastic region $\eta(\mathrm{MPa\ s})$, viscoelastic stiffness $C_1(\mathrm{MPa})$, initial yield stress σ_Y (MPa), viscosity coefficient in plastic region K $(\mathrm{MPa\ s})$, kinematic hardening coefficient $C_2(\mathrm{MPa})$, non-linear hardening $C_3(\mathrm{MPa})$, and non-linear hardening γ_3. The eighth parameter, namely the Young's modulus, was chosen from experimental measurement ($E = 26.9$ GPa). The inverse method approach was used to extract constitutive inelastic parameters from the strain measurements on two tests:

- test A: repetitive progressive loading in tension,
- test B: creep in tension at 29 MPa.

The RPL was chosen to activate mainly viscoplastic phenomena and the creep test at 29 MPa (under initial yield stress) was chosen to activate mainly viscoelastic phenomena. Fig. 4.8 – coming from Poilâne et al.[47] – shows RPL simulation (left) and creep simulation (right). The used parameter has been identified by UD flax yarn composite tests at room temperature and standard speed ($\dot{\varepsilon} = 1e^{-6}s^{-1}$). The total strain (in red) is partitioned by three contributions (elastic in black, viscoelastic in dotted line, viscoplastic in blue). Elastic contribution is naturally activated all over the test. Viscoelastic contribution is very low at room temperature and standard speed. Creep test at 29 MPa mainly shows elastic contribution, as expected, and viscoplastic contribution is major over 50 MPa.

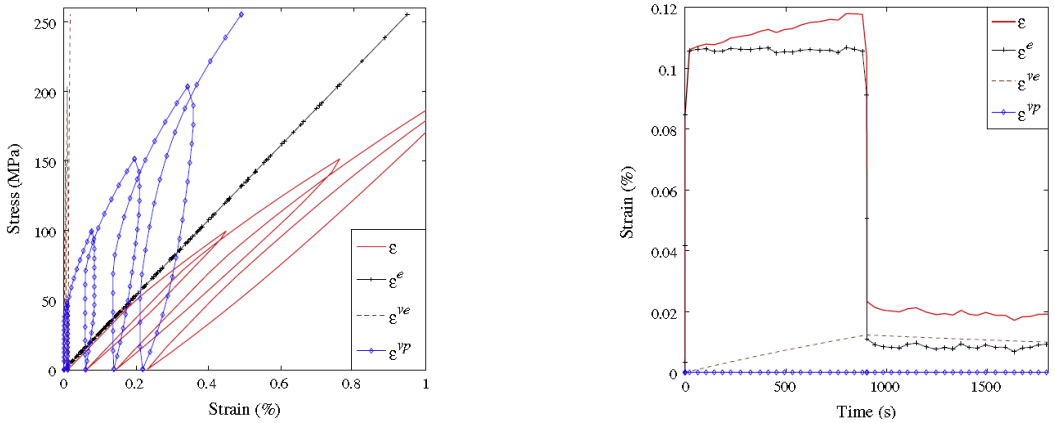

(a) RPL test (b) Creep test at 29 MPa

Fig. 4.8 Simulation response according to elastic contribution, viscoelastic contribution and viscoplastic contribution, the tests were conducted on UD flax yarn composite at room condition and standard speed

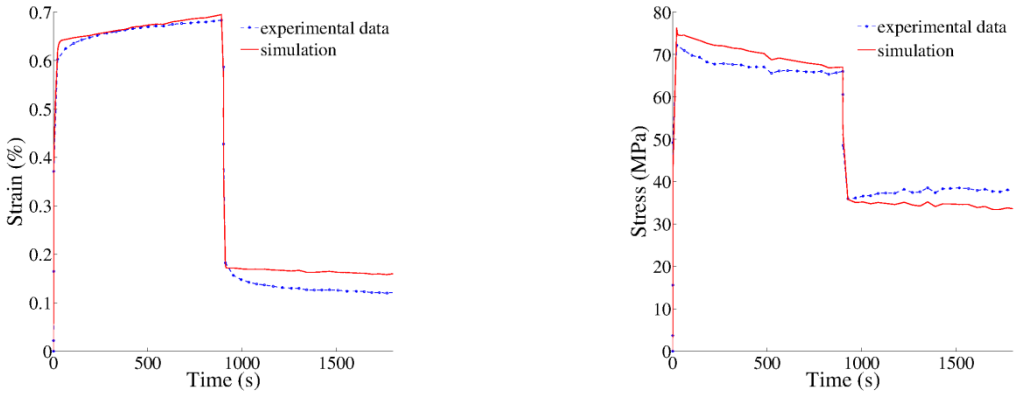

(a) Creep test at 126 MPa

(b) Relaxation test at 0.33%

Fig. 4.9 Experimental data and simulation, the tests were conducted on unidirectional twisted yarn/epoxy composite at room condition and standard speed

At room temperature, the proposed model allows us to correctly simulate the behavior of flax yarn reinforced epoxy composite in repetitive progressive loading, creep test and relaxation test (see Fig. 4.9). In conclusion, for "unidirectional" twisted yarn/epoxy composite at room condition and standard speed, the first region of monotonic tensile curves is quasi-elastic and the second region is viscoelastoplastic. This model cannot describe the three-region mechanical behavior described in Section 4.1 but constitutes a good base to analysis purely unidirectional flax epoxy composite. This analysis will be treated in the next section.

4.3 Toward a more global model

The phenomenological model presented in previous section did not need "strengthening parameter" to correctly simulate standard flax fiber composite in normal condition. The idea of a strengthening phenomenon is due to one of the stronger assumption researchers make in case of bast fiber reinforced polymer: the possibility for microfibrils to realign themselves during longitudinal loading (microfibril being the main component of bast fibers as we seen in Section 1.3), even when fibers are trapped inside the matrix. The re-orientation of microfibrils has been demonstrated experimentally on elementary fiber and bundle of fibers under tensile test[97]. It has been correlated to experimental tensile curve by an inverse approach using finite element model[99]. Consequently, the first need to test our model for more complex cases than previous one was to improve the direction of the fibers inside composite. Indeed, it is clear that twisted flax yarn as reinforcement is not the best candidate to activate the reorientation of microfibrils inside a composite. It is known that in case of twisted yarn some of the fibers are oriented into the main direction, but globally fiber orientation follows a statistical distribution

with major part of fibers aligned not in the longitudinal direction. Inside the purely unidirectional flax ply (Flaxtape^{TM}), the fibers are mainly oriented in the longitudinal direction (see Fig. 2.7 and Fig. 3.1). In this product, there are no any weft yarn and no any sewing to link the fibers together. The reinforcement inside the final composite products is constituted by a mix of elementary fibers and technical fibers (bundle forms) as described in Chapter 2. Consequently, these reinforcements are mainly oriented in the same direction in the composite, inside we find "optimal organization" in term of mechanical behavior analysis.

We have previously showed that temperature impacts the apparent behavior of flax fiber reinforced polymers[48]. Firstly, the rigidity of epoxy matrix decreases with increasing temperature. Particularly, the mechanical properties of thermosetting media drastically decrease when temperature nears to the glass transition temperature T_g of the material. Secondly, high temperature activates viscoelastic properties of bast fibers[100]. One macroscopic consequence of temperature increase is to make possible a description of tensile curve by three apparent regions as we shown in Section 4.1. Note also that the increase of specimen moisture itself promotes viscous effects of flax composite and makes also visible a three-region apparent tensile curve[48]. Temperature and humidity decrease the material rigidity. Another way, more simple, is to decrease the strain rate of the tensile test. When the strain rate is low, viscous effects are more visible[47]. The mechanisms which are responsible to viscous effects are easier to activate with "low strain rate", "high testing temperature" or "high specimen moisture". Eventually, to test our model with unidirectional flax composite we choose repetitive progressive load at four different stress rate ($10\,MPa\,s^{-1}$ to $0.01\,MPa\,s^{-1}$). For the lower speed, experiment curve is constituted by three apparent regions instead of two, the first region being quasi-elastic and the third region showing increase tangent rigidity.

Firstly, we have tried to describe the increasing apparent rigidity by the viscous parameters combining the previous model. Note that the increase of apparent tangent modulus can be described by the viscous parameters of previous constitutive model. The previous phenomenological model was possible to fit on experimental data with the same set of inelastic parameters (but different values).

Table 4.1 Elastic and inelastic material parameters for unidirectional flax/epoxy composite (UD110)

Parameter	Definition	Identified value
$E\ (MPa)$	Young's modulus	3.15×10^4
$\eta\ (MPa\ s)$	Viscosity coefficient in elastic region	1.98×10^6
$C_1\ (MPa)$	Viscoelastic stiffness	7.72×10^4
$\sigma_Y\ (MPa)$	Initial yield stress	2.38×10^1
$K\ (MPa\ s)$	Viscosity coefficient in plastic region	1.92×10^7
$C_2\ (MPa)$	Kinematic hardening coefficient	3.92×10^4
$C_3\ (MPa)$	Nonlinear hardening	4.26×10^4
γ_3	Nonlinear hardening (recall)	1.62×10^3

Fig. 4.10 shows the best fits we obtained for both extreme strain rates. The eight identified parameters are given in Table 4.1. It is clearly visible that the test simulation at the lowest stress rate does not correlate very well with the experimental data (Fig. 4.10(b)). In that case, the increase of apparent tangent modulus – visible on fourth and fifth load – was not possible to simulate. Moreover, depth look on Fig. 4.10(a) shows that this behavior was neither possible to simulate on seventh load of the test at $10\ MPa\ s^{-1}$. Something like a strengthening effect has not been taken into account with our model for a strain above 1% (depending on the stress rate). Consequently for this under-estimation of apparent rigidity, the permanent strains predicted by our model of are lower than the experimental ones, loop after loop.

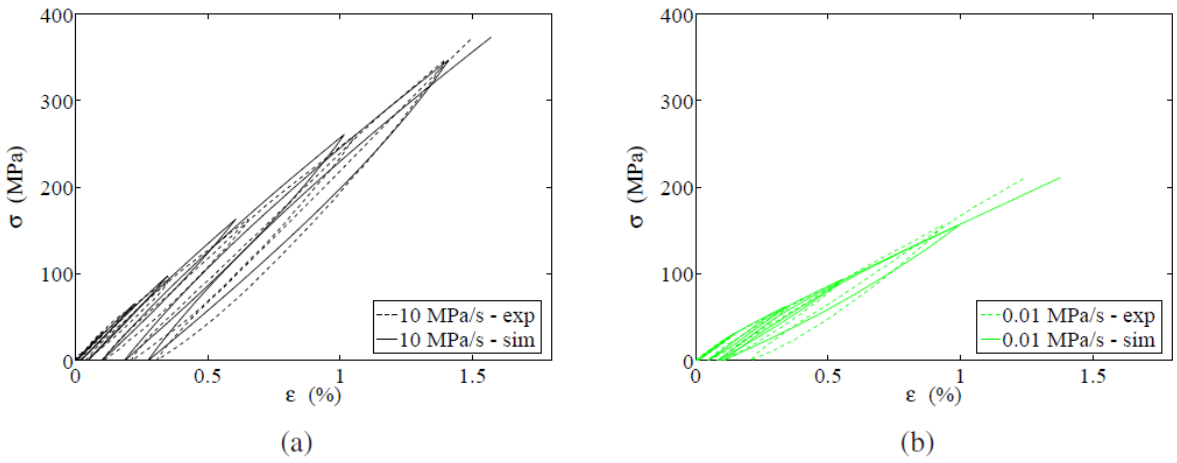

Fig. 4.10 RPL experiment and simulation with the phenomenological model

Testing the idea of using strengthening parameter seems now a good option to improve the phenomenological model. Fig. 4.11 shows the first result we have obtained with the same data as used for Fig. 4.10 when we "replace" the nonlinear hardening C_3 and γ_3 with two strengthening parameters. The fitting of experimental data by simulation is clearly improved at the lowest stress rate (Fig. 4.11(b)).

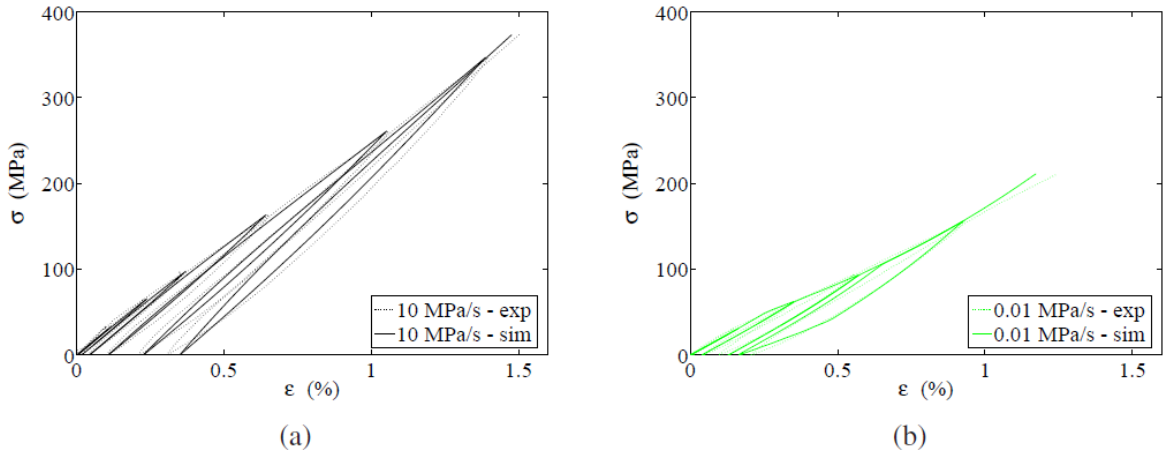

Fig. 4.11 RPL experiment and new simulation with two strengthening parameters

Although this new approach is not totally validated at this day – it is necessary now to mix the two models with both non-linear hardening parameters and strengthening parameters – it offers an elegant solution because it seems easy to correlate the cyclic strengthening to a reinforcement reorientation by longitudinal loading in case of unidirectional flax composite. In a near future, analysis of such upgraded model will help at exploring the origin of the mechanical behavior of plant-based reinforced organic polymers.

4.4 Conclusion

In conclusion, an apparent cyclic strengthening in tensile is not possible to simulate with our previous viscoelastoplastic model. For an adapted material and specific tests, the difference between experimental data and simulation – once the viscoelastoplastic parameters identified – is noticeable. Low stress rates in tensile were used here, but we make the assumption that high temperature tests or tensile tests on moisturized specimens should offer good possibilities also. Finally, we propose as strong assumption that the addition of a strengthening phenomenon to the initial model[47] offers a good solution to improve simulation.

Chapter 5 WATER SORPTION OF UNIDIRECTIONAL FLAX FIBER COMPOSITE

Not only flax fibers but also most of plant fibers such as sisal, bamboo and wood, etc. mainly comprised of cellulose are sensitive to changes in atmospheric conditions, particularly moisture[101][102]. There is a limited resistance to moisture sorption because of their hydrophobicity. Swelling by water uptake can lead to micro cracking and low dimensional stability of the composite and decrease the mechanical properties[103]. In addition, plant fibers are easy to be infiltrated or wetted with polar water, on the contrary, not easy to be accessed by non-polar resin and which results in an interface which is not as good as artificial fibers with mature crafts manship. These problems represent a major obstacle for composite materials reinforced by plant fibers. It is therefore important to characterize the phenomenon sorption behavior of moisture of the plant fibers. The aim here is to investigate the water sorption behavior of UD flax fiber composite.

Sorption test is a technique used to study the uptake of moisture of a material. It is intended to measure the amount of water absorbed by the sample over the time to a potential level of saturation, the speed of water penetration into the material, and the sorption kinetics. Experimentally, measuring the water sorption of a material is performed by a gravimetric analysis. This method consists in measuring the water content absorbed as a function of exposure time. Sorption test is very useful in plant fiber reinforced polymer, because it offers the opportunity to analysis quality of composite production (efficiency of fiber treatment, compatibility between reinforcement and matrix…).

The first step is to remove any traces of moisture within the material. For this, the samples are placed in an oven for 22 hours at a temperature of 80℃. To ensure unidirectional sorption, the edges of the samples can be sealed by a high temperature silicone layer with a negligible water sorption ($< 1\%$). Taking into account the mass of the silicone border, the mass of the sample in this state is measured and recorded as W_0. After oven-dry step the samples are submerged in water at a temperature stabilized at 20℃ and humidity 45% according to the standard test method ASTM D5229/D5229M[104]. A value of the sample mass is carried out at regular intervals to determine the rate of water absorbed versus time. The average amount of absorbed moisture in a material is measured, taken as the ratio of the mass of the moisture in

the material to the mass of the oven-dry material and expressed as a percentage. The water sorption ratio M at time t can be evaluated by the relative weight uptake as follows:

$$M = \frac{M^t - M^0}{M^{00}} \tag{5.1}$$

where: M^t = current specimen mass, M^{00} = oven-dry specimen mass, M^0 = mass of oven-dry specimen sealed with silicon.

5.1 Mechanism of water sorption in flax fiber reinforcement

As described in the Section 1.3, flax fibers are mainly composed of cellulose (including crystalline and amorphous cellulose) and hemicelluloses with multiple hydroxyl groups (OH) on the glucose chain. Cellulose has hydroxyl groups which allow it to form hydrogen bonds with water. Fig. 5.1 illustrates an example of the water adsorption mechanism by a glucose molecule (basic molecule of the cellulose). The glucose molecule contains three hydroxyl groups, and three water molecules are attracted to the hydroxyl groups to form hydrogen bonds. Hydrophilicity of plant fibers is mainly due to the hydroxyl groups (OH) on the surface of the molecules. With a ratio of three hydroxyl groups per glucose repeat unit the amount of water that can be absorbed is substantial[105].

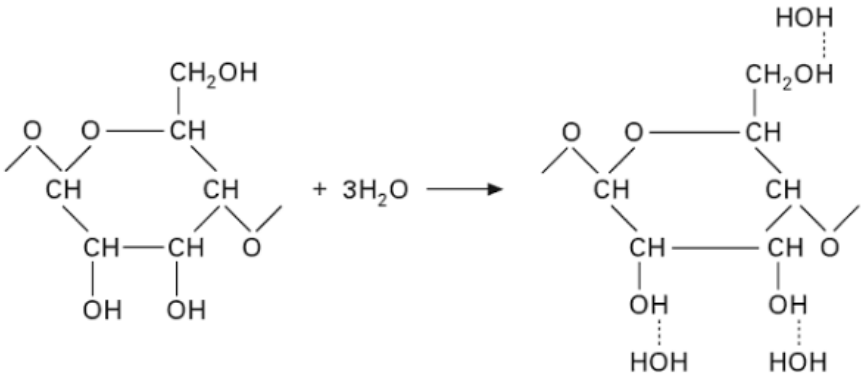

Fig. 5.1 Adsorption of water hydrogen bonding to hydroxyl groups in a cellulose molecule

Besides the moisture adsorption of water molecules on the surface of the cellulose fibers, other two mechanisms also play roles in moisture uptake. One is the capillary action through the lumen and another is capillary bridges between the fibers[106]. The interactions between fiber and water originate from the non-crystalline region and extend to the crystalline region[107]. However, lignin mainly comprised of aromatics[108] has little effect on water

sorption. The interaction of cellulose fiber with water is enhanced by tiny cracks formed on the fibers and, the cracks allow penetration of water inside enable the cellulose molecules-bonding that make up its walls. The water penetrates the cracks on the fiber, searching new cellulose chains, which increases the surface area of the fiber resulting in a greater water contact with the cellulose. During exposure to the water, the cellulose fiber swells, its volume increases, mainly in the transverse direction.

5.2 Mechanism of water sorption in polymer

Generally speaking, the equilibrium solubility of water in typical polymer is very small and a limiting form of Flory's equation could make estimation as expressed below[109]:

$$\delta = e^{-\left[1.34+\frac{v}{RT}(k_1-k_2)^2\right]} \tag{5.2}$$

where δ is the volume fraction of liquid absorbed at equilibrium, v is the molar volume of liquid, R is the universal gas constant, T is the absolute temperature, and k_1 and k_2 are the solubility parameters of the liquid and polymer respectively. For the commonly used polymers, the equilibrium solubility of water will range from about 0.02 to 0.2% by wt. Hence the uptake of water in amounts much greater than these values must be attributed to other causes. In our lab previous studies, thermoset epoxy system based on Araldite LY5150 associated with an amine hardener Aradur 5021 and an accelerator XB3471 give an equilibrium solubility of water 3% by weight at a stabilized temperature 20°C[49]. Fedoras proposed the diffusion rate of liquid depends on the cavity[109]. Firstly, water diffuses into the polymer a rate which depends on the geometry of the test specimen and the chemical nature of the polymer and then after some time the water contacts inclusion which will be dissolved. When the inclusion first begins to dissolve, the solution is relatively concentrated, and which make an enhancement in the increase of diffusion rate of water. The increase of porosity volume is equal to the water exist in the polymer. In our lab previous observation, the water uptake performance of pure epoxy resin in the sorption process is closed to Fickian behavior which will be described below.

5.3 Fickian diffusion model

5.3.1 Fick's laws

A simple model to describe the diffusion of a solvent into a solid material is given by Fick's laws (1855)[110]. They are based on the assumption that the flow of the penetrant (water for example) in the material is proportional to the concentration gradient. Fick's first law relates the diffusive flux to the concentration under the assumption of steady state. It postulates that the flux goes from regions of high concentration to regions of low concentration, with a magnitude that is proportional to the concentration gradient (spatial derivative), or in simplistic terms the concept that a solute will move from a region of high concentration to a region of low concentration across a concentration gradient. The rate of diffusion is characterized by the diffusion coefficient D. Thus, the Fick's first law in one (spatial) dimension is expressed by the following equation.

$$\mathrm{J} = -\mathrm{D}\frac{\mathrm{d}\varphi}{\mathrm{dx}} \tag{5.3}$$

where J is the "diffusion flux", of which the dimension is amount of substance per unit area per unit time ($\mathrm{mol\,m^2 s^{-1}}$); D is the diffusion coefficient or diffusivity, its dimension is area per unit time ($\mathrm{m^2 s^{-1}}$); φ (for ideal mixtures) is the concentration, of which the dimension is amount of substance per unit volume ($\mathrm{mol\,m^{-3}}$); x is position (m). D is proportional to the squared velocity of the diffusing particles, which depends on the temperature, the viscosity of the fluid, and the size of the particles. The negative sign in Equation (5.3) indicates that the flow is directed from high concentration areas to low concentration areas. In two or more dimensions the gradient operator ∇ can be used which generalizes the first derivative, obtaining:

$$\mathrm{J} = -\mathrm{D}\nabla\varphi. \tag{5.4}$$

The Fick's second law involving time predicts how diffusion causes the concentration to change with time. It is a partial differential equation in one dimension written as below:

$$\mathrm{div\,J} = \frac{\mathrm{d}\varphi}{\mathrm{dt}} \tag{5.5}$$

$$= -\mathrm{D}\frac{\partial^2\varphi}{\mathrm{dx}^2}. \tag{5.6}$$

The diffusion coefficient and equilibrium sorption of penetrant in the materials are key parameters in the part of considering the behavior in the Fickian diffusion. For the utilization of the Fick's second law, several hypotheses have been implemented:

1. the temperature and moisture distributions inside the material are uniform,
2. the moisture content and the temperature of the environment are constant.

To achieve the points above, rigorous sorption experiments are performed with optimization of test procedures in order to avoid unnecessary errors. The material is exposed to the environment on one side or on two sides with both sides being parallel.

5.3.2 Common sorption types

The overall effect can be modeled conveniently considering only the diffusional mechanism in polymeric media[111][112][113][114]. According to the diffusion behavior of relative mobility of the penetrant and of the polymer segments, there are three different categories of diffusion behavior in polymeric:

- *Case I or Fickian* diffusion, in which the rate of diffusion is much less than that of the polymer segment mobility. The equilibrium inside the polymer is rapidly reached and it is maintained with independence of time.
- *Case II (and Super Case II)*, in which penetrant mobility is much greater than other relaxation processes. This diffusion is characterized by the development of a boundary between the swollen outer part and the inner glassy core of the polymer. The boundary advances at a constant velocity and the core diminishes in size until an equilibrium penetrant concentration is reached in the whole polymer[102].
- *Anomalous or Pseudo-Fickian* the former diffusion occurs when the penetrant mobility and the polymer segment relaxation are comparable. It is then, an intermediate behavior between Case I and Case II diffusion. The latter diffusion curves resemble true *Fickian* curves inasmuch as they do not exhibit any inflection in slope. The initial portion of the curves is linear, but only over a small part of the total concentration change, the approach to final equilibrium is very slow.

These three main cases of diffusion can be distinguished theoretically by the shape of the sorption curve represented by:

$$\frac{M}{M^{\infty}} = kt^{n} \tag{5.7}$$

where M is the moisture content at time t, M^{∞} is its maximum moisture content at the equilibrium state, and k and n are the diffusion kinetic parameters. The diffusion exponent n indicates the case of diffusion. Diffusion obeys Fickian law, while n is equal to 0.5. Other mechanisms has been established for diffusion phenomenon in polymers and categorized based on the exponent n, as follow:

- $n < 0.5$ *pseudo-Fickian,*
- $n = 0.5$ *case I,*
- $0.5 < n < 1$ *anomalous,*
- $n = 1$ *case II,*
- $n > 1$ *super case II.*

The major sorption curves are as shown in Fig. 5.2.

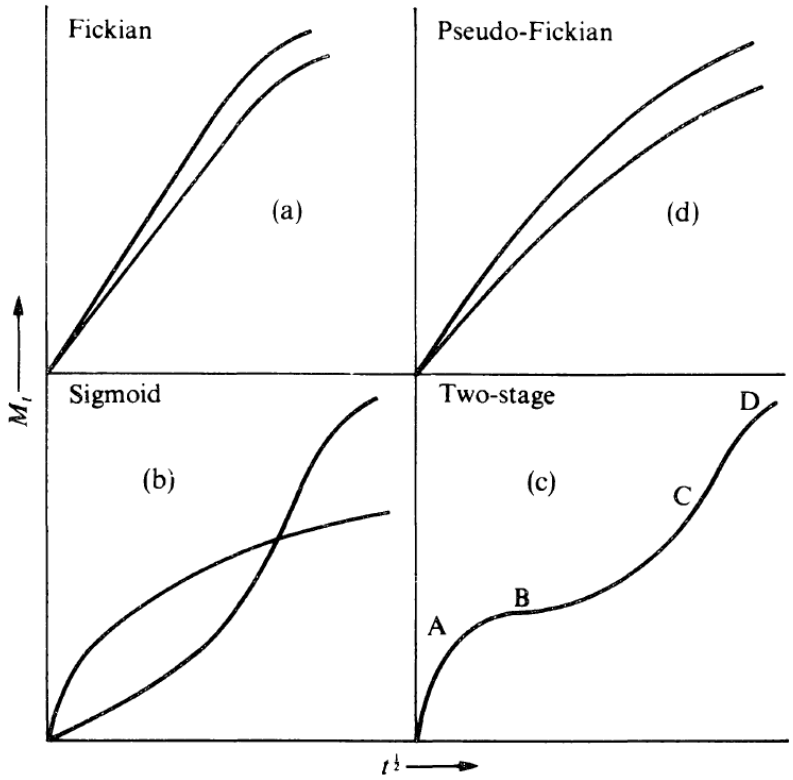

Fig. 5.2 "Non-Fickian" or "anomalous" sorption curves compared with Fickian-type curves[115]

Two models able to describe two-stage sorption types – two-phase model and Langmuir's model – have gained important applications and concerns in the composite technology community[116][117][118][49]. They will be presented later.

5.3.3 Diffusion, sorption, and permeability coefficients

Using the assumption of Fick's laws described previously the percentage moisture content as a function of time can be calculated from the following equation[119][120][121][122]:

$$\frac{M - M^0}{M^\infty - M^0} = 1 - \frac{8}{\pi^2}\sum_{n=0}^{\infty}\frac{1}{(2n+1)^2}\exp\left[-\frac{(2n+1)^2\pi^2 Dt}{h^2}\right] \tag{5.8}$$

which is obtained by integrating the solution to Equation (5.6)[115][123] over the thickness of plate, h. Sorption ratio of penetrant in the solid material as a function of square root of time can be characterized by two zones: an initial linear region followed by a plateau curve versus the abscissa in the Fickian diffusion. For the initial part (M/M^∞ smaller than 0.6) the initial slope ($t < t_x$) is constant, which is illustrated in the following equation and Fig. 5.3:

$$\frac{M - M^0}{M^\infty - M^0} = \frac{4}{h}\sqrt{\frac{Dt}{\pi}} \tag{5.9}$$

where h is the thickness of specimen, n is the summation index, M^0 is the initial moisture content (for the oven-dry specimens, the value M^0 is zero), D is the diffusion coefficient which is a key parameter complies with the equation as below in the initial part of the sorption curve.

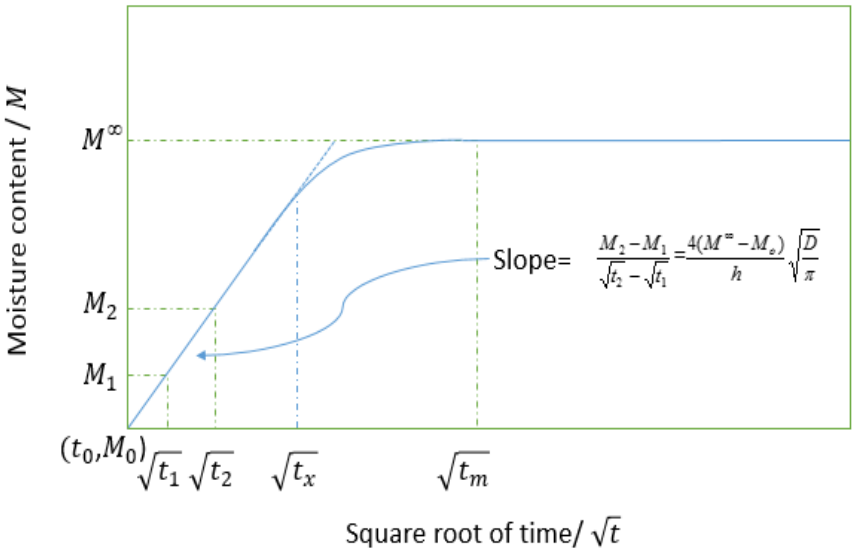

Fig. 5.3 Illustration of the relationship between the initial slope part and the moisture content with the square root of time[121]

In addition, the mass square of absorbed water varies linearly with the immersion time t in the initial part. The diffusion coefficient D in Fickian law by Equation (5.9) is transformed as below:

$$D = \frac{\pi}{16t}\left(\frac{(\mathrm{M}-\mathrm{M}^0)h}{\mathrm{M}^\infty-\mathrm{M}^0}\right)^2 \tag{5.10}$$

$$= \pi\left(\frac{h\theta}{4M^\infty}\right)^2 \tag{5.11}$$

where the coefficient θ is the slope of the linear part in the sorption curve when the abscissa is the square root of time (as in Fig. 5.3). For the second half-sorption – M/M^∞ upper than 0.6 – Shen et al.[121] proposed the following approximation:

$$\frac{\mathrm{M}-\mathrm{M}^0}{\mathrm{M}^\infty-\mathrm{M}^0} = 1-\exp\left[-7.3\left(\frac{\mathrm{Dt}}{\mathrm{h}^2}\right)^{0.75}\right]. \tag{5.12}$$

In the case of epoxy matrix, due to its hydrophobic nature the amount of water uptake is negligible. The increasing water sorption is caused, among other factors, by the higher hydrophilic nature of flax fiber compared to the epoxy matrix, the greater interfacial area (capillary effect comparing the epoxy matrix only), and the presence of percolated porosities when occurs[49]. Solubility as related to chemical nature of penetrant and polymer, is the capacity of a polymer to uptake a penetrant. Here, the sorption coefficient S which defines

volume of penetrant exists in per unit volume of polymer with per unit pressure is calculated using the following equation:

$$S = \frac{M^e}{M^{00}} \tag{5.13}$$

where M^e is the mass of the penetrant at equilibrium swelling and M^{00} is the initial mass of the specimen as described above. The permeability coefficient, P, is defined as volume of the penetrant which passes per unit time through unit area of polymer having unit thickness, with a unit pressure difference across the system. The permeability coefficient which implies the net effect of sorption and diffusion is given by the relation[124]:

$$P = DS. \tag{5.14}$$

Typical units for P are $(cm^2 s^{-1} Pa^{-1})$, those units $\times 10^{-10}$ are defined as the barrier the standard unit of P.

5.4 Model for two-stage sorption type

5.4.1 Two-phase model

The previous sorption results in our laboratory about textile flax yarn composite encouraged us to analyze the sorption behavior with a two-phase model[116][49]. In this model, the moisture transport has also been successfully predicted and interpreted. The two-phase model consists of two Fickian diffusions in parallel. Both the Fickian diffusion models involve separate diffusion coefficient (D_1 and D_2) and saturation levels ($M_1^\infty - M_1^0$) and ($M_2^\infty - M_2^0$), respectively, which can be represented by the equation as below:

$$\begin{aligned} M - M^0 = \quad & (M_1^\infty - M_1^0)\left(1 - \frac{8}{\pi^2}\sum_{n=0}^{\infty}\frac{1}{(2n+1)^2}\exp\left[-\frac{(2n+1)^2\pi^2 D_1 t}{h^2}\right]\right) \\ & +(M_2^\infty - M_2^0)\left(1 - \frac{8}{\pi^2}\sum_{n=0}^{\infty}\frac{1}{(2n+1)^2}\exp\left[-\frac{(2n+1)^2\pi^2 D_2 t}{h^2}\right]\right) \end{aligned} \tag{5.15}$$

with

$$M^\infty = M_1^\infty + M_2^\infty \tag{5.16}$$

$$M^0 = M_1^0 + M_2^0. \tag{5.17}$$

M^0, M_1^0 and M_2^0 are the initial moisture of the test specimen and two Fickian phases. After oven drying we consider these parameters as null. The sum of the two moisture uptake of diffusion gives out the total moisture uptake in the tested specimen in which one of the Fickian diffusion is faster and in dominance in regard to another, as described in Fig. 5.4.

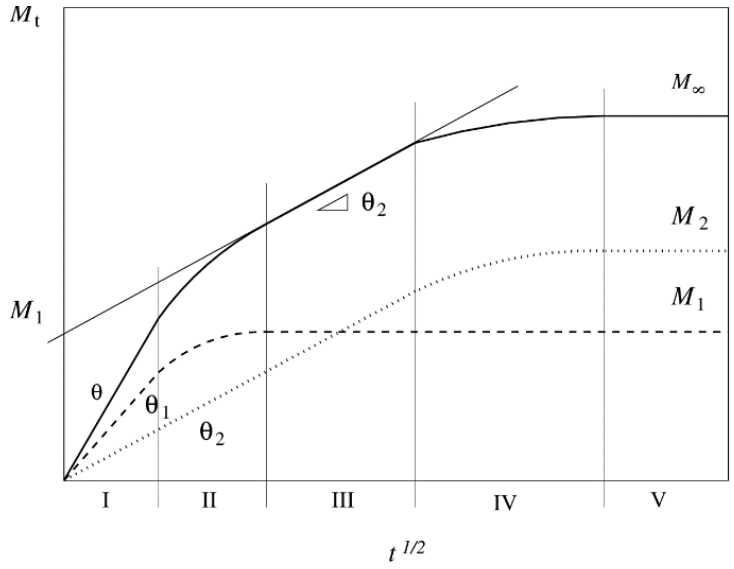

Fig. 5.4 Two-phase model[49]

5.4.2 Langmuir's model

This model developed by Carter, and Kibler is based on the Langmuir theory of adsorption on surface with the idea assuming the moisture uptake is dominated by the mobile and bound water molecules[116][117][118]. The free mobile molecules diffuse with a concentration and stress independent diffusion coefficient D_γ and are absorbed (become bound) with a probability per unit time γ at certain sites (e.g. porosity or hydrogen bonding). Molecules are emitted from the bound phase, thereby becoming free mobile, with a probability β per time unit.

The total moisture uptake in an initially dry one-dimensional specimen satisfies the following coupled set of equations:

$$M - M^0 = (M^\infty - M^0)\left(\frac{\beta}{\gamma+\beta}e^{\gamma t}y(t) + \frac{\beta}{\gamma+\beta}\left(e^{-\beta t} - e^{-\gamma t}\right) + 1 - e^{-\beta t}\right) \tag{5.18}$$

where

$$y(t) = 1 - \frac{8}{\pi^2}\sum_{n=0}^{\infty}\frac{1}{(2n+1)^2}\exp[-(2n+1)^2 kt] \tag{5.19}$$

where

$$k = 1 - \frac{\pi^2 D_\gamma}{h^2}. \tag{5.20}$$

5.5 Factors that affect sorption performance in composite material

The sorption behavior of water in composite reinforced by plant fiber depends on several parameters. Besides, the chemical and physical properties of plant fibers and matrix have fundamental impact on the sorption behavior, both the internal structure of composite such as fraction of components (matrix, fiber, porosity), fiber orientation, interface quality, etc., and the external environment e.g. temperature, humidity, etc., have obvious influence on the sorption performance of water into plant fiber composites. Kreze et al.[125] reported that, for cellulose fiber forming polymers, the influence of the crystalline regions (their size and orientation) on the adsorption character is less important than that of the amorphous regions, the size and organization of porosities, and the interaction properties of the surface. In long unidirectional flax fiber/resin composite, the structure is heterogeneous and anisotropic, so the diffusion coefficient is not the same in all directions. The penetration of water inside composite material is governed by different mechanisms involving diffusion of water molecules inside porosities (and micro cavities present between the polymer chains), capillary transport in porosities and defects at the fiber/matrix interface. The latter is important in case of poor interfacial adhesion between the fibers and the matrix – derived from a poor wettability or incomplete impregnation of the fibers by the matrix – and when the detachment of the matrix/fibers has begun. In order to promote the use of plant fiber composite materials, vary properties of them should be clearly understood. This is one of the reasons why we study sorption performance of our UD flax fiber composite.

5.5.1 Influence of environmental conditions

The water sorption is a process of diffusion phenomena that are thermally activated. Sreekala et al.[126] investigated oil palm fiber reinforced phenol formaldehyde (PF) composites and oil palm/glass hybrid fiber reinforced PF composites at different sorption temperature (30°C, 50°C, 70 °C and 90°C) and showed results that upon reinforcing PF resin with oil palm fiber, a large increase in sorption (10 wt%) takes place and thereafter it decreases. The lowest sorption was observed for composite having 40 wt% fiber loading. Beyond 40 wt% fiber loading the sorption again increased. The decreased water sorption could be due to the increased fiber-matrix adhesion according sorption results. The value globally increases with increasing temperature. However, the value shows its maximum at 30°C except in the case of 40 wt% fiber loaded composite in which case maximum sorption is observed at 90°C. The

lowest sorption in this case is observed at 50°C. In addition, Chen et al.[127] showed equilibrium moisture content of bamboo/vinylester composites increase with the increasing relative humidity.

5.5.2 Effect of composite structure and treatment of fiber

Shanks et al.[128] reported that flax fiber washed in sodium hydroxide 30°C for 1 h or using butyl acrylate (BA) as polymerization initiator give a lower sorption of water compared with other untreated systems of polylactic acid with flax fibers composite. In our team, Cherif et al.[46] studied effects of the conventional textile treatments of woven flax on the water sorption of their composites. Results show that textile treatment with bleach, mercerization and leach can decrease the moisture uptake for the similar fiber and porosity component textile flax fiber composites. In the study of Arbelaiz et al.[129] about short flax fiber reinforced polypropylene, water uptake increases with the increasing proportion of flax fiber content and water uptake show a slight decrease by the 5 wt% epolene E43-modified for fiber. In the structure of hemp fiber reinforced unsaturated polyester composites, Dhakal et al.[130] give a clear results of water sorption by unsaturated polyester reinforced by 3, 4 and 5 layers of hemp fiber reinforced specimens, corresponding to 0, 0.15, 0.21 and 0.26 fiber volume fractions, respectively, immersed at room temperature for 888 h. The saturation has been measured to be 0.88, 5.63, 8.16 and 11%, respectively. Besides, compared with the room temperature above, the same original specimens influenced by temperature have a distinguishable increase in the water sorption at 100°C which reach 1.95, 7.37, 9.12 and 13.5%, respectively.

5.5.3 Effect of sorption on composite mechanical properties

Moisture sorption exerts big influence on the tensile mechanical properties, especially for plant fiber composite such as flax as reinforcement. Assarar et al.[45] analyzed the influence of water ageing on tensile mechanical properties of flax composites processed with epoxy resin prepreg and glass fiber epoxy composites and damage events. Results showed that the ultimate stress decreases as immersion time for flax fiber composites as for glass fiber composites – 13% during the first day and 9% during the first ten days, respectively – but the ultimate strain increases for the flax fiber composite, which is not the case for the glass fiber composite. As shown in Fig. 5.5, decrease of tensile mechanical property performances is very obvious for flax fiber composite comparing with glass fiber composite over time.

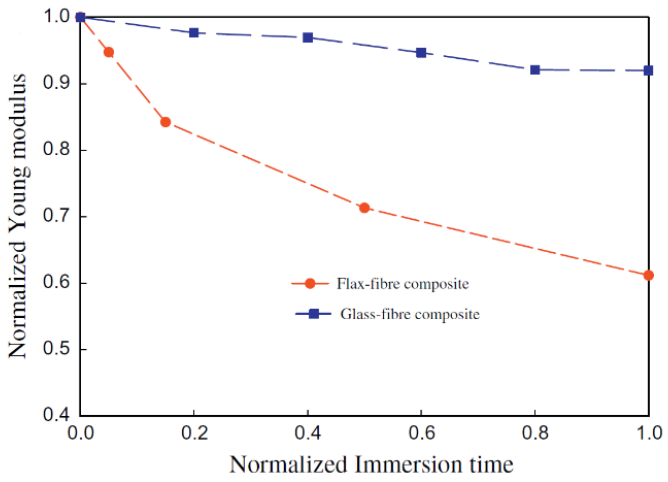

Fig. 5.5 Evolution of the normalized Young's modulus according to the normalized immersion time[45]

The dramatic decline in mechanical properties of bio-based composite is mainly due to the aged reinforcement and degradation of fiber/matrix interface region rather than the polymer. According to the report of Baschek et al.[131], though pure polymers having different or opposite mechanical change ways by water aging at low and high temperatures, there is no such large proportion of the decline in the mechanical properties (Young's modulus). For instance at low moisture content from 0.4 to 1.2 $\%wt$, PES and PA12 show a slight increase in the changes of Young's modulus at temperature 77 K, inversely, a notable decrease appears at 293 K. In the study of Dhakal et al.[132], water sorption proportion does not match a linear relation with the tensile mechanical property change of hemp/unsaturated polyester composite. For fiber volume fraction 0 and 0.26 (water uptake 0.88and 11%, respectively) the ultimate tensile stress increases, on the contrary it decreases for fiber volume fraction 0.15 and 0.21 (water uptake 5.63 and 8.16%, respectively).

5.6 Water sorption of UD flax composite

5.6.1 Description and procedure

Our experiment has been done with common water at standard laboratory atmosphere, an atmosphere (environment) having a temperature of $23 \pm 2℃$ and a relative humidity of $50 \pm 10\%$. In our case, the samples are taken out from the water bath and tissue papers are used to dry the samples surfaces meticulously each time. The samples were re-immersed in water to permit the continuation of the kinetic of sorption until saturation in excess water was established. When the weight reaches the saturation point, which means the weight gain are

nearly constant. We can obtain the saturation state of moisture gains in the sorption test M^{∞}. Fig. 5.6 shows the percentage of water absorbed for four UD samples after immersing water ageing at 20℃, as a function of square root of immersing time.

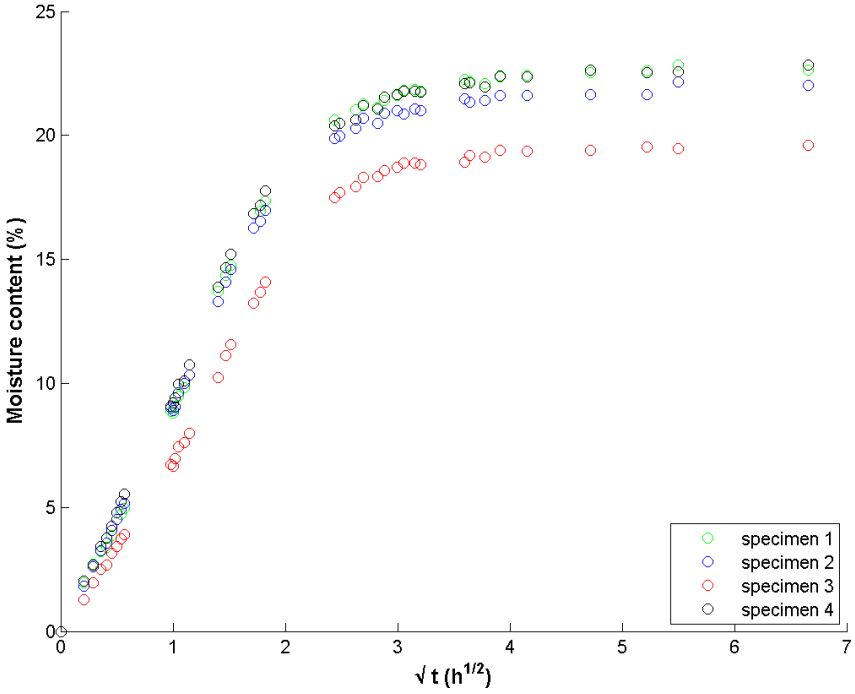

Fig. 5.6 Moisture uptake of four UD flax composites.

The moisture uptake seems to increase linearly with the square root of time and gradually approaches the equilibrium plateau. The curves show that UD flax composite specimens rapidly gain much more moisture during the beginning part (the first stages: $0-2\ days$) with a faster rate of moisture uptake comparing the plateau part which could be considered reaching the equilibrium at a certain value, where no more water was absorbed and the content of water in the composites remained the same.

5.6.2 Diffusion mechanism

To identify the diffusion mechanism and kinetics in our UD specimens, the analysis was performed base on the shape of the sorption curve and adjusting experimental data to the equation as below:

$$ln\left(\frac{\mathrm{M}}{\mathrm{M}^{\infty}}\right) = ln\,\mathrm{k} + \mathrm{n}\,ln\,\mathrm{t} \tag{5.21}$$

which is derived from Equation (5.7).

In Equation (5.21), the constant values n and k are determined by linear regression analysis. The exponent value of n indicates the type of sorption transport mechanism, while the parameter, k, represents the extent of interaction between the water and UD flax composite, which is showed in Fig. 5.7 and Table 5.1 with specific values.

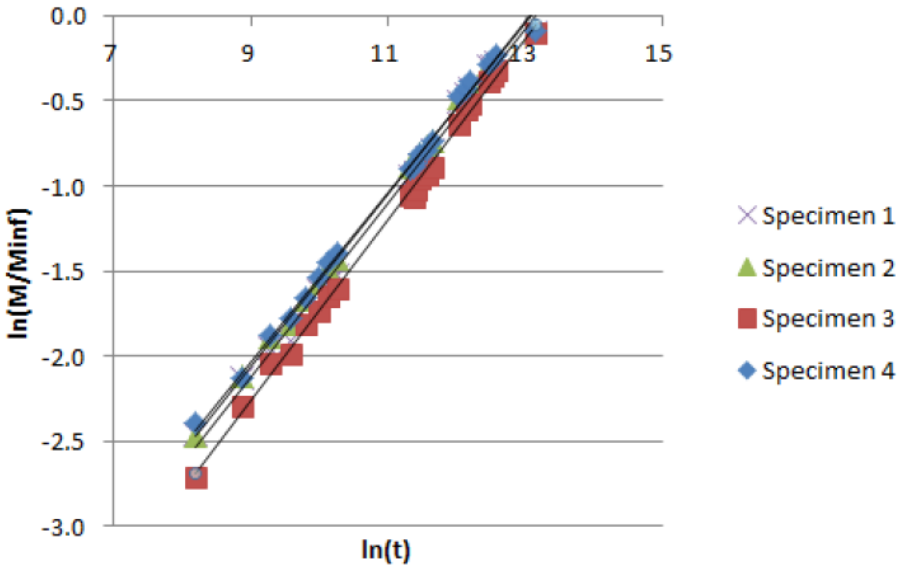

Fig. 5.7 Plot of sorption case for UD flax/epoxy composite

The values of diffusion coefficient n are very similar for all the specimens and they are close to the value $n = 0.5$ (Table 5.1). The values of k exhibit the trends similar to sorption results, i.e., these results in general according to this descending sequence: Sample 4, Sample 2, Sample 1, Sample 3. For some other organic solvents and polymer systems reported by Aminabhavi et al.[133], values of k could increase systematically with increasing temperature.

Table 5.1 Diffusion constant of UD flax composite (UD110-3)

	n	$k \times 10^3$
Specimen 1	0.517	1.1
Specimen 2	0.513	1.2
Specimen 3	0.535	0.8
Specimen 4	0.503	1.4

From the results listed in the Table 5.1, all the n values can be clearly rounded about 0.5. Consequently, considering small experiment error water sorption behavior of UD flax/epoxy composite could be known as a Fickian diffusion mechanism. The same behavior that moisture uptake in plant fiber reinforced polymers follows a Fickian law was reported for other plant fiber reinforced polymers[126][127].

5.6.3 Diffusion, sorption, and permeability coefficients

Table 5.2 shows the values of diffusion, sorption and permeability coefficients of UD flax composites. It is clear from Table 5.2 that the permeability coefficient is larger than $2.00 \times 10^{-7}\, mm^2 s^{-1}\, Pa^{-1}$ except for Sample 3. The different penetration may be due to the development of microcracks in the interface and the bulk of the material. The different porosities existing in the composite may also play a role. The development of microcracks makes possible peeling and surface dissolution of the composite in the sorption environment.

Table 5.2 Sorption parameters for UD flax/epoxy composite, Fick's model (UD110-3).

	Diffusion $D \times 10^7 (mm^2 s^{-1})$	Sorption $S\ (g\ g^{-1})$	Permeability $P \times 10^7 (mm^2 s^{-1} Pa^{-1})$	Saturation M^{∞} (%)
Specimen 1	9.40	0.225	2.12	22.5
Specimen 2	9.93	0.217	2.15	21.7
Specimen 3	7.75	0.197	1.53	19.7
Specimen 4	10	0.224	2.24	22.4

5.6.4 Water uptake by composite components

As we know, there are three main phases in our UD flax composite: unidirectional flax fibers, epoxy resin, and porosities. However, the moisture uptake in the saturation equilibrium for each phase is quite different. We consider it is 3% for our epoxy resin matrices in water uptake by weight, and assume the porosities in our UD composite are all full filled up by the water when it is reached equilibrium state meanwhile utilize the density value of water of $1000\ kg\ m^{-3}$. For UD reinforcement, it could be different in water uptake. The proportions of water uptake by each phase in the composite were calculated here as showed in Fig. 5.8. where:

$$\mathrm{M}^{\infty} = \mathrm{M}_{\mathrm{f}}^{\infty} + \mathrm{M}_{\mathrm{m}}^{\infty} + \mathrm{M}_{\mathrm{p}}^{\infty} \tag{5.23}$$

where n stand for reinforcement, m matrix, and p porosities.

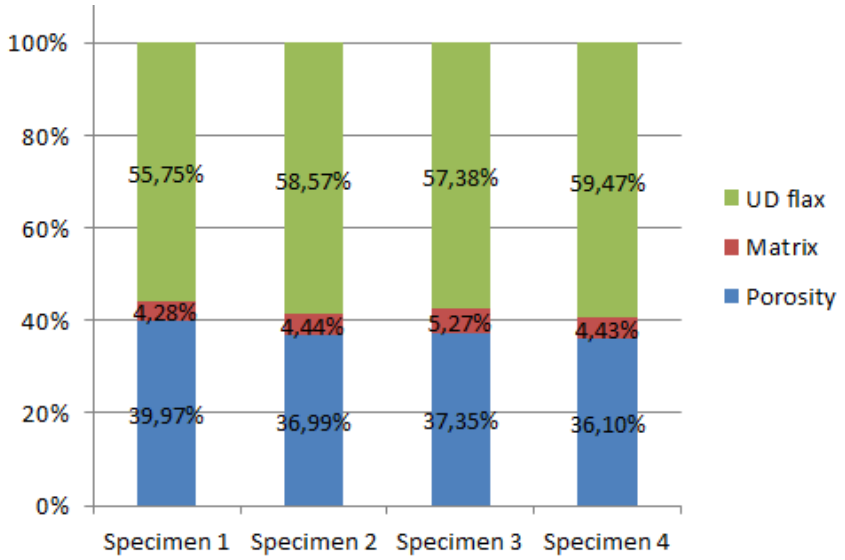

Fig. 5.8 Water sorption ratio of each component in UD flax composite specimens.

5.6.5 Discussion

The diffusion constants n and k (Table 5.1) seem to indicate a Fickian mechanism of sorption. Now, we compare the experimental diffusion results with theoretical predictions in order to discuss deviation from the regular Fickian model described by the Equation (5.8). In our laboratory previous studies, two phases (see Section 5.4) were considered to be used in the analysis of sorption behavior in flax textile composite[49] and which give a favorable result about the water diffusion in the composite. Another famous sorption model is the Langmuir's model (also exposed in Section 5.4). The plain curve on Fig. 5.9(a), calculated by using Equation (5.8), shows the theoretical water uptake behavior adjusted with Fickian diffusion model for the specimen 1. Respectively, the plain curve on Fig. 5.9(b) and Fig. 5.9(c) show the theoretical water uptake behavior adjusted from two phases Fickian model and Langmuir's model. The three curves are very similar, which suggests the Fickian model to be correct.

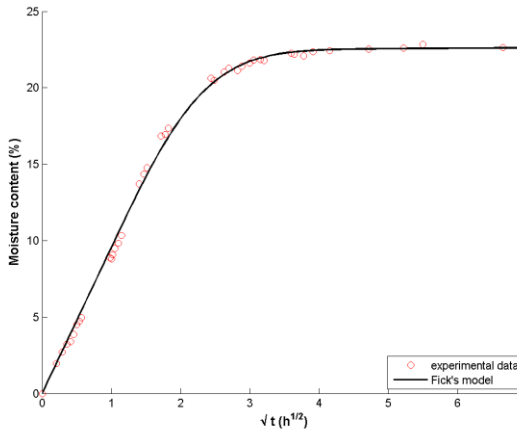

(a) Standard Fick's model fitting

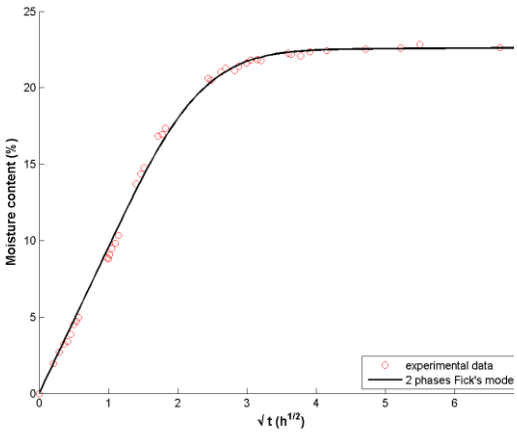

(b) Two-phase Fick's model fitting

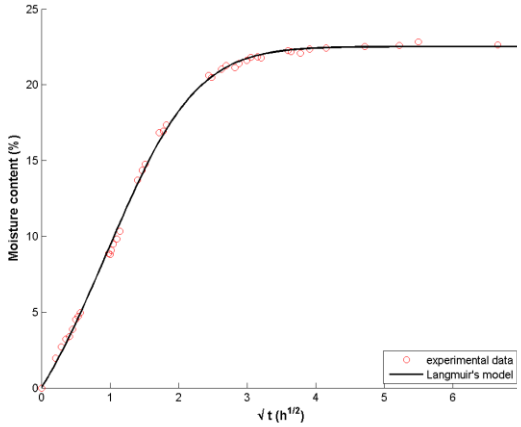

(c) Langmuir's model fitting

Fig. 5.9 Typical comparison between three sorption models for UD flax composite (Specimen 1).

For the example of two phases Fick's model applied to specimen 1, the theoretical diffusion coefficient is $D_1 = 9.45\ 10^{-7}\ mm^2 s^{-1}$ for one phase and $D_2 = 0.18\ 10^{-7}\ mm^2 s^{-1}$ for the second one (Table 5.3). D_1 is very close to the diffusion coefficient obtained by standard Fick's model, which is $D = 9.40\ 10^{-7}\ mm^2 s^{-1}$ (Table 5.2). The sorption coefficients are $M_1^{\infty} = 22.4\%$ and $M_2^{\infty} = 0.44\%$, respectively, and $M = 22.5\%$ when measured by the Fick's model. In fact, for the tested unidirectional composites, one phase of two-phase Fick's model is insignificant (Table 5.3). The two phases Fickian sorption was developed with idea that there is one slow sorption kinetic and one quick kinetic of sorption, simultaneously. In our study, the only case for which the slower phase was detected is the sorption kinetic of specimen 1 (Table 5.3), the diffusion coefficient D_2 being very lower than D_1.

Table 5.3 Sorption parameters for UD flax/epoxy composite, two-phase Fick's model (UD110-3).

	Phase 1		Phase 2	
	Diffusion $D_1 \times 10^7 (mm^2 s^{-1})$	Saturation $M_1^\infty (\%)$	Diffusion $D_2 \times 10^7 (mm^2 s^{-1})$	Saturation $M_2^\infty (\%)$
Specimen 1	9.45	22.4	0.18	0.44
Specimen 2	9.93	21.7	5.52	0
Specimen 3	7.75	19.7	8.02	0
Specimen 4	10	22.3	9.61	0.05

For the same specimen 1, the sorption parameters measured by Langmuir model are $= 9.66\ 10^{-7} mm^2 s^{-1}$, $M = 22.5\%$, $\beta = 3.06 \cdot 10^{-6} s^{-1}$ and $\gamma = 1.09 \cdot 10^{-6} s^{-1}$ (Table 5.4). The kinetic is supposed Fickian when γ tends to zero which can be analyzed from Equation (5.18) and is confirmed in case of UD composite both by Fig. 5.9 and Table 5.4. Considering now that γ is the probability per unit of time for a molecule to be bond and β is the probability per unit of time for a molecule to be mobile[117][118], both two-phase Fickian model and Langmuir model explain that the water is very mobile inside the tested composite.

Table 5.4 Sorption parameters for UD flax/epoxy composite, Langmuir's model (UD110-3).

	Phase 1		Phase 2	
	Diffusion $D \times 10^7 (mm^2 s^{-1})$	Saturation $M^\infty (\%)$	Beta value $\beta \times 10^6 (s^{-1})$	Gamma value $\gamma \times 10^6 (s^{-1})$
Specimen 1	9.66	22.5	3.06	1.09
Specimen 2	10.77	21.8	2.74	0.70
Specimen 3	6.25	19.6	3.38	1.26
Specimen 4	11.31	22.5	2.37	0.57

5.7 Conclusion

Finally for the tested unidirectional composite, the penetration of water is very easy and very rapid. The ratio of porosity and reinforcement is not the only cause, because similar composite in term of component ratio were tested in our team with lower diffusion and

sorption coefficients, as we can see in Fig. 5.10. The main differences between UD composite and others in Fig. 5.10 are:

- reinforcement not twisted for unidirectional composite (Section 2.1.2),
- high level of pectin for unidirectional composite (Section 1.3.2),
- no mesh in the reinforcement as in textile composite (Section 2.1.2),
- reinforcement not treated for unidirectional composite (Section 2.1.2).

In conclusion, we assume that the water penetrates rapidly in the flax and in all linear open channels (both constituting the first phase), which is enhanced by high level of pectin and low interface efficiency. The second phase is constituted by the matrix itself and the close porosities, the latter being very small compared to the total volume.

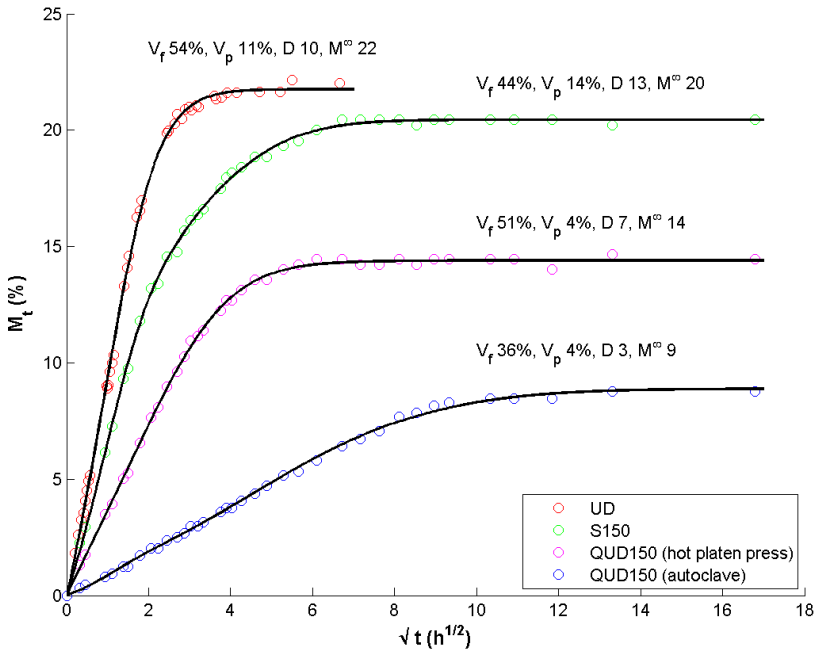

Fig. 5.10 Typical comparison of sorption curves for several flax/epoxy composites, Langmuir's model has been applied.

CONCLUSION

L'objectif principal de ce travail de doctorat était de caractériser le comportement d'un composite unidirectionnel de fibre de lin du point de vue de ses propriétés mécaniques. Le composite de fibre de lin purement unidirectionnel (le renfort est constitué de fibres de lin unidirectionnelles, la matrice est une époxyde) a été fabriqué en optimisant les paramètres du procédé. Des méthodes multiples (analyse thermogravimétrique, microscopie optique et électronique, et mesure de température de transition vitreuse, etc.) ont été utilisées pour caractériser les propriétés de base du renfort de lin et du composite associé. Pour le pli unidirectionnel, l'analyse thermogravimétrique montrent que les fibres de lin ont une stabilité thermique jusqu'à $160°C$. Le taux de perte de poids maximal se produit à environ $330°C$. La microstructure du composite de lin montre que les fibres sont organisées en faisceaux ou sous forme de fibres élémentaires distribuées aléatoirement. La température de transition vitreuse mesurée se situe entre $80°C$ et $100°C$, selon le pourcentages des différentes constituants. La mesure globale des fractions volumiques des différents composants du composite lin unidirectionnel développée en combinant les dimensions et la masse des plaques tout en connaissant la densité de chaque

In this PhD work, the main objective is to characterize the behavior of unidirectional (UD) flax fiber composite at the aspects of mechanical properties. Purely unidirectional flax fiber composite (reinforcement is unidirectional flax fibers, matrix is epoxy) has been manufactured considering affection of process parameters. Multiple methods (thermogravimetric analysis, optical microscopy, scanning electron microscopy and glass transition temperature measurement etc.) have been used for characterizing basic properties of flax reinforcement or it's composite. For the unidirectional Flaxtape^{TM}, thermogravimetric analysis shows that flax fibers have thermal stability when the temperature is lower than 160 °C. Maximum weight loss rate occurs at about 330°C. The microstructures of flax composite show that flax fibers exist in buddle forms or in elementary fibers randomly distributed in the matrix. T_g tests give results that UD flax fiber composite herein is approximately between 80°C-100°C, depending on the constituent fractions. Global measurement of different component ratios in UD flax composite has been developed combining measuring the dimensions and the mass of plates while knowing the density of each

composant. Un soin particulier a été pris dans la mesure du volume des plaques composites élaborées par thermo-compression. L'enveloppe surfacique de la plaque composite a été reconstruite numériquement, car elle n'est pas plane.

La distribution d'orientation du renfort joue un rôle important dans les propriétés mécaniques du composite. J' analyse dans la thèse la désorientation des plis unidirectionnels à l'aide d'un traitement d'image et de la notion des tenseurs de structure. La distribution statistique d'orientation du renfort au sein du pli a été obtenue en mesurant les orientations locales des fibres.

Un modèle permettant d'établir les propriétés effectives du renfort fibreux a été développé en prenant en compte le taux de porosités ainsi que la distribution d'orientation des fibres. Après avoir introduit le paramètre d'orientation dans la loi des mélanges, nous montrons que le renfort de lin unidirectionnel possède des propriétés effectives dans l'axe meilleures que le renfort torsadé d'un composite textile quasi-unidirectionnel testé par ailleurs au laboratoire, pour des fractions volumiques comparables. Ces propriétés sont par ailleurs cohérentes avec celle des composites associés, le composite

component. Special care has been taken in the measurement of the volume of composite plates developed by thermo-compression. Precisely, the composite plate surface was reconstructed with a software due to it is not flat.

Orientation distribution of UD flax fiber play an important role in the mechanical behavior performance. I analyzed the disorientation of UD flax ply reinforcement by optical measurement combining to structure tensor method. Statistical distribution of reinforcement orientation was obtained by using image analysis of local orientation of fibers.

Effective mechanical properties of fibrous UD reinforcement identification theory has been developed by taking not only the efficiency porosities but also UD flax fiber orientation distribution into account. Once I introduced the orientation parameter into the rule of mixture model, we shows that unidirectional flax fibers exhibited a higher effective mechanical properties in longitudinal tension aspect – with similar composite phase system – than previous twisted flax yarn included in a textile quasi-UD composite previously made in our laboratory. The results of effective mechanical properties of both UD flax fiber and textile flax fiber

unidirectionnel possédant des propriétés meilleures que le composite quasi-unidirectionnel. Les différentes fractions volumiques et la distribution d'orientation des fibres ont l'effet attendu sur les propriétés mécaniques des composites étudiés. Le coefficient de Poisson par contre, ne montre pas d'influence notable sur les propriétés mécaniques.

Il est connu que le comportement mécanique des composite à fibres végétales n'est pas linéaire et dépend des conditions d'essai (vitesse de chargement, température, et taux d'humidité ...) , deux domaines typiques sont aisément détectables en traction. Des essais monotones, des chargements répétés progressifs (CRP) et des tests de fluage selon la méthode standard ont été effectués pour étudier ce comportement global. Les essais mécaniques sont de ce fait non seulement utilisés pour développer la théorie d'identification des propriétés mécaniques effectives du renfort, mais aussi pour l'analyse phénoménologique du matériau. Un comportement mécanique global en trois domaines du composite à fibres végétales a été identifié avec un modèle antérieurs à huit paramètres. Il est clair que des phénomènes de déformation élastiques, viscoplastiques et viscoélastiques sont activés. Cependant, il existe encore une

are also consistent with their composite tensile mechanical properties of UD flax composites showing higher tensile mechanical properties than that of textile flax composite. Both components ratio and orientation distribution have then regular effect law on the mechanical behavior of the studied composite. Poisson ratio, however, as an essential attributes of flax fiber does not show affection on composite mechanical property performance.

As it is well known, mechanical behavior of plant fiber composites exhibit non-linear behavior which depends on experimental conditions (strain rate, temperature, and humidity…): two apparent regions are visible under tensile loading. Monotonic test, repetitive progressive load (RPL), and creep test according to standard method were performed to study this global behavior. Mechanical tests are then not only for development of the identification theory of effective mechanical properties of reinforcement, but also for phenomenological analysis of the material. Global behavior with three regions in tensile mechanical behavior of plant fiber composite has been identified with eight parameters previous model. It is evident that elastic, viscoplastic and

marge d'amélioration de la prédiction du comportement mécanique en traction du composite lin unidirectionnel. Une piste d'amélioration intégrant des paramètres de renforcement est abordée dans la thèse.

Enfin, le comportement en sorption d'eau du composite unidirectionnel a été étudié. Les paramètres de sorption du composite ont été identifiés. Nous en concluons que la sorption du composite unidirectionnel est conforme à la loi de Fick. Les résultats montrent que l'absorption d'humidité est fortement affectée par la conformation unidirectionnelle des fibres de lin et des porosités existant dans le composite, tandis que le comportement de pénétration de l'humidité diffère de celui du composite à renfort torsadé étudié précédemment dans notre laboratoire. Pour le composite à fil de lin, les deux phases du modèle Fickian semblent avoir donné de meilleurs résultats que le simple modèle de Fick. Cependant, pour approfondir le comportement en sorption de notre composite unidirectionnel à fibre de lin, deux modèles importants – Langmuir et un modèle de Fick à deux phases – ont été appliqués sur le composite unidirectionnel. Compte tenu de la probabilité qu'une molécule soit liée et de la probabilité qu'une mobile soit mobile, les deux modèles Fickian et le modèle de Langmuir montrent que l'eau est très

viscoelastic phenomena are activated in the strain. However, there still is a room for improvement about the precise prediction of the tensile mechanical behavior of UD flax composite. In the thesis, an improvement track integrating reinforcement parameters is discussed.

Last but not least, water absorption behavior of UD composite has been investigated. The sorption parameters of UD flax fiber composite have been identified. As a result on UD composite, the sorption behavior is in line with the common Fickian theory. Result shows that the moisture uptake are strongly affected by the unidirectional conformation of flax fibers and porosities existing in the composite, meanwhile the penetration behavior of moisture differs to that of twisted reinforcement composite previously studied in our laboratory. For flax yarn composite in our laboratory, two phases Fickian model seem to have given a better results than simple Fickian model. However for a deep view to understand the sorption behavior of our UD flax fiber composite, two important models – Langmuir's and two-phases Fickian cases – were applied on the UD composite. Considering the probability for a water molecule to be bond and the probability for a molecule to be mobile,

mobile à l'intérieur du composite testé. La pénétration rapide est favorisée par tous les canaux linéaires ouverts, un niveau élevé de pectine dans le renfort et une faible efficacité d'interface.

both two-phases Fickian model and Langmuir's model explain that the water is very mobile inside the tested composite. Rapid penetration can be enhanced by all linear open channels, high level of pectin and low interface efficiency.

REFERENCE

[1] Westman M P, Fifield L S, Simmons K L, et al. Natural fiber composites: a review. Pacific Northwest National Laboratory, 2010.

[2] Shah D U. Developing plant fibre composites for structural applications by optimising composite parameters: a critical review. Journal of Materials Science, 2013, 48(18): 6083-6107.

[3] Reux F. Worldwide composites market: Main trends of the composites industry. 5th innovative composites summit-JEC ASIA 2012, 2012: 26-28.

[4] Stamboulis A, Baillie C A, Peijs T. Effects of environmental conditions on mechanical and physical properties of flax fibers. Composites Part A: Applied Science and Manufacturing, 2001, 32(8): 1105-1115.

[5] Pickering K L, Efendy M G A, Le T M. A review of recent developments in natural fibre composites and their mechanical performance. Composites Part A: Applied Science and Manufacturing, 2016, 83: 98-112.

[6] Rao K M M, Rao K M. Extraction and tensile properties of natural fibers: Vakka, date and bamboo. Composite structures, 2007, 77(3): 288-295.

[7] Bledzki A K, Gassan J. Composites reinforced with cellulose based fibres. Progress in polymer science, 1999, 24(2): 221-274.

[8] Nam T H, Ogihara S, Tung N H, et al. Effect of alkali treatment on interfacial and mechanical properties of coir fiber reinforced poly (butylene succinate) biodegradable composites. Composites Part B: Engineering, 2011, 42(6): 1648-1656.

[9] Baley C. Analysis of the flax fibres tensile behaviour and analysis of the tensile stiffness increase. Composites Part A: Applied Science and Manufacturing, 2002, 33(7): 939-948.

[10] Kalia S, Kaith B S, Kaur I. Pretreatments of natural fibers and their application as reinforcing material in polymer composites—a review. Polymer Engineering & Science, 2009, 49(7): 1253-1272.

[11] Morvan C, Andème-Onzighi C, Girault R, et al. Building flax fibres: more than one brick in the walls. Plant Physiology and Biochemistry, 2003, 41(11): 935-944.

[12] Bos H L, Van Den Oever M J A, Peters O C J J. Tensile and compressive properties of flax fibres for natural fibre reinforced composites. Journal of Materials Science, 2002, 37(8): 1683-1692.

[13] Koksharov S, Aleeva S, Lepilova O. Nanostructural biochemical modification of flax

fiber in the processes of its preparation for spinning. Autex Research Journal, 2015, 15(3): 215-225.

[14] Dymińska L, Gągor A, Hanuza J, et al. Spectroscopic characterization of genetically modified flax fibers. Journal of Molecular Structure, 2014, 1074: 321-329.

[15] Moriana R, Vilaplana F, Karlsson S, et al. Correlation of chemical, structural and thermal properties of natural fibres for their sustainable exploitation. Carbohydrate polymers, 2014, 112: 422-431.

[16] Nguong C W, Lee S N B, Sujan D. A review on natural fibre reinforced polymer composites. Materials and Metallurgical Engineering, 7(1):33—40, 2013.

[17] Duchemin B, Thuault A, Vicente A, et al. Ultrastructure of cellulose crystallites in flax textile fibres. Cellulose, 2012, 19(6): 1837-1854.

[18] Bismarck A, Aranberri□Askargorta I, Springer J, et al. Surface characterization of flax, hemp and cellulose fibers; surface properties and the water uptake behavior. Polymer composites, 2002, 23(5): 872-894.

[19] Dittenber D B, GangaRao H V S. Critical review of recent publications on use of natural composites in infrastructure. Composites Part A: Applied Science and Manufacturing, 2012, 43(8): 1419-1429.

[20] Kalia S, Dufresne A, Cherian B M, et al. Cellulose-based bio-and nanocomposites: a review. International Journal of Polymer Science, 2011, 2011.

[21] Scheller H V, Ulvskov P. Hemicelluloses. Annual review of plant biology, 2010, 61: 263-289.

[22] Gibson L J. The hierarchical structure and mechanics of plant materials. Journal of the Royal Society Interface, 2012: rsif20120341.

[23] Célino A, Fréour S, Jacquemin F, et al. The hygroscopic behavior of plant fibers: A review. Frontiers in chemistry, 2013, 1.

[24] Wojtasik W, Kulma A, Dymińska L, et al. Fibres from flax overproducing β-1, 3-glucanase show increased accumulation of pectin and phenolics and thus higher antioxidant capacity. BMC biotechnology, 2013, 13(1): 1-16.

[25] Moriana R, Vilaplana F, Karlsson S, et al. Correlation of chemical, structural and thermal properties of natural fibres for their sustainable exploitation. Carbohydrate polymers, 2014, 112: 422-431.

[26] Lebo S E, Gargulak J D, McNally T J. Lignin. Kirk-Othmer encyclopedia of chemical technology, 2001.

[27] Jouanin L, Lapierre C. Lignins: biosynthesis, biodegradation and bioengineering.

Academic Press, 2012.

[28] Batra S K. Other long vegetable fibers. Handbook of Fiber Chemistry, Third Edition. CRC Press, 2006

[29] Wambua P, Ivens J, Verpoest I. Natural fibres: can they replace glass in fibre reinforced plastics?. composites science and technology, 2003, 63(9): 1259-1264.

[30] Dittenber D B, GangaRao H V S. Critical review of recent publications on use of natural composites in infrastructure. Composites Part A: Applied Science and Manufacturing, 2012, 43(8): 1419-1429.

[31] Madsen B, Lilholt H. Physical and mechanical properties of unidirectional plant fibre composites—an evaluation of the influence of porosity. Composites Science and Technology, 2003, 63(9): 1265-1272.

[32] Baley C. Influence of kink bands on the tensile strength of flax fibers. Journal of materials science, 2004, 39(1): 331-334.

[33] Cosgrove D J. Growth of the plant cell wall. Nature reviews molecular cell biology, 2005, 6(11): 850-861.

[34] Schrick K, Fujioka S, Takatsuto S, et al. A link between sterol biosynthesis, the cell wall, and cellulose in Arabidopsis. The Plant Journal, 2004, 38(2): 227-243.

[35] Lamy B, Pomel C. Influence of fiber defects on the stiffness properties of flax fibers-epoxy composite materials. Journal of materials science letters, 2002, 21(15): 1211-1213.

[36] Mehdi Khennache, « Caractérisation biologique, chimique, physique et mécanique de différents lots de fibres de lin, transformées ou non, pour une application en matériaux composites biosourcés », PhD in progress, University of Rouen Normandy.

[37] Van de Velde K, Baetens E. Thermal and mechanical properties of flax fibres as potential composite reinforcement. Macromolecular Materials and Engineering, 2001, 286(6): 342-349.

[38] Carrier M, Loppinet-Serani A, Denux D, et al. Thermogravimetric analysis as a new method to determine the lignocellulosic composition of biomass. Biomass and Bioenergy, 2011, 35(1): 298-307.

[39] Souto-Maior J F A, Reis A V, Pedreiro L N, et al. Phosphated crosslinked pectin as a potential excipient for specific drug delivery: preparation and physicochemical characterization. Polymer International, 2010, 59(1): 127-135.

[40] Gassan J, Bledzki A K. Thermal degradation of flax and jute fibers. Journal of

Applied Polymer Science, 2001, 82(6): 1417-1422.

[41] Charlet K, Eve S, Jernot J P, et al. Tensile deformation of a flax fiber. Procedia Engineering, 2009, 1(1): 233-236.

[42] Pillin I, Kervoelen A, Bourmaud A, et al. Could oleaginous flax fibers be used as reinforcement for polymers?. Industrial Crops and Products, 2011, 34(3): 1556-1563.

[43] Arbelaiz A, Cantero G, Fernandez B, et al. Flax fiber surface modifications: effects on fiber physico mechanical and flax/polypropylene interface properties. Polymer composites, 2005, 26(3): 324-332.

[44] Saville B P. Physical testing of textiles. Elsevier, 1999.

[45] Assarar M, Scida D, El Mahi A, et al. Influence of water ageing on mechanical properties and damage events of two reinforced composite materials: Flax–fibres and glass–fibres. Materials & Design, 2011, 32(2): 788-795.

[46] Cherif Z E, Poilâne C, Falher T, et al. Influence of textile treatment on mechanical and sorption properties of flax/epoxy composites. Polymer composites, 2013, 34(10): 1761-1773.

[47] Poilâne C, Cherif Z E, Richard F, et al. Polymer reinforced by flax fibres as a viscoelastoplastic material. Composite Structures, 2014, 112: 100-112.

[48] Scida D, Assarar M, Poilâne C, et al. Influence of hygrothermal ageing on the damage mechanisms of flax-fibre reinforced epoxy composite. Composites Part B: Engineering, 2013, 48: 51-58.

[49] Cherif Z E, Poilâne C, Vivet A, et al. About optimal architecture of plant fibre textile composite for mechanical and sorption properties. Composite Structures, 2016, 140: 240-251.

[50] Hughes M, Carpenter J, Hill C. Deformation and fracture behaviour of flax fibre reinforced thermosetting polymer matrix composites. Journal of Materials Science, 2007, 42(7): 2499-2511.

[51] Chauhan S R, Patnaik A, Kaith B S, et al. Analysis of Mechanical Behavior of Phenol Formaldehyde Matrix Composites Using Flax-g-Poly (MMA) as Reinforcing Materials. Journal of Reinforced Plastics and Composites, 2009, 28(16): 1933-1944.

[52] Cuinat-Guerraz N, Dumont M J, Hubert P. Environmental resistance of flax/bio-based epoxy and flax/polyurethane composites manufactured by resin transfer moulding. Composites Part A: Applied Science and Manufacturing, 2016, 88: 140-147.

[53] Adekunle K, Cho S W, Ketzscher R, et al. Mechanical properties of natural fiber

hybrid composites based on renewable thermoset resins derived from soybean oil, for use in technical applications. Journal of Applied Polymer Science, 2012, 124(6): 4530-4541.

[54] Crossley R, Schubel P, Stevenson A. Furan matrix and flax fibre as a sustainable renewable composite: Mechanical and fire-resistant properties in comparison to phenol, epoxy and polyester. Journal of Reinforced Plastics and Composites, 2014, 33(1): 58-68.

[55] Le Duigou A, Bourmaud A, Gourier C, et al. Multi-scale shear properties of flax fibre reinforced polyamide 11 biocomposites. Composites Part A: Applied Science and Manufacturing, 2016, 85: 123-129.

[56] Arbelaiz A, Fernandez B, Ramos J A, et al. Mechanical properties of short flax fibre bundle/polypropylene composites: Influence of matrix/fibre modification, fibre content, water uptake and recycling. Composites Science and Technology, 2005, 65(10): 1582-1592.

[57] Le Duigou A, Bourmaud A, Davies P, et al. Long term immersion in natural seawater of Flax/PLA biocomposite. Ocean Engineering, 2014, 90: 140-148.

[58] Aydın M, Tozlu H, Kemaloglu S, et al. Effects of alkali treatment on the properties of short flax fiber–poly (lactic acid) eco-composites. Journal of Polymers and the Environment, 2011, 19(1): 11-17.

[59] Kaith B S, Singha A S, Kumar S, et al. Mercerization of flax fiber improves the mechanical properties of fiber-reinforced composites. International Journal of Polymeric Materials, 2008, 57(1): 54-72.

[60] Baiardo M, Zini E, Scandola M. Flax fibre–polyester composites. Composites Part A: Applied Science and Manufacturing, 2004, 35(6): 703-710.

[61] Frechette J. Flax-filled composite: U.S. Patent Application 10/045,519. 2001-10-26.

[62] Oksman K. High quality flax fibre composites manufactured by the resin transfer moulding process. Journal of reinforced plastics and composites, 2001, 20(7): 621-627.

[63] Yan L, Chouw N, Yuan X. Improving the mechanical properties of natural fibre fabric reinforced epoxy composites by alkali treatment. Journal of Reinforced Plastics and Composites, 2012, 31(6): 425-437.

[64] Goutianos S, Peijs T, Nystrom B, et al. Development of flax fibre based textile reinforcements for composite applications. Applied composite materials, 2006, 13(4): 199-215.

[65] Baiardo M, Zini E, Scandola M. Flax fibre–polyester composites. Composites Part A: Applied Science and Manufacturing, 2004, 35(6): 703-710.

[66] Schuster J, Govignon Q, Bickerton S. Processability of biobased thermoset resins and flax fibres reinforcements using vacuum Assisted resin transfer moulding. Open Journal of Composite Materials, 2014, 2014.

[67] Oksman K, Skrifvars M, Selin J F. Natural fibres as reinforcement in polylactic acid (PLA) composites. Composites science and technology, 2003, 63(9): 1317-1324.

[68] Kannan T G, Wu C M, Cheng K B, et al. Effect of reinforcement on the mechanical and thermal properties of flax/polypropylene interwoven fabric composites. Journal of Industrial Textiles, 2013, 42(4): 417-433.

[69] Adekunle K, Cho S W, Ketzscher R, et al. Mechanical properties of natural fiber hybrid composites based on renewable thermoset resins derived from soybean oil, for use in technical applications. Journal of Applied Polymer Science, 2012, 124(6): 4530-4541.

[70] Li X, Panigrahi S, Tabil L G. A study on flax fiber-reinforced polyethylene biocomposites. Applied Engineering in Agriculture, 2009, 25(4): 525.

[71] Bourmaud A, Le Duigou A, Gourier C, et al. Influence of processing temperature on mechanical performance of unidirectional polyamide 11–flax fibre composites. Industrial Crops and Products, 2016, 84: 151-165.

[72] Gourier C, Bourmaud A, Le Duigou A, et al. Influence of PA11 and PP thermoplastic polymers on recycling stability of unidirectional flax fibre reinforced biocomposites. Polymer Degradation and Stability, 2017, 136: 1-9.

[73] Pucci M F, Liotier P J, Seveno D, et al. Wetting and swelling property modifications of elementary flax fibres and their effects on the Liquid Composite Moulding process. Composites Part A: Applied Science and Manufacturing, 2017.

[74] Liu M, Baum A, Odermatt J, et al. Oxidation of lignin in hemp fibres by laccase: Effects on mechanical properties of hemp fibres and unidirectional fibre/epoxy composites. Composites Part A: Applied Science and Manufacturing, 2017, 95: 377-387.

[75] Mahjoub R, Yatim J M, Sam A R M, et al. Characteristics of continuous unidirectional kenaf fiber reinforced epoxy composites. Materials & Design, 2014, 64: 640-649.

[76] Liu K, Takagi H, Osugi R, et al. Effect of physicochemical structure of natural fiber on transverse thermal conductivity of unidirectional abaca/bamboo fiber composites.

Composites Part A: Applied Science and Manufacturing, 2012, 43(8): 1234-1241.

[77] Ntenga R, Béakou A, Atéba J A, et al. Estimation of the elastic anisotropy of sisal fibres by an inverse method. Journal of materials science, 2008, 43(18): 6206-6213.

[78] Brahim S B, Cheikh R B. Influence of fibre orientation and volume fraction on the tensile properties of unidirectional Alfa-polyester composite. Composites Science and Technology, 2007, 67(1): 140-147.

[79] Kalia S, Kaith B S, Kaur I. Pretreatments of natural fibers and their application as reinforcing material in polymer composites—a review. Polymer Engineering & Science, 2009, 49(7): 1253-1272.

[80] Zhang L, Miao M. Commingled natural fibre/polypropylene wrap spun yarns for structured thermoplastic composites. Composites Science and Technology, 2010, 70(1): 130-135.

[81] ISO E N. 527-5 (2009) Plastics—determination of tensile properties—Part 5: test conditions for unidirectional fibre-reinforced plastic composites. ISO international standards, West Conshohocken, 2009.

[82] Gillham J K. The TBA torsion pendulum: a technique for characterizing the cure and properties of thermosetting systems. Polymer international, 1997, 44(3): 262-276.

[83] Vergnaud J M, Bouzon J. Cure of thermosetting resins: modelling and experiments. Springer Science & Business Media, 2012.

[84] Varna J, Joffe R, Berglund L A, et al. Effect of voids on failure mechanisms in RTM laminates. Composites Science and technology, 1995, 53(2): 241-249.

[85] Thomason J L. The interface region in glass fibre-reinforced epoxy resin composites: 2. Water absorption, voids and the interface. Composites, 1995, 26(7): 477-485.

[86] Berthelot J M. Composite materials: mechanical behavior and structural analysis. Springer Science & Business Media, 2012.

[87] Jähne B. Spatio-temporal image processing: theory and scientific applications. Springer Science & Business Media, 1993.

[88] Naouar N, Vidal-Sallé E, Schneider J, et al. Meso-scale FE analyses of textile composite reinforcement deformation based on X-ray computed tomography. Composite Structures, 2014, 116: 165-176.

[89] Harris B. The mechanical behaviour of composite materials. Symposia of the Society for Experimental Biology. Cambridge University Press, p. 37-73, 1980.

[90] Hull D, Clyne T W. An introduction to composite materials. Cambridge university press, 1996.

[91] Madsen B. Properties of plant fibre yarn polymer composites – an experimental study. PhD Thesis, Technical University of Denmark, Department of Civil Engineering; 2004. 206 p.

[92] Karine Charlet, “Contribution à l’étude de composites unidirectionnels renforcés par des fibres de lin : relation entre la microstructure de la fibre et ses propriétés mécaniques”, PhD Thesis, University of Caen Basse-Normandie, 2008

[93] Eik M, Puttonen J, Herrmann H. The effect of approximation accuracy of the orientation distribution function on the elastic properties of short fibre reinforced composites. Composite Structures, 2016, 148: 12-18.

[94] Altendorf H, Jeulin D, Willot F. Influence of the fiber geometry on the macroscopic elastic and thermal properties. International Journal of Solids and Structures, 2014, 51(23): 3807-3822.

[95] Hine P, Parveen B, Brands D, et al. Validation of the modified rule of mixtures using a combination of fibre orientation and fibre length measurements. Composites Part A: Applied Science and Manufacturing, 2014, 64: 70-78.

[96] Hohe J, Beckmann C, Paul H. Modeling of uncertainties in long fiber reinforced thermoplastics. Materials & Design, 2015, 66: 390-399.

[97] Bourmaud A, Morvan C, Bouali A, et al. Relationships between micro-fibrillar angle, mechanical properties and biochemical composition of flax fibers. Industrial Crops and Products, 2013, 44: 343-351.

[98] Keckes J, Burgert I, Frühmann K, et al. Cell-wall recovery after irreversible deformation of wood. Nature materials, 2003, 2(12): 810-813.

[99] Del Masto A, Trivaudey F, Guicheret-Retel V, et al. Nonlinear tensile behaviour of elementary hemp fibres: a numerical investigation of the relationships between 3D geometry and tensile behaviour. Journal of Materials Science, 2017, 52(11): 6591-6610.

[100] Placet V. Characterization of the thermo-mechanical behaviour of Hemp fibres intended for the manufacturing of high performance composites. Composites Part A: Applied Science and Manufacturing, 2009, 40(8): 1111-1118.

[101] Sanjay M R, Arpitha G R, Naik L L, et al. Applications of Natural Fibers and Its Composites: An Overview. Natural Resources, 2016, 7(03): 108.

[102] Espert A, Vilaplana F, Karlsson S. Comparison of water absorption in natural cellulosic fibres from wood and one-year crops in polypropylene composites and its influence on their mechanical properties. Composites Part A: Applied science and

manufacturing, 2004, 35(11): 1267-1276.

[103] Alomayri T, Assaedi H, Shaikh F U A, et al. Effect of water absorption on the mechanical properties of cotton fabric-reinforced geopolymer composites. Journal of Asian ceramic societies, 2014, 2(3): 223-230.

[104] Standard A. D5229/D5229M-12 “Standard Test Method for Moisture Absorption Properties and Equilibrium Conditioning of Polymer Matrix Composite Materials." ASTM International, West Conshohocken, PA, 2012, DOI: 10.1520/D5229_D5229M-12.

[105] Westman M P, Fifield L S, Simmons K L, et al. Natural fiber composites: a review. Pacific Northwest National Laboratory, 2010.

[106] Hearle J W S, Morton W E. Physical properties of textile fibres. Elsevier, 2008.

[107] Bledzki A K, Mamun A A, Lucka-Gabor M, et al. The effects of acetylation on properties of flax fibre and its polypropylene composites. Express Polymer Letters, 2008, 2(6): 413-422.

[108] Palmer N A, Sattler S E, Saathoff A J, et al. Genetic background impacts soluble and cell wall-bound aromatics in brown midrib mutants of sorghum. Planta, 2008, 229(1): 115-127.

[109] Fedors R F. Osmotic effects in water absorption by polymers. Polymer, 1980, 21(2): 207-212.

[110] Fick A. Ueberdiffusion. Annalen der Physik, 1855, 170(1): 59-86.

[111] Masaro L, Zhu X X. Physical models of diffusion for polymer solutions, gels and solids. Progress in polymer science, 1999, 24(5): 731-775.

[112] Comyn J. Polymer permeability. Barking England: Elsevier Applied science publishers.1985.

[113] Sperling L H. Introduction to Physical Polymer Science (Fourth Edition), Wiley-Interscience.2006.

[114] Kishimoto A, Matsumoto K. Effect of film thickness upon the sorption of organic vapors in polymers slightly above their glass transition temperatures. Journal of Polymer Science Part A: General Papers, 1964, 2(2): 679-687.

[115] Crank J. The Mathematics of Diffusion: 2d Ed. Clarendon Press, 1975.

[116] Célino A, Fréour S, Jacquemin F, et al. Characterization and modeling of the moisture diffusion behavior of natural fibers. Journal of Applied Polymer Science, 2013, 130(1): 297-306.

[117] Carter H G, Kibler K G. Langmuir-type model for anomalous moisture diffusion in

composite resins. Journal of Composite Materials, 1978, 12(2): 118-131.

[118] Startsev V O, Panin S V, Startsev O V. Sorption and diffusion of moisture in polymer composite materials with drop-weight impact damage. Mechanics of Composite Materials, 2016, 51(6): 761-770.

[119] Dhakal H N, Zhang Z Y, Richardson M O W. Effect of water absorption on the mechanical properties of hemp fibre reinforced unsaturated polyester composites. Composites Science and Technology, 2007, 67(7): 1674-1683.

[120] Joliff Y, Rekik W, Belec L, et al. Study of the moisture/stress effects on glass fibre/epoxy composite and the impact of the interphase area. Composite Structures, 2014, 108: 876-885.

[121] Shen C H, Springer G S. Moisture absorption and desorption of composite materials. Journal of Composite Materials, 1976, 10(1): 2-20.

[122] Crank J, Park G S. Methods of Measurement, in Diffusion in Polymers. Academic Press, London, 1968, Chap. 1.

[123] Shewmon P & Janßen M. (Eds.)Diffusion in solids. Springer, 2016.

[124] Ashley R J. Permeability and plastics packaging, In: Polymer permeability. Springer Netherlands, 1985: 269-308.

[125] Kreze T, Stana-Kleinschek K, Ribitsch V. The sorption behaviour of cellulose fibres. Lenzinger Berichte, 2001, 80: 28-33.

[126] Sreekala M S, Kumaran M G, Thomas S. Water sorption in oil palm fiber reinforced phenol formaldehyde composites. Composites Part A: Applied science and manufacturing, 2002, 33(6): 763-777.

[127] Chen H, Miao M, Ding X. Influence of moisture absorption on the interfacial strength of bamboo/vinylester composites. Composites Part A: Applied Science and Manufacturing, 2009, 40(12): 2013-2019.

[128] Shanks R A, Hodzic A, Ridderhof D. Composites of poly (lactic acid) with flax fibers modified by interstitial polymerization. Journal of applied polymer science, 2006, 99(5): 2305-2313.

[129] Arbelaiz A, Fernandez B, Ramos J A, et al. Mechanical properties of short flax fibre bundle/polypropylene composites: Influence of matrix/fibre modification, fibre content, water uptake and recycling. Composites Science and Technology, 2005, 65(10): 1582-1592.

[130] Dhakal H N, Zhang Z Y, Richardson M O W. Effect of water absorption on the mechanical properties of hemp fibre reinforced unsaturated polyester composites.

Composites Science and Technology, 2007, 67(7): 1674-1683.

[131] Baschek G, Hartwig G, Zahradnik F. Effect of water absorption in polymers at low and high temperatures. Polymer, 1999, 40(12): 3433-3441.

[132] Dhakal H N, Zhang Z Y, Richardson M O W. Effect of water absorption on the mechanical properties of hemp fibre reinforced unsaturated polyester composites. Composites Science and Technology, 2007, 67(7): 1674-1683.

[133] Aminabhavi T M, Naik H G. Sorption/desorption, diffusion, and swelling characteristics of geomembranes in the presence of halo-organic liquids. Journal of applied polymer science, 1999, 72(3): 349-359.

APPENDIX

All types of products tested in the laboratory.

UD70

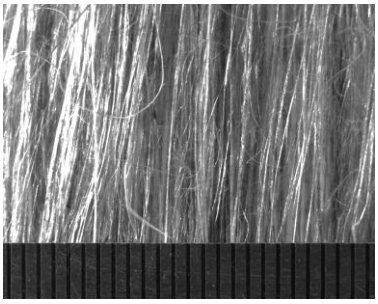

UD110

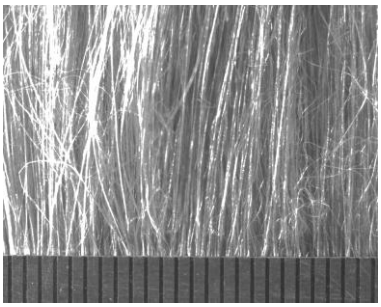

UD200

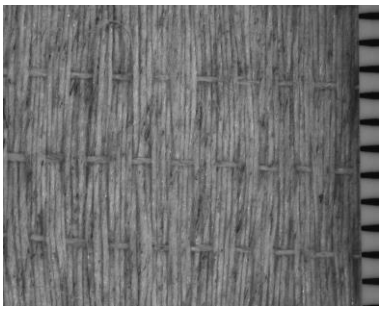

QUD150

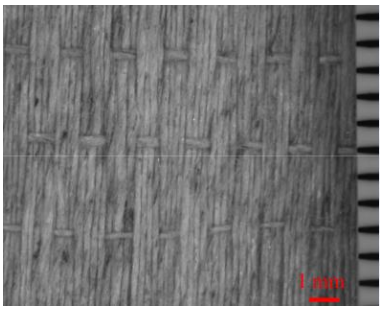

QUD180

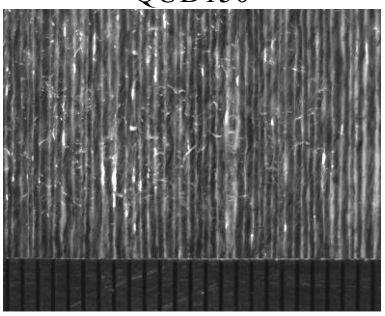

QUD200

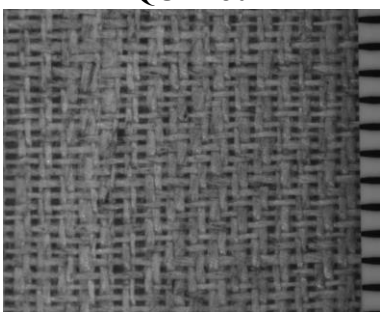

S150

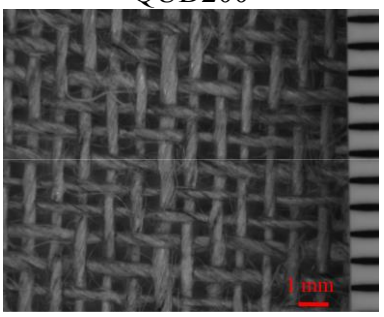

S200

S300

S550

Haomiao Yang

Abstract

In this Ph.D work, unidirectional flax fiber composite (UD biobased composite) has been designed and manufactured based on the hot platen press process. Plant fiber composites usually exhibit two regions under tensile load, but three regions have been identified in this work. A phenomenological model, previously developed to describe the tensile mechanical behavior of twisted plant yarn composites, has been tested with the UD biobased composite. We show that the addition of a strengthening phenomenon to the previous model is necessary to simulate correctly the third region. A second mechanical model has also been developed for experimental identification of the effective mechanical properties of flax reinforcement when embeded in matrix. A statistical distribution of local orientation of UD reinforcement was obtained allowing taking the fiber orientation into account. To that end, structure tensor method was applied to optical images of flax ply. Furthermore, this model allows the effect of porosity on mechanical properties to be studied. Both models provide effective forecast of the mechanical behavior of unidirectional flax fiber composite. Besides the mechanic models, sorption behavior of UD flax composite also has been analyzed. Langmuir's model and Fick's model were applied on our UD composite. The results show that the unidirectional configuration of the flax reinforcement promotes the water sorption from the associated composites.

Keywords: Plant fiber; UD composite; Mechanical properties; Fiber orientation; Sorption behavior

Résumé

Dans cette thèse, un composite unidirectionnel à renfort lin (composite UD biosourcé) a été développé et élaboré par la technique de presse à chaud. Le comportement en traction des composites à renfort végétal montre en général deux domaines, mais un troisième domaine est identifié dans ce travail. Un modèle phénoménologique développé précédemment pour décrire le comportement en traction d'un composite à renfort en fils torsadés a été testé avec le composite UD biosourcé. Nous montrons que l'ajout d'un phénomène de consolidation au modèle précédent est nécessaire pour simuler correctement le troisième domaine. Un second modèle mécanique a été par ailleurs développé pour identifier expérimentalement les propriétés mécaniques effectives du renfort en lin lorsqu'il est piégé dans la matrice. La distribution statistique de l'orientation locale du renfort a été mesurée pour pouvoir prendre en compte l'orientation des fibres. Pour cela, la technique du tenseur de structure a été appliquée sur des images optiques du pli de lin. Par ailleurs, ce modèle permet d'étudier l'influence des porosités sur les propriétés mécaniques. Les deux modèles permettent d'effectuer des prévisions efficaces du comportement mécanique du composite de fibre de lin unidirectionnel. En complément des modèles de mécanique, le comportement en sorption du composite de lin UD a également été analysé. Le modèle de Langmuir et le modèle de Fick ont été appliqués sur nos composites UD. Les résultats montrent que la configuration unidirectionnelle du renfort de lin favorise la sorption d'eau des composites associés.

Mots clés : Fibre végétale ; Composites UD ; Propriétés mécaniques ; Orientation des fibres ; Sorption